

2021 年度

博士学位論文

**Effects of targeting inhibitors of plasmacytoid dendritic cell
migration in immune diseases**

(特異的形質細胞様樹状細胞遊走抑制剤の免疫疾患に対する治療効果)

富山大学

和漢医薬学総合研究所

未病分野 腸管疾患ユニット

薬科学専攻

張 玥 (ZHANG YUE)

学籍番号 31761308

**Effects of targeting inhibitors of plasmacytoid dendritic cell
migration in immune diseases**

This thesis was submitted to the
Graduate School of Medicine and Pharmaceutical Sciences
University of Toyama
to the fulfillment of the degree of
Doctor of Philosophy in Pharmaceutical Sciences.

ZHANG YUE

Division of Gastrointestinal Pathophysiology

Institute of Natural Medicine

University of Toyama

Japan

September 2021

Contents

Abstract.....	1
Abbreviations	4
Introduction	6
Objective.....	10
Chapter 1 Therapeutic benefit in allergic dermatitis derived from the inhibitory effect of byakkokaninjinto on the migration of plasmacytoid dendritic cells	
1. Introduction	11
2. Materials and methods	13
3. Results	16
4. Discussion	23
5. Conclusion	25
6. Tables	26
Chapter 2 Suppression of plasmacytoid dendritic cell migration to colonic isolated lymphoid follicles abrogates the development of colitis	
1. Introduction	36
2. Materials and methods	38
3. Results	43
4. Discussion	61
5. Conclusion	65
6. Tables	66
Conclusion and Future Directions	71
References	72
Acknowledgements	83

Abstract

Trafficking of dendritic cells (DCs) *in vivo* is essential in maintaining immunological homeostasis by orchestrating innate and adaptive immune responses. DCs respond to foreign substances and activate immunocytes such as T cells and B cells via migration to inflamed sites and lymph nodes (LNs). DCs are mainly divided into 2 subtypes: conventional DCs (cDCs) and plasmacytoid DCs (pDCs). pDCs rarely exist in peripheral tissues in the normal state but accumulate in infected sites and rapidly secrete massive amounts of type-I interferon (IFN) once viral infection occurs. Chemokine (C-C motif) ligand 19 (CCL19) and chemokine (C-C motif) ligand 21 (CCL21), as ligands of C-C chemokine receptor type 7 (CCR7) expressed on mature pDCs guide pDCs into the LNs.

Migration of pDCs towards LNs is involved in the pathogenesis of many immune diseases via interaction with other immunocytes. Infiltration of pDCs has been found in the skin of systemic sclerosis patients. Depletion of B220⁺ PDCA-1⁺ pDCs reduces skin thickness in a skin fibrosis model. In addition, increase of pDCs has been found in inflamed sites in patients with contact dermatitis and atopic dermatitis. Accordingly, pDCs are required for the pathogenic mechanism and defense mechanism of skin disorders, such as atopic dermatitis.

Furthermore, pDCs reportedly play a pivotal role in the onset of inflammatory bowel disease (IBD). A large number of pDCs infiltrate in the colonic mucosa of IBD patients. pDCs are increased in the inflamed colon of ulcerative colitis (UC) patient and Crohn's disease patients. Also, it is reported that pDCs are decreased in the peripheral blood of UC patients. The population of pDCs is increased in the mouse colon in a dextran sulfate sodium (DSS)-induced colitis model, and the depletion of pDCs suppresses the inflammation in the colon of DSS-induced colitis mice. On the contrary, the depletion of pDCs aggravates severe colitis in a *Citrobacter rodentium*-induced colitis model by impairing gut barrier functions. Thus, pDCs are considered to play various roles in the pathology of many inflammatory diseases, while the roles of pDCs remain unclear.

To the best of our knowledge, few agents have been found to effectively and potently regulate pDC functions, especially pDC migration. Therefore, we utilized traditional Japanese herbal medicines as a resource for drug discovery. Traditional Japanese herbal medicines have been widely used for various immune diseases, such as rheumatoid arthritis and IBD. Kampo formulas or compounds in natural medicines have been used in the study of inflammatory diseases. Our study focused on the pDC migration in allergic dermatitis model and DSS-induced colitis model. Furthermore, Kampo formulas and compounds in natural medicines were used in the disease models to elucidate the effect and role of inhibition of pDC migration in inflammatory diseases.

1. Therapeutic benefit in allergic dermatitis derived from the inhibitory effect of

byakkokaninjinto on the migration of plasmacytoid dendritic cells

pDCs have been reportedly related to inflammatory skin disorders for the increase and accumulation in inflamed sites in patients with contact dermatitis. Even pDCs are increased in the lesional skin of atopic dermatitis patients. Similarly, pDCs also infiltrate in the skin of systemic sclerosis patients and meanwhile, depletion of pDCs reduces skin thickness in a skin fibrosis model.

CCR7-driven migration of pDCs to the lymph nodes is considered play a pivotal role in pathogenesis of immune diseases via activating T cells or B cells. Therefore, our study focused on the inhibition of pDC migration. We screened 86 kinds of Kampo formulas and examined that byakkokaninjinto was the inhibitor of pDC migration by reducing the number of migrated bone marrow-derived pDCs (BMpDCs) and suppressing the velocity and directionality of BMpDC migration in a chemotaxis assay. Furthermore, *Gypsum Fibrosum* and *Ginseng Radix* which are the components of byakkokaninjinto, obviously suppressed the velocity of BMpDC migration. *Gypsum Fibrosum* significantly suppressed the directionality of BMpDC migration. Besides, byakkokaninjinto had no effect on the expression of CCR7 on BMpDCs. Then the effect of byakkokaninjinto on a 1-fluoro-2,4-dinitrobenzene-induced allergic contact dermatitis model was investigated. Orally administration of byakkokaninjinto markedly relieved ear swelling in the late-phase response of allergic reactions.

These findings prove that byakkokaninjinto which has an inhibitory effect on pDC migration may contribute to ameliorate the occurrence of allergic contact dermatitis. Inhibition of pDC migration is anticipated to become a therapeutic agent for pDC-related diseases, such as atopic dermatitis.

2. Suppression of plasmacytoid dendritic cell migration to colonic isolated lymphoid follicles abrogates the development of colitis

It has been reported that pDCs participate in the onset of IBD. Infiltration of pDCs is found in the colonic mucosa of IBD patients. And highly enrichment of pDCs correlates with disease severity of IBD patients. In a DSS-induced colitis model, pDCs is increased in the mouse colon. And depletion of pDCs suppresses inflammation in the colon. However, depletion of pDCs also impairs gut barrier function and causes heavy colitis in a pathogenic bacterium induced colitis model. In another Wiskott-Aldrich syndrome (WAS) disease model, ablating type-I IFN signaling in WAS protein null mice rescues colitis and makes pDCs show tolerance to further stimulation. On the other hand, pDC has been reported that it does not have a major role in the pathology of colitis caused by deficiency in WAS protein. Therefore, these contradictory reports suggest that pDCs perform multiple functions in the intestine.

Our study targets the inhibition of pDC migration. 80 compounds in natural medicines were

searched for inhibitors of pDC migration using BMpDCs. Astragaloside IV (As-IV) and oxymatrine (Oxy) suppressed the migration of BMpDC by reducing the number of migrated BMpDCs and suppressing the velocity and directionality of BMpDC migration in a chemotaxis assay. Meanwhile, As-IV and Oxy had no effect on bone marrow-derived conventional DCs. To elucidate the pathogenesis role of pDCs in the intestinal immunity, DSS-induced colitis model was established. The number of pDCs was markedly increased in the colonic lamina propria (LP) of DSS-induced colitis model. Intraperitoneal injection of As-IV or Oxy reduced symptoms of colitis but not affect the number of pDCs in the colonic LP. By the immunohistochemical staining, expression of CCL21 was obviously observed in colonic isolated lymphoid follicles (ILFs). As-IV or Oxy reduced the accumulation of pDCs in colonic ILFs. Furthermore, migration of BMpDCs to colonic ILFs was significantly decreased by treatment with As-IV or Oxy in a BMpDC adoptive transfer model.

These findings prove that accumulation of pDCs in the ILFs is relative to the onset and progression of colitis. As-IV and Oxy exert preventive effects on colitis by suppressing pDC migration to colonic ILFs. The inhibitor of pDC migration may become a potential therapeutic approach for treating colonic inflammatory diseases.

Conclusion

CCR7-driven migration of pDCs to the lymph nodes leads to activation of T cells or B cells. In this study, we discovered inhibitors of pDC migration toward the lymphoid tissues. Our present results have demonstrated that the migration of pDCs toward the lymphoid tissues is involved in the pathogenesis of immune diseases such as contact dermatitis and colonic inflammation. Inhibition of pDC migration contributes to alleviate these diseases. Therefore, the inhibitors of pDC migration may have potentials to become the useful lead drugs for immunological diseases.

Abbreviations

As-IV: Astragaloside IV

Ber: berberine

BM: bone marrow

BMcDC: bone marrow-derived cDC

BMpDC: bone marrow-derived pDC

CCL19: chemokine (C-C motif) ligand 19

CCL21: chemokine (C-C motif) ligand 21

CCL25: chemokine (C-C motif) ligand 25

CCR7: C-C chemokine receptor type 7

CCR9: C-C chemokine receptor type 9

CD: Crohn's disease

cDC: conventional dendritic cell

CFSE: carboxyfluorescein diacetate succinimidyl ester

Cur: curcumin

CXCL12: Chemokine (C-X-C motif) ligand 12

CXCR4: C-X-C chemokine receptor type 4

DAI: disease activity index

DC: Dendritic cell

DNFB: 1-fluoro-2,4-dinitrobenzene

DSS: dextran sulfate sodium

FBS: fetal bovine serum

GALT: gut-associated lymphoid tissue

i.p.: intraperitoneal

IBD: inflammatory bowel disease

IFN: interferon

IL: interleukin

ILF: isolated lymphoid follicle

IPA: Ingenuity Pathway Analysis

IPR: immediate-phase response

Iso: isofraxidine

LN: lymph node

LP: lamina propria

LPR: late-phase response

LPS: Lipopolysaccharide

MLN: mesenteric lymph node

ODN: oligodeoxynucleotides

Oxy: oxymatine

pDC: plasmacytoid dendritic cell

PI: propidium iodide

SLE: systemic lupus erythematosus

UC: ulcerative colitis

vLPR: very-late-phase response

WAS: Wiskott-Aldrich syndrome

WASp: Wiskott-Aldrich syndrome protein

Introduction

*** Immune functions of plasmacytoid dendritic cells**

There are various immunoreactions *in vivo* contribute to body homeostasis. Dendritic cells (DCs) which are known as the high ability of antigen presenting cells distribute to various tissues and organs. DCs are derived from a common myeloid progenitor which is derived from hematopoietic stem cells in the bone marrow and migrate to the inflamed sites and lymph nodes (LNs) depend on the stimulation of chemokines to regulate the immune responses. DCs are defined as the conventional dendritic cells (cDCs) and the plasmacytoid dendritic cells (pDCs). pDCs are known for secretion of massive type-I interferon (IFN) in the context of viral infection to induce antiviral responses. Besides, migration of pDCs into the LNs and antigen presentation to T cells activate the T cells differentiation into Treg cells, Th1 cells, Th2 cells or Th17 cells which induces immunoreactions and contributes to maintain immunological homeostasis (Seth et al., 2011, McKenna et al., 2005). Thus, pDCs participate the innate immune response and the adaptive immune response. Moreover, activation of T cells evoked by pDCs arouses anti-inflammatory activity or pro-inflammatory activity *in vivo* (Takagi et al., 2011). Therefore, the pathophysiological role of pDCs in the immune diseases is complicated.

*** Migration of pDCs**

Migration of pDCs, which is mediated by chemokines, into the LN is important for exerting its immune functions. Various types of chemokine receptors are expressed on pDCs and several chemokines drive migration to different sites (Tiberio et al., 2018). In the study of mouse pDCs, C-C chemokine receptor type 9 (CCR9) was usually used in the study of pDCs in the small intestine. CCR9 expressed on pDCs guides pDCs into the small intestine via its ligand chemokine (C-C motif) ligand 25 (CCL25) (Wendland et al., 2007). C-X-C chemokine receptor type 3 (CXCR3) induces pDC precursors migrate to inflamed LNs under bacterial infection (Tiberio et al., 2018). C-X-C chemokine receptor type 4 (CXCR4) allows migration of pDCs into splenic white pulp (Tiberio et al., 2018). C-C chemokine receptor type 7 (CCR7) expressed on pDCs leads pDCs migrate into the LNs. CCR7 drives mature pDCs migrate into T cell areas of the gut-associated lymphoid tissue (GALT) (Seth et al., 2011). For the human pDCs, CCR7 allows the human pDCs recruit to LNs (Tiberio et al., 2018). Therefore, CCR7 is imperative for pDC migration to LNs both in mouse and human. In addition, migration of pDC into LNs arouses activation of T cells and leads immune regulation. So, trafficking of pDCs driven by CCR7 is imperative for pDCs exerting its immune functions in organs and tissues.

*** pDCs in immune diseases: skin disorders**

Atopic dermatitis and contact dermatitis as the common skin disorders are caused by the contact

of allergen. The hypersensitivity response to the allergen results in the impairment of skin barrier (Owen et al., 2018). The symptoms of these skin disorders are usually accompanied with weeping eczema, edema, itch and skin thickening (Owen et al., 2018). Prednisolone is used as therapy for dermatitis patients; however, side effects of Prednisolone restrict its dosage and administration period (Vatti et al., 2014). Therefore, it is hoped that a new therapeutic agent with lower side effects or with a different action mechanism of steroids for reducing the dose of steroids is developed.

Recent studies refer to dermatitis have reported the involvement of abnormal distribution of pDCs in the lesional skin of dermatitis patients. pDCs are increased in the lesional skin of patients with allergic contact dermatitis and psoriasis. Th17 cells activated by pDCs induce the secretion of massive interleukin (IL)-17. Hypersecretion of IL-17 aggravates the skin inflammation (Garzorz-Stark et al., 2018). Infiltration of pDCs is found in the lesional skin of patients with atopic dermatitis (Lebre et al., 2008). Similarly, increased pDCs in the lesional skin of patients with atopic dermatitis are proved by interaction with peripheral neural addressin of vascular endothelium (Hashizume et al., 2005). Infiltration of pDCs and massive secretion of IFN- α are found in the lesional skin of systemic sclerosis patients. Although the aberrant distribution of pDCs in atopic dermatitis patients was demonstrated, the pathological role of pDCs involved in the pathogenesis of dermatitis is unclear. In a mouse skin fibrosis model, depletion of B220⁺ PDCA-1⁺ pDCs downregulates the skin thickness (Ah Kioon et al., 2018).

These studies prove that pDC is involved in the pathogenesis of skin disorders, but the pathogenic mechanism of pDCs in the skin disorders still remains unclear.

* pDCs in immune diseases: colonic inflammations

Inflammatory bowel disease (IBD) has been defined as ulcerative colitis (UC) and Crohn's disease (CD). UC is the inflammation in surface mucosa of rectum. Bloody stool, diarrhea and fever as the main symptoms are appeared in UC patients (Zhang and Li, 2014). CD causes the ulceration and fibrogenesis of entire gastrointestinal tract. Acute abdomen, chronic diarrhea and body weight losses as the main symptoms are appeared in CD patients (Zhang and Li, 2014). Th17 cells are considered as the indicator of IBD patients (Geremia et al., 2014). Besides, macrophages and DCs are also involved in the progression of IBD because of secreting the cytokines which promote Th17 cell proliferation (Geremia et al., 2014). However, the pathogenesis of IBD is not identified. Mesalamine and Prednisolone are used as therapies for IBD patients. Mesalamine is commonly used in the treatment of mild to moderate IBD patients (Solitano et al., 2020). Prednisolone is used as anti-inflammatory agent (Vatti et al., 2014). However, the current therapeutic drugs for IBD have insufficient therapeutic effect and cause several side effects.

Recently, many studies indicated that pDCs play a key role in the pathogenesis of IBD. pDCs are increased in the colonic mucosa of both UC patients and CD patients (Baumgart et al., 2011). pDCs are markedly increased in the flare of IBD patient's colonic mucosa, and the up-regulated inflammatory cytokines secreted by peripheral blood pDCs disrupt the immune tolerance which results in flare-up of IBD (Baumgart et al., 2011). Similarly, infiltration of pDCs in the inflamed colonic tissues is associated with disease severity (Liu, Dasgupta et al., 2019). pDCs have been reported to increase in the peripheral blood (Mitsialis et al., 2020). On the contrary, there is a report showing that the decrease of pDCs in peripheral blood of UC patients result in pDC migration from peripheral blood into the intestinal mucosa (Baird et al., 2016). Although the aberrant distribution of pDCs in IBD patients was revealed by clinical studies, the pathological role of pDCs involved in the pathogenesis of colitis is unclear. Dextran sulfate sodium (DSS)-induced colitis model is commonly used in the study of IBD because of the similar pathological condition in UC patients. DSS caused the impairment of colonic epithelium. Diarrhea, bleeding, body weight loss and even mortality are the main symptoms of DSS-induced colitis model (Eichele and Kharbanda, 2017). Infiltration of macrophages and DCs are involved in the DSS-induced colitis (Eichele and Kharbanda, 2017). Recently, pDCs have been reported to be related to the progression of colitis in experimental colitis models. pDCs are increased in the colonic LP of DSS-induced colitis model, and depletion of pDCs abrogates colonic inflammation (Arimura et al., 2017). Studies of pDCs using other colitis models have also been reported. In *Citrobacter rodentium*-induced colitis model, depletion of pDCs promotes the activation of cDCs in LNs and causes the decrease of Foxp3⁺ T cells. These impaired gut barrier functions result in the exaggeration of colitis (Pöysti et al., 2021). In a Wiskott-Aldrich syndrome (WAS) protein (WASp) knock-out developed spontaneous colitis model, disruption of IFN- α signaling in pDCs relieves the colitis (Prete et al., 2013). However, in the deficiency of WASp caused colitis model, pDCs are proved unassociated with the pathology of colitis caused by deficiency in WASp or interleukin (IL)-10 (Sawai et al., 2018).

These findings prove that pDCs are commit to the pathogenesis of colonic inflammations. However, previous studies have yielded inconsistent results about the pathogenic roles of pDCs.

* Therapeutic agents: Kampo formulas and compounds in natural medicine

Kampo formulas are composed of natural medicines and exert therapeutic effects on patients individually according to the different symptoms and different ages (Takayama et al., 2018). Most of Kampo formulas are prescribed individually to improve the different kinds of diseases (Takayama et al., 2018). Kampo formulas are used for treating many immunological diseases.

In the treatment of skin disorders, byakkokaninjinto and shoseiryuto have been used as cures for patients with skin disorders (Arumugam and Watanabe, 2017, chapter 1). Byakkokaninjinto and

Jumihaidokuto which have effect on suppressing inflammation are used in atopic dermatitis patients (Arumugam and Watanabe, 2017, chapter 10). Hochuekkito protects the skin from bacterial infections (Arumugam and Watanabe, 2017, chapter 10). As one of the components of byakkokaninjinto, *Ginseng Radix* has been used as its antiviral effects (Im et al., 2016) and promoted the recovery from illness (Arumugam and Watanabe, 2017).

Saireito, tokishakuyakusan and jumihaidokuto have been used as cures for patients with gastrointestinal diseases (Arumugam and Watanabe, 2017, chapter 1). Tokishakuyakusan and jumihaidokuto have been used as treatment for IBD because of the anti-inflammatory effects. Daikenchuto is used as treatment for CD for its effect of enhancing blood circulation (Arumugam and Watanabe, 2017, chapter 5). As one of the components of Kampo formula, As-IV has been reported to upregulate the colonic stem cells and suppress symptoms of 2,4,6-trinitrobenzene sulfonic acid-induced colitis model by modulating the energy metabolism (Jiang, Sun et al., 2017). Oxy is extracted from *Sophora flavescens* Aiton. Oxy exerts its anti-inflammatory effects by regulating the differentiation of Th1 and Th17 cells in a DSS-induced colitis model (Chen et al., 2017). Similarly, Oxy relieves the DSS-induced colitis by suppressing the differentiation of Th17 cells and promoting the differentiation of Treg cells (Wang et al., 2019).

Therefore, both Kampo formulas and compounds extracted from natural medicines are used as therapeutic agent for immunological diseases such as dermatitis and colitis. However, there is little study targeting on the pDCs which elucidates the therapeutic role of Kampo formulas or compounds in the immunological disease.

Objective

pDCs migrate into inflamed sites and rapidly secrete massive amounts of type-I IFN once affected by viral infections. Moreover, pDCs have been reported to be involved in the pathogenesis of many immune diseases through regulating the innate immune response and the adaptive immune response.

pDCs are infiltrated in the lesional skin of patients with inflammatory skin disorders. However, the pathophysiological roles of pDCs in the inflammatory diseases are not apparent. I speculated that whether the inhibition of pDC migration might have the potential to ameliorate inflammatory dermatitis. Thus, I investigated the inhibitors of pDC migration during Kampo formulas. Then a (1-fluoro-2,4-dinitrobenzene) DNFB-induced allergic contact dermatitis model was established to investigate the effect of inhibition of pDC migration in the skin disorders. We aimed to elucidate the effect of byakkokaninjinto which exerted an inhibitory effect on pDC migration on ear swelling of an allergic contact dermatitis model.

Infiltration of pDCs was found in the IBD patients and DSS-induced colitis model. However, the pathophysiological role of pDCs in the colitis is not apparent. I speculated that whether the inhibition of pDC migration might have the potential to ameliorate colonic inflammatory diseases. 80 compounds were screened to select the specific inhibitors of pDC migration. As-IV and Oxy which were selected as a specific inhibitor exerted inhibitory effect on pDC migration in vitro. Further, a DSS-induced colitis model was established to elucidate the effect of inhibiting pDC migration in colonic inflammation in vivo. The number of pDCs in the colon with colitis and As-IV or Oxy treated colon was not altered. We assumed that whether As-IV or Oxy caused a restriction in distribution of pDCs in ILFs. We aimed to prove that restriction in distribution of pDCs in ILFs ameliorated the symptoms of DSS-induced colitis.

Above all, our study is to elucidate the pathophysiological role of pDCs in the inflammatory diseases.

Chapter 1

Therapeutic benefit in allergic dermatitis derived from the inhibitory effect of byakkokaninjinto on the migration of plasmacytoid dendritic cells

1. Introduction

Dendritic cells (DCs) play a critical role in immune regulation. In particular, DCs possess a strong ability to present antigens to CD4⁺ T cells. DCs, as versatile immunocytes, play roles in the induction of T cell activation at the beginning of an immune response and in immune tolerance. During these processes, DCs need to migrate to organs and tissues to exert their functions. The migration of DCs is induced by chemokines and depends on chemokine concentration gradients (Sokol and Luster, 2015). In general, DCs have been divided into conventional dendritic cells (cDCs) and plasmacytoid dendritic cells (pDCs). The bone marrow is the primary site of pDC production, and pDCs migrate through the circulation to the thymus, secondary lymphoid organs and peripheral tissues. In the normal state, pDCs rarely exist in peripheral tissues, but once viral infection occurs, pDCs accumulate in infected sites and rapidly secrete massive amounts of type-I (interferon) IFN. pDCs are activated by viruses; subsequently, they extend, form dendrites and express the costimulators MHCII, CD40, CD80 and CD86 for antigen presentation (Swiecki and Colonna, 2015). Consequently, the migration of pDCs is important in facilitating the immune functions of these cells.

Chemokine (C-C motif) ligand 19 (CCL19) and Chemokine (C-C motif) ligand 21 (CCL21), as ligands of C-C chemokine receptor type 7 (CCR7), are highly expressed in secondary lymphoid tissues (Hauser and Legler, 2016). The numbers of 120G8⁺ B220^{int} CD11c^{int} pDCs are decreased in the peripheral lymph nodes and mesenteric lymph nodes of CCR7-deficient mice (Liu et al., 2011). Thus, CCR7 is required for pDC migration to the lymph nodes both under steady-state conditions and during viral infections (Seth et al., 2011).

pDCs have been reportedly related to inflammatory skin disorders (Saadeh et al., 2016). Infiltrated pDCs have been found in the skin of systemic sclerosis patients, whereas pDCs in the peripheral blood have been found to be decreased, and depletion of B220⁺ PDCA-1⁺ pDCs reduces skin thickness in a skin fibrosis model (Ah Kioon et al., 2018). Similarly, pDCs are increased, and pDCs accumulate in inflamed sites in patients with contact dermatitis (Garzorz-Stark et al., 2018, Lebre et al., 2008). Otherwise, it has been reported that pDCs are increased in the lesional skin of atopic dermatitis patients (Garzorz-Stark et al., 2018, Lebre et al., 2008, Hashizume et al., 2005). Therefore, pDCs play essential roles in the pathogenic mechanism and defense mechanisms of many inflammatory skin disorders, including atopic dermatitis.

Kampo formulas have been used according to individual situations. Many Kampo formulas target the immune system, and their therapeutic effects on immunological diseases have been

demonstrated in clinical studies (Wang and Kaneko, 2018; Takayama et al., 2018). However, the precise mechanisms of Kampo formulas are not well understood. In addition, little is known about the effects of Kampo formulas on the function of DCs, a target for immunological diseases, even though DCs play a key role in immune responses.

Byakkokaninjinto, a traditional Japanese Kampo formula, has been frequently used in Japan and originates from the classical Chinese records of 'Shang Han Lun' and 'Jin Gui Yao Lue'. Byakkokaninjinto is composed of *Gypsum Fibrosum*, *Ginseng Radix*, *Glycyrrhizae Radix*, *Anemarrhenae Rhizoma* and *Oryzae Fructus* (**Table 1**). *Gypsum Fibrosum*, as the basic component of byakkokaninjinto, is composed of calcium sulfate, and Kampo formulas containing *Gypsum Fibrosum* are used for their suppressive effects on heat and inflammation (Lin et al., 2019). *Anemarrhenae Rhizoma* has anti-inflammatory effects (Wang, Cai et al., 2018). *Ginseng Radix* has been used as an antiviral drug (Im et al., 2016). Therefore, byakkokaninjinto is widely applicable for the treatment of many disorders, such as oral dryness caused by diabetes, dermatitis, eczema, urticaria, pneumonia and the common cold (Karuppagounder et al., 2017). Dermatitis is one of the indications of byakkokaninjinto, and the efficacy of byakkokaninjinto in clinically curing atopic dermatitis and allergic contact dermatitis has been reported (Karuppagounder et al., 2017, Shimizu, 2013). In addition, it has been reported that byakkokaninjinto induces therapeutic effects on spontaneous atopic dermatitis-like skin lesions in NC mice (Tohda et al., 2000) and IgE-mediated triphasic skin reaction (Tatsumi et al., 2001). However, the anti-inflammatory mechanism underlying the effects of byakkokaninjinto on these dermatitis remains uncertain.

In this study, we investigated the effects of 86 Kampo formulas on pDC migration and demonstrated that byakkokaninjinto exerted therapeutic effects on an (1-fluoro-2,4-dinitrobenzene) DNFB-induced allergic contact dermatitis model by inhibiting pDC migration.

2. Materials and methods

2.1 Mice

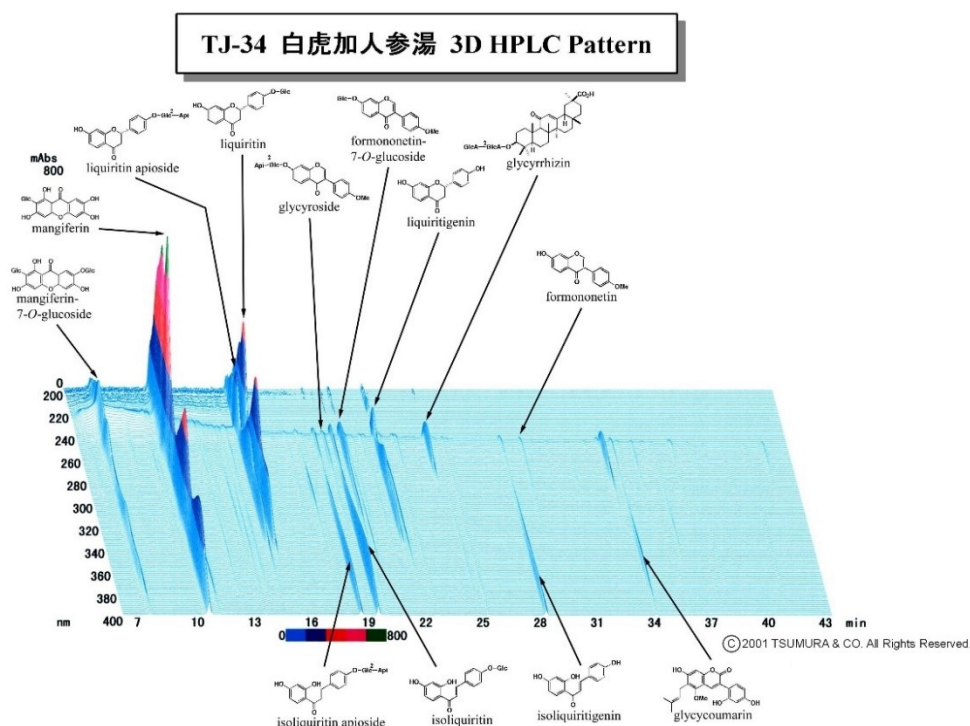
Male BALB/c mice (6-10 weeks old) were purchased from Japan SLC (Shizuoka, Japan). All mice were housed under standard vivarium conditions ($23.5 \pm 0.5^{\circ}\text{C}$, 12-hour light/dark cycle, and food and water provided ad libitum). This study was performed in strict accordance with the recommendations of the Guide for the Care and Use of Laboratory Animals by the National Institutes of Health. The Animal Experiment Committee at the University of Toyama approved all the animal care procedures and experiments (authorization No. A2012 INM4, A2015 INM-3 and A2018 INM-4).

2.2 Preparation of Kampo formulas and each component extracts

Kampo formula extracts and component extracts were provided as dried powders by the Joint Usage/Research Center for Science-Based Natural Medicine, Institute of Natural Medicine, University of Toyama and the Knowledge Cluster Initiative Program (Second Stage) of the Ministry of Education, Culture, Sports, Science and Technology of Japan. Each herbal extract was obtained using a standard method. In brief, each formula and each herbal component was extracted in water at 100°C for 50 min, evaporated under reduced pressure, and freeze-dried to obtain a powder extract. The 86 Kampo formula extracts were screened. Detailed information about the herbal components of the 86 Kampo formula extracts and detailed information of herbal component extracts were stated (**Table 2**).

For a mouse allergic contact dermatitis model study, byakkokaninjinto (TJ-34) was purchased from Tsumura Co. (Tokyo, Japan) as a dried powder with the 3D-HPLC data (Figure 1) and was evaluated as a therapeutic drug for the symptoms of DNFB-induced allergic contact dermatitis.

Figure 1. 3D-HPLC data of byakkokaninjinto.



2.3 BMpDC generation

Bone marrow-derived plasmacytoid dendritic cells (BMpDCs) were generated from bone marrow cells according to a method described previously (Gotoh et al., 2008). Briefly, bone marrow cells were collected from the femur and tibia of male BALB/c mice (6-10 weeks old) and incubated in RPMI 1640 medium (Wako, Osaka, Japan) supplemented with 10% FBS (Equitech-Bio, Kerrville, TX, USA), 55 μ M 2-mercaptoethanol, 100 units/mL penicillin, 100 μ g/mL streptomycin, 292 μ g/mL glutamine (Invitrogen, Carlsbad, CA, USA) and 100 ng/mL Flt3 ligand (R&D Systems, Minneapolis, MN, USA). On day 7-9, immature BMpDCs were collected and stimulated with 2 μ M CpG-oligodeoxynucleotides (ODN-2216; Hokkaido System Science, Hokkaido, Japan) for 24 hours to induce maturation.

2.4 Chemotaxis assay

Mature BMpDCs were suspended in modified RPMI 1640 medium (Sigma, St. Louis, MO, USA) containing 1% FBS and then incubated with each Kampo formula extract or herbal medicine extract for 3 hours at 37°C. Chemotaxis experiments with BMpDCs were performed in an EZ-TAXIScan™ chamber according to the manufacturer's protocol (GE Healthcare Japan, Tokyo, Japan). A BMpDC suspension (1×10^6 cells/mL) was injected into one side of the chamber,

and 1 μl of CCL21 (250 $\mu\text{g}/\text{mL}$) was injected into the opposite side of the chamber. A concentration gradient of CCL21 was formed, and the migration of the BMpDCs toward the more concentrated side of a CCL21 gradient was observed. BMpDC migration was recorded with a CCD camera located beneath the chamber every 30 seconds for 1 hour. At the end of the chemotaxis assay, the number of migrated BMpDCs during 30 minutes and the velocity and directionality of the migrating BMpDCs were analyzed by the TAXIScan Analyzer 2.

2.5 Viability assay and analysis of CCR7 expression level

Treatment with byakkokaninjinto to mature BMpDCs was performed in the same way as the chemotaxis assay. Mature BMpDCs were suspended in modified RPMI 1640 medium containing 1% FBS and then incubated with byakkokaninjinto for 3 hours at 37°C. Subsequently, BMpDCs were stained with Via-Probe (Becton Dickinson, San Jose, CA, USA), anti-mouse mPDCA-1-APC (Miltenyi Biotec, Bergisch Gladbach, Germany) and anti-mouse CD11c-FITC (BD Biosciences, San Jose, CA, USA). To analyze the expression level of CCR7 on BMpDCs, BMpDCs were stained with anti-mouse CD197 (CCR7)-PE-Cy7 (eBioscience).

2.6 Flow cytometry and antibodies

Mature BMpDCs were suspended in FACS buffer (0.01 M phosphate-buffered saline (PBS) containing 1% BSA and 0.2% NaN_3) and stained with the following antibodies: anti-mouse mPDCA-1-APC (Miltenyi Biotec), anti-mouse CD11c-FITC (BD Biosciences), anti-mouse MHC class II-PE (eBioscience, San Diego, CA, USA), and anti-mouse CD197 (CCR7)-PE-Cy7 (eBioscience). Cell proportions were analyzed with a BD FACSCantoII flow cytometer (BD Biosciences).

2.7 DNFB-induced allergic contact dermatitis mouse model

Male BALB/c mice (6 weeks old) were administered intraperitoneally 10 μg DNP-OVA with 1 mg aluminum hydrogel on day 0. Byakkokaninjinto (0.5 g/kg or 1.0 g/kg) in 0.5% methylcellulose was administered orally on day 13. Skin lesions were induced by painting the ear with 0.1% DNFB in ethanol on day 14. Ear swelling induced with DNFB was evaluated by measuring ear thickness at 1 hour, 2 days and 7 days after DNFB painting.

2.8 Statistical analysis

The results are expressed as the mean \pm SEM. Significant differences among groups were evaluated by one-way analysis of variance (ANOVA) followed by Dunnett's test for multiple comparisons, and significant differences between groups were evaluated with an unpaired Student's t-test. A *P* value less than 0.05 was considered significant.

3. Results

3.1 Effects of Kampo formulas on the migration of BMpDCs

To identify drugs that regulate DC migration, 86 Kampo formula extracts were screened using an EZ-TAXIScan chemotaxis assay. The chemotactic responses of BMpDCs were observed following stimulation with the CCR7 ligand CCL21, and BMpDCs migrated toward the more concentrated side of the CCL21 concentration gradient (Figure 2A). Among the 86 Kampo formula extracts, byakkokaninjinto significantly suppressed the migration of BMpDCs from 25 minutes to 30 minutes at each time point (Figure 2A and B, $p < 0.05$), and shimotsuto significantly accelerated the migration of BMpDCs (Figure 3). The other 84 Kampo formula extracts did not show significant effects on BMpDC migration. Compared with the vehicle, byakkokaninjinto obviously decreased the number of migrated BMpDCs during 30 minutes (Figure 2B). In addition, we also performed a detailed analysis of the inhibitory effect of byakkokaninjinto by analyzing the velocity and directionality of BMpDC migration (Figure 2C). The velocity of the migration of BMpDCs treated with byakkokaninjinto ($0.08 \pm 0.00 \mu\text{m}/\text{sec}$) was significantly slower than that of BMpDCs treated with the vehicle ($0.11 \pm 0.00 \mu\text{m}/\text{sec}$) (Figure 2C, $p < 0.05$). In addition, the direction of BMpDC migration was calculated as the radian of cells migrating toward the more concentrated side of the concentration gradient of CCL21. The directionality of the migration of BMpDCs treated with byakkokaninjinto ($0.48 \pm 0.03 \text{ rad}$) was significantly lower than that of those treated with the vehicle ($0.67 \pm 0.03 \text{ rad}$) (Figure 2C, $p < 0.05$). These results indicate that byakkokaninjinto has a notable inhibitory effect on pDC migration.

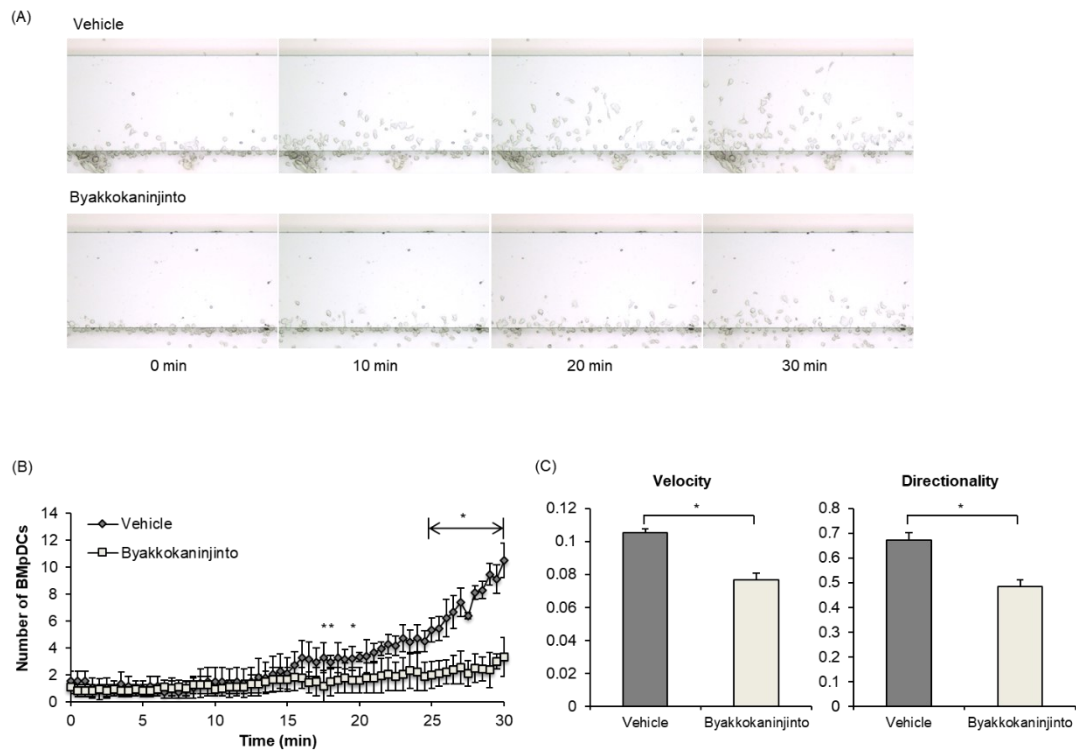


Figure 2. The effects of byakkokaninjinto on the migration of BMpDCs. Chemotactic responses were induced in BMpDCs by stimulation with the CCR7 ligand CCL21. Time-lapse images of the migration of BMpDCs treated with byakkokaninjinto (0.1 mg/mL) or the vehicle were recorded in an EZ-TAXIScan chemotaxis assay (A). The number of byakkokaninjinto-treated BMpDCs that migrated during 30 minutes is indicated by the line graph (B). Data are expressed as the mean \pm SE (* $p < 0.05$, vs the vehicle; $n = 3$). The effects of byakkokaninjinto on the velocity and directionality of BMpDC migration are represented by the bar chart (C). Data are expressed as the mean \pm SE (* $p < 0.05$, vs the vehicle; $n = 3$).

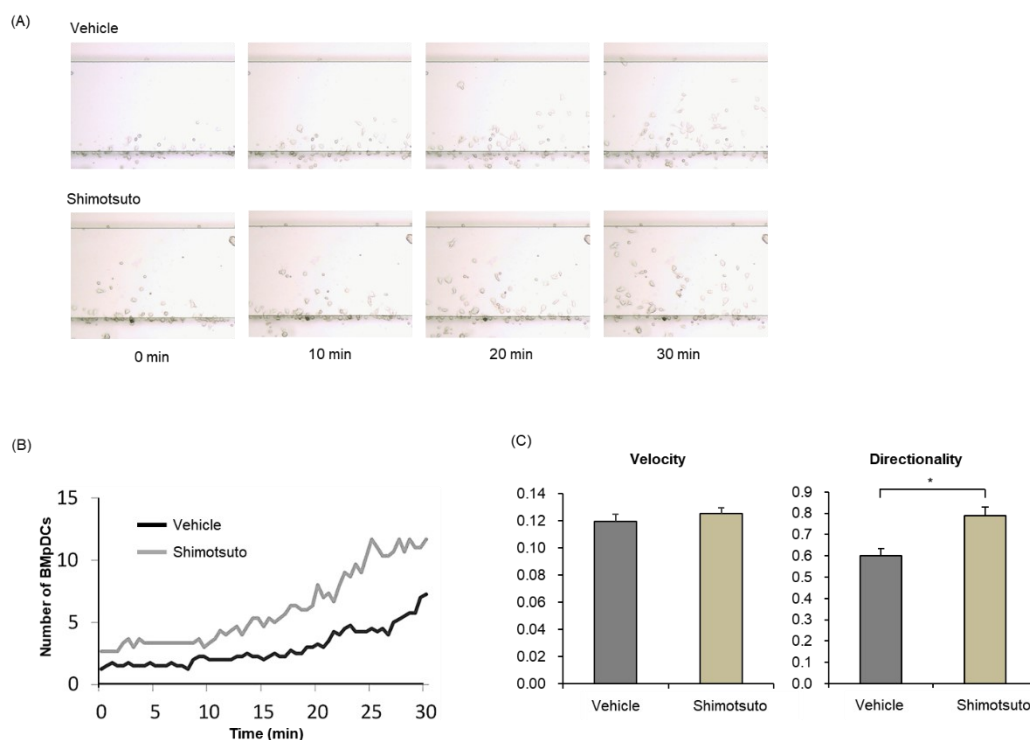


Figure 3. The effects of shimotsuto on the migration of BMpDCs. Chemotactic responses were induced in BMpDCs by stimulation with the CCR7 ligand CCL21. Time-lapse images of the migration of BMpDCs treated with shimotsuto (0.1 mg/mL) or the vehicle were recorded in an EZ-TAXIScan chemotaxis assay (A). The typical data for the number of shimotsuto-treated BMpDCs that migrated during 30 minutes is indicated by the line graph (B). The effects of shimotsuto on the velocity and directionality of BMpDC migration are represented by the bar chart (C). Data are expressed as the mean \pm SE (* $p < 0.05$, vs the vehicle; $n = 3$).

3.2 Viability assay with BMpDCs treated with byakkokaninjinto

To verify that the inhibitory effect of byakkokaninjinto on BMpDC migration is not due to toxic side effects, we examined the viability of BMpDCs treated with byakkokaninjinto. BMpDCs treated with byakkokaninjinto or the vehicle were stained with Via-Probe, an anti-CD11c antibody and an anti-mPDCA-1 antibody. Dead BMpDCs ($CD11c^{int}$ mPDCA-1⁺ Via-Probe⁺) were detected by flow cytometry. The proportion of dead BMpDCs following vehicle treatment was $4.3 \pm 0.5\%$, and the proportion following byakkokaninjinto treatment was $3.6 \pm 0.2\%$ (Figure 4). Thus, byakkokaninjinto has no toxic side effects on BMpDCs.

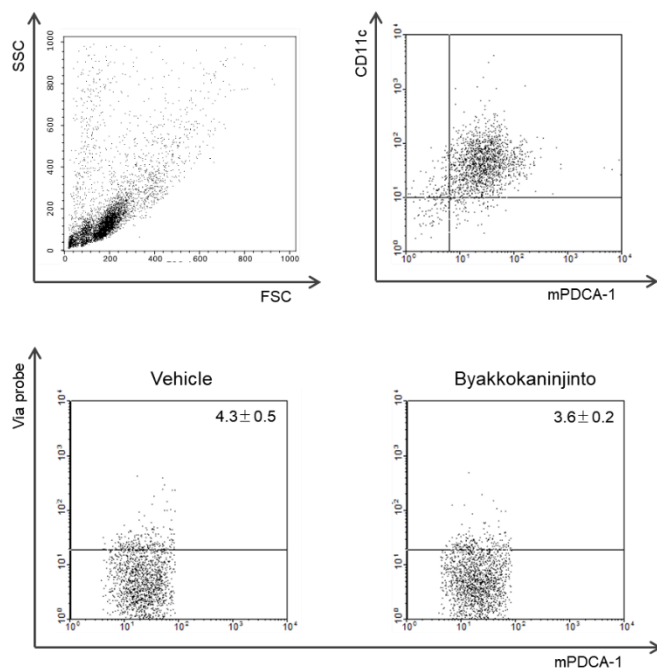


Figure 4. The detection of cell death caused by byakkokaninjinto. The toxicity of byakkokaninjinto to BMpDCs was detected by flow cytometry. The percentage of dead BMpDCs (CD11c^{int} mPDCA-1⁺ Via-Probe⁺) was determined. Dot plots show representative data. Data are expressed as the mean \pm SE (n = 3).

3.3 Expression level of CCR7 on BMpDCs treated with byakkokaninjinto

The maturation of BMpDCs is accompanied by the upregulation of CCR7 expression, which leads to increased sensitivity to CCL21. Thus, the expression level of CCR7 on BMpDCs was analyzed by flow cytometry. The expression level of CCR7 on BMpDCs treated with byakkokaninjinto was comparable to that on BMpDCs treated with the vehicle (Figure 5), indicating that byakkokaninjinto has no effect on the expression of CCR7 on BMpDCs.

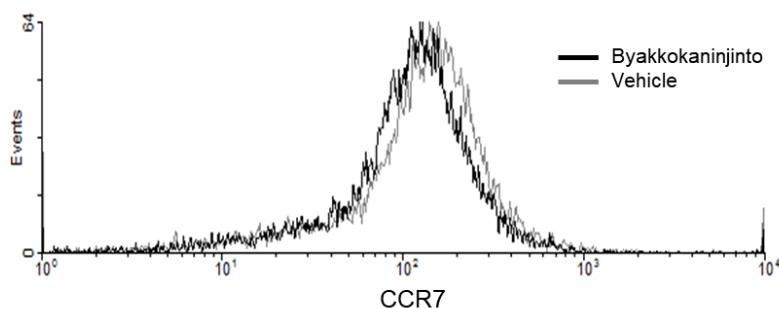


Figure 5. The effects of byakkokaninjinto on CCR7 expression in BMpDCs. The expression of CCR7 on BMpDCs treated with 0.1 mg/mL byakkokaninjinto (black line) or the vehicle (gray

line) was detected by flow cytometry. Representative CCR7 expression data are represented by the line graph.

3.4 Effects of the components of byakkokaninjinto on BMpDC migration

Byakkokaninjinto is composed of *Gypsum Fibrosum*, *Ginseng Radix*, *Glycyrrhizae Radix*, *Anemarrhenae Rhizoma* and *Oryzae Fructus*. We examined the effect of each component extract on the migration of BMpDCs. BMpDCs were treated with one component of byakkokaninjinto (0.02 mg/mL, 0.05 mg/mL, or 0.1 mg/mL) or the vehicle for 3 hours. The number of BMpDCs chemotaxing towards the CCL21 concentration gradient following treatment with each component extract or vehicle was increased during 30 minutes. At the dose of 0.1 mg/mL, the number of migrated BMpDCs was obviously decreased by the treatment of *Gypsum Fibrosum*, *Ginseng Radix* and *Glycyrrhizae Radix* (Figure 6) There was no effect of *Anemarrhenae Rhizoma* and *Oryzae Fructus* on the number of migrated BMpDCs (Figure 6A). To confirm the effect of each component, the value of the velocity and the directionality of BMpDC migration under treatment of each component of byakkokaninjinto (0.02 mg/mL, 0.05 mg/mL, or 0.1 mg/mL) were examined. The velocity of BMpDC migration in the vehicle treatment group was 0.12 ± 0.00 $\mu\text{m}/\text{sec}$. Treatment with *Gypsum Fibrosum* (0.10 mg/mL) or *Ginseng Radix* (0.10 mg/mL) for 3 hours significantly reduced the velocity of BMpDC migration by 24.7% and 13.3%, respectively (Figure 6B, $p < 0.05$). In addition, the inhibitory effect of *Gypsum Fibrosum* on the velocity of BMpDC migration was dose dependent (Figure 6B).

The directionality of BMpDC migration in the vehicle group was 0.62 ± 0.04 rad. Treatment with *Gypsum Fibrosum* (0.10 mg/mL) significantly reduced the directionality of BMpDC migration by 37.5% (Figure 6C, $p < 0.05$), and the inhibitory effect of *Gypsum Fibrosum* on the directionality of BMpDC migration was dose dependent (Figure 6C). Therefore, these results indicate that *Gypsum Fibrosum* is an active component in the inhibitory effect of byakkokaninjinto on BMpDC migration.

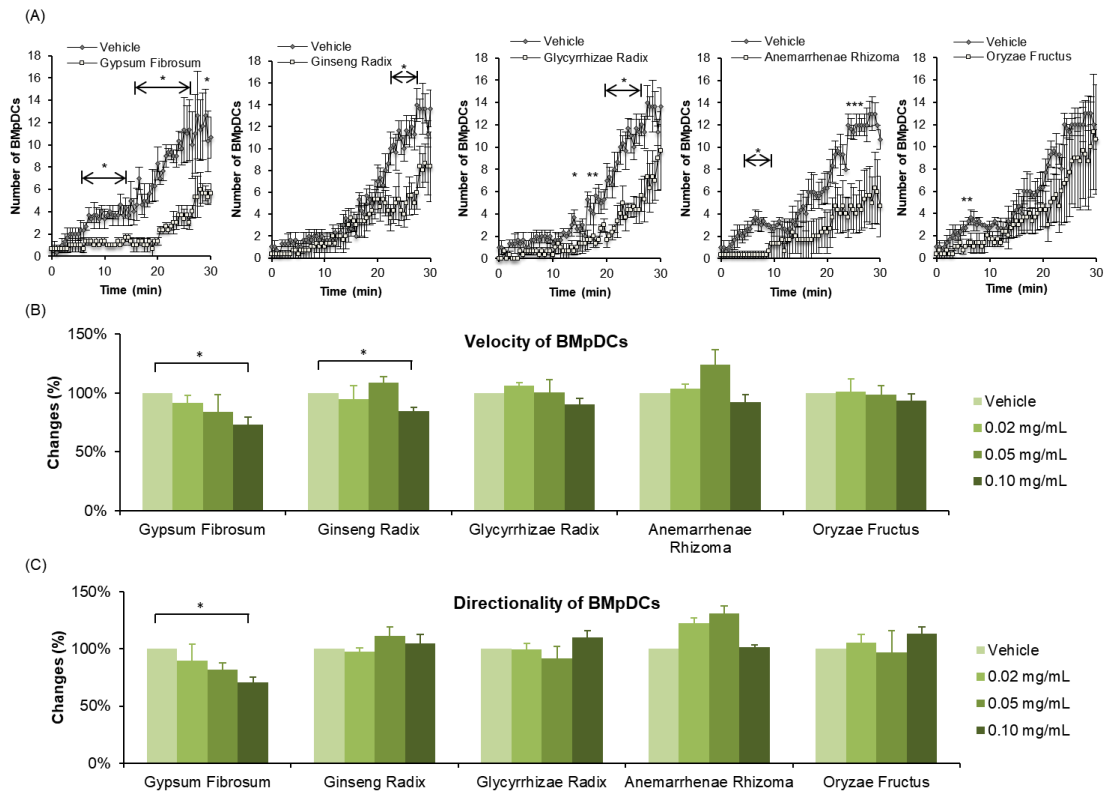


Figure 6. The effects of byakkokaninjinto components on BMpDC migration. The number of migrated BMpDCs with treatment of each component (0.10 mg/mL) is indicated by the line graph (A). Data are expressed as the mean \pm SE (* $p < 0.05$, vs the vehicle; $n = 3$). The effects of each component of byakkokaninjinto at doses of 0.02 mg/mL, 0.05 mg/mL and 0.10 mg/mL on the velocity and directionality of BMpDC migration were measured by an EZ-TAXIScan chemotaxis assay. The bar chart shows the change rates of BMpDC migration velocity (B) and directionality (C) induced by treatment at each dose versus treatment with the vehicle. Data are expressed as the mean \pm SE (* $p < 0.05$, vs the vehicle; $n = 3$).

3.5 Effects of byakkokaninjinto on an DNFB-induced allergic contact dermatitis model

There are several inconsistent reports on the role of pDCs in the onset of dermatitis, which remains controversial. In the present study, we used a murine model of DNFB-induced allergic contact dermatitis that exhibits allergic contact dermatitis symptoms (ear swelling) with an immediate-phase response (IPR) at 1 hour, a late-phase response (LPR) at 2 days and a very-late-phase response (vLPR) at 6-10 days after DNFB administration (Itoh et al., 2009). Oral administration of byakkokaninjinto exhibited a tendency to suppress ear swelling during the IPR in a dose-dependent manner and then markedly prevented ear swelling during the LPR. However, byakkokaninjinto had no effect on ear swelling during the vLPR (Figure 7).

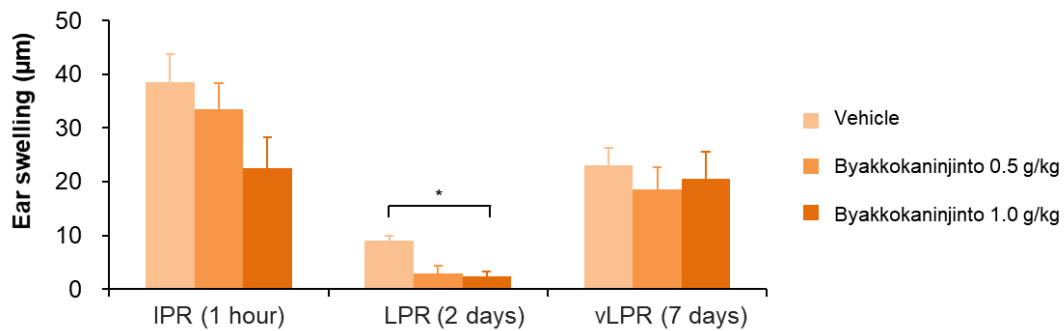


Figure 7. The effects of byakkokaninjinto on DNFB-induced allergic contact dermatitis model. Byakkokaninjinto (0.5 g/kg or 1.0 g/kg) was given by oral administration to DNFB-induced allergic contact dermatitis model mice 1 day before DNFB sensitization. Ear swelling was monitored during the IPR (1 hour), LPR (2 days) and vLPR (7 days). The bar chart shows the ear thicknesses of mice treated with 0.5 g/kg or 1.0 g/kg byakkokaninjinto or the vehicle during the IPR, LPR and vLPR. Data are expressed as the mean \pm SE (* $p < 0.05$, vs the vehicle; $n = 5$).

4. Discussion

The present study revealed that byakkokaninjinto inhibits the migration of BMpDCs and that *Gypsum Fibrosum*, one of the components of byakkokaninjinto, has a potent inhibitory effect on BMpDC migration. Furthermore, it suggested that pDCs are involved in the onset of allergic contact dermatitis and that byakkokaninjinto suppresses the onset of allergic contact dermatitis by inhibiting pDC migration.

Byakkokaninjinto significantly inhibited the migration of BMpDCs without inducing cellular toxicity in BMpDCs or enhancing the expression of CCR7 on BMpDCs. These results indicated that the inhibitory effect of byakkokaninjinto on BMpDC migration was caused by the inhibition of CCR7 signaling cascades. The activation of the CCR7 signaling pathway elicited by CCL21 is related to trimeric GTP-binding proteins, Jak family proteins and Rho family proteins (Hauser and Legler, 2016). Rho, Rac and Cdc42, members of the Rho family of proteins, play crucial roles in DC migration (Ridley, 2015). In particular, it has been reported that BMpDCs derived from DOCK2-deficient mice hardly migrate toward the more concentrated side of a concentration gradient of CCL21 (Gotoh et al., 2008). Furthermore, RAC1 activation induced by CCL21 is almost abolished in DOCK2-deficient BMpDCs, although wild-type BMpDCs exhibit RAC1 activation (Gotoh et al., 2008). Accordingly, Rho family proteins, including RAC1-DOCK2, are essential in the migration of pDCs. Thus, it is assumed that byakkokaninjinto inhibits the signaling pathway of RAC1-DOCK2 to suppress pDC migration.

We investigated the effect of each component of byakkokaninjinto on BMpDC migration and demonstrated that *Gypsum Fibrosum* and *Ginseng Radix* have inhibitory effects on BMpDC migration. However, the effective doses (0.1 mg/mL) of *Gypsum Fibrosum* and *Ginseng Radix* were higher than the amount contained in byakkokaninjinto. Moreover, makyokansekito, which contains the same dose of *Gypsum Fibrosum* as byakkokaninjinto, showed no inhibitory effect on the migration of pDCs. In addition, a high dose of *Ginseng Radix* is contained in many Kampo formulas, such as daikenchuto and shikunshito. However, these Kampo formulas had no effect on the migration of pDCs. In general, pharmacological effects of Kampo formulas containing many herbal components are characterized by synergistic effects or additive effects of multiple herbal components, and thus are complicated (Zhou et al., 2016). These results suggest that the inhibitory effect of byakkokaninjinto on pDC migration is attributed to the synergistic effects of multiple herbal medicines in byakkokaninjinto, including *Gypsum Fibrosum* and *Ginseng Radix*.

It has been reported that pDCs highly infiltrate the lesional skin of patients with contact dermatitis (Garzorz-Stark et al., 2018, Wollenberg et al., 2002) or atopic dermatitis (Lebre et al., 2008, Hashizume et al., 2005), whereas the proportion of CD304⁺ BDCA4⁺ pDCs does not change in the peripheral blood mononuclear cell population (Lebre et al., 2008). Conversely, BDCA2⁺ pDCs are not recruited into the lesional skin of patients with atopic dermatitis (Vittorakis et al.,

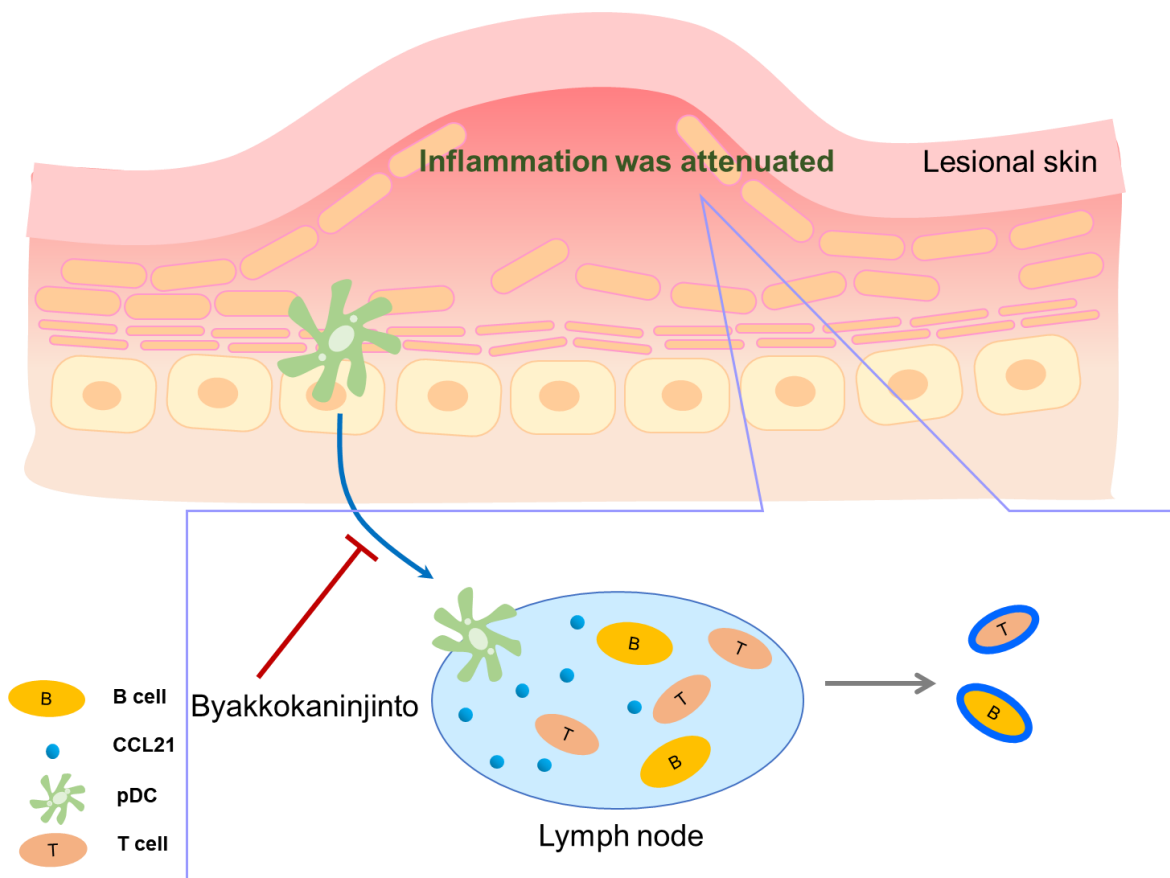
2014, Wollenberg et al., 2002). Even in patients with atopic dermatitis, the proportion of CD123⁺ pDCs in the blood is higher than that in normal subjects (Hashizume et al., 2005). In ovalbumin-induced dermatitis model mice, Wang et al. reported that the infiltration of pDCs was increased in the inflamed skin and that treatment with the immunostimulatory sequence CpG reduced pDC infiltration and skin inflammation (Wang et al., 2008), suggesting that pDCs play pivotal roles in the onset and development of dermatitis. However, in DNFB-induced dermatitis model similar to our used model, it is also reported that pDCs prevent the ear swelling response by inducing systemic tolerance (Goubier et al., 2008, Dubois et al., 2009). Accordingly, the role and distribution of pDCs in dermatitis remain poorly understood. In this study, we demonstrated that byakkokaninjinto had an inhibitory effect on pDC migration and suppressed the initiation of DNFB-induced allergic contact dermatitis. Therefore, the migration of pDCs to inflamed sites or the lymph nodes contributes to the onset and development of allergic contact dermatitis.

pDCs are well known for their capacity to present antigens (Reizis, 2019, Suzuki et al., 2018, Villadangos and Young, 2008) and secrete type-I IFN in response to viral infections (Reizis, 2019, Swiecki and Colonna, 2015). Acquired immune responses are carried out through pDC migration to inflamed sites and mature pDC migration from the inflamed sites to the lymph nodes, where they perform antigen presentation. Consequently, the inhibition of pDC migration by byakkokaninjinto may have a beneficial effect on allergic dermatitis via the suppression of immune responses.

5. Conclusion

In conclusions, CCL21 induced pDCs migrate into LNs to activate T cells or B cells. Byakkokaninjinto exerted an inhibitory effect on migration of pDCs into LNs so that activation of T cells or B cells was inhibited. And this process prevented the progression of allergic contact dermatitis. So pDC migration may be involved in the onset of allergic contact dermatitis. And byakkokaninjinto is anticipated to be a therapeutic agent for disorders related to the pDC migration (Graphic conclusion 1).

Graphic conclusion 1



6. Tables

Table 1. Components and their percentages in byakkokaninjinto

Components	Full botanical plant names	Percentage (%)
<i>Gypsum Fibrosum</i>	Natural hydrous calcium sulfate	48
<i>Ginseng Radix</i>	<i>Panax ginseng</i> C. A. Meyer	5
<i>Glycyrrhizae Radix</i>	<i>Glycyrrhiza uralensis</i> Fischer	6
<i>Anemarrhenae Rhizoma</i>	<i>Anemarrhena asphodeloides</i> Bunge	16
<i>Oryzae Fructus</i>	<i>Oryza sativa</i> Linne	25

Table 2. Components of 86 kinds of Kampo prescriptions

No	Kampo prescriptions	Components
1.	Anchusan	<i>Cinnamomi Cortex, Corydalis Tuber, Ostreae Testa, Foeniculi Fructus, Amomi Semen, Glycyrrhizae Radix, Alpiniae Officinari Rhizoma</i>
2.	Inchinkoto	<i>Artemisiae Capillaris Flos, Gardeniae Fructus, Rhei Rhizoma</i>
3.	Eppikajutsuto	<i>Ephedrae Herba, Gypsum Fibrosum, Zingiberis Rhizoma, Ziziphi Fructus, Glycyrrhizae Radix, Atractylodis Rhizoma</i>
4.	Orengedokuto	<i>Ephedrae Herba, Gypsum Fibrosum, Zingiberis Rhizoma, Ziziphi Fructus, Glycyrrhizae Radix, Atractylodis Rhizoma</i>
5.	Kakkonto	<i>Puerariae Radix, Ephedrae Herba, Zingiberis Rhizoma, Ziziphi Fructus, Cinnamomi Cortex, Paeoniae Radix, Glycyrrhizae Radix</i>
6.	Kamiuntanto	<i>Pinelliae Tuber, Poria Sclerotium, Bambusae Caulis, Citri Unshiu Pericarpium, Ziziphi Semen, Glycyrrhizae Radix, Ziziphi Fructus, Aurantii Fructus Immaturus, Polygalae Radix, Scrophulariae Radix, Ginseng Radix, Rehmanniae Radix, Zingiberis Rhizoma</i>
7.	Kamikihito	<i>Astragali Radix, Angelicae Acutilobae Radix, Gardeniae Fructus, Ginseng Radix, Atractylodis Rhizoma, Poria Sclerotium, Ziziphi Semen, Longan Arillus, Bupleuri Radix, Polygalae Radix, Ziziphi Fructus, Glycyrrhizae Radix, Zingiberis Rhizoma, Saussureae Radix</i>
8.	Kamishoyosan	<i>Bupleuri Radix, Paeoniae Radix, Angelicae Acutilobae Radix, Poria Sclerotium, Gardeniae Fructus, Moutan Cortex, Glycyrrhizae Radix, Zingiberis Rhizoma, Menthae Herba, Atractylodis Rhizoma</i>
9.	Kihito	<i>Astragali Radix, Angelicae Acutilobae Radix, Ginseng Radix, Atractylodis Rhizoma, Poria Sclerotium, Ziziphi Semen, Longan Arillus, Polygalae Radix, Ziziphi Fructus, Glycyrrhizae Radix, Zingiberis Rhizoma, Saussureae</i>

	<i>Radix</i>
10. Keishito	<i>Cinnamomi Cortex, Paeoniae Radix, Zingiberis Rhizoma, Ziziphi Fructus, Glycyrrhizae Radix</i>
11. Keishibukuryogan	<i>Cinnamomi Cortex, Poria Sclerotium, Paeoniae Radix, Persicae Semen, Moutan Cortex</i>
12. Goshuyuto	<i>Euodiae Fructus, Ziziphi Fructus, Zingiberis Rhizoma, Ginseng Radix</i>
13. Goreisan	<i>Alismatis Tuber, Poria Sclerotium, Polyporus, Atractylodis Rhizoma, Cinnamomi Cortex</i>
14. Saikokaryukotsuboreito	<i>Bupleuri Radix, Pinelliae Tuber, Poria Sclerotium, Cinnamomi Cortex, Ziziphi Fructus, Zingiberis Rhizoma, Ginseng Radix, Fossilia Osis Mastodi, Ostreae Testa, Rhei Rhizoma</i>
15. Saikokeishito	<i>Bupleuri Radix, Pinelliae Tuber, Scutellariae Radix, Glycyrrhizae Radix, Cinnamomi Cortex, Paeoniae Radix, Ziziphi Fructus, Ginseng Radix, Zingiberis Rhizoma</i>
16. San'Oshashinto	<i>Rhei Rhizoma, Scutellariae Radix, Coptidis Rhizoma</i>
17. Sansoninto	<i>Ziziphi Semen, Poria Sclerotium, Anemarrhenae Rhizoma, Cnidii Rhizoma, Glycyrrhizae Radix</i>
18. Shikunshito	<i>Ginseng Radix, Atractylodis Rhizoma, Poria Sclerotium, Glycyrrhizae Radix, Ziziphi Fructus, Zingiberis Rhizoma</i>
19. Shimotsuto	<i>Angelicae Acutilobae Radix, Paeoniae Radix, Cnidii Rhizoma, Rehmanniae Radix</i>
20. Shakuyakukanzoto	<i>Paeoniae Radix, Glycyrrhizae Radix</i>
21. Juzentaihoto	<i>Astragali Radix, Cinnamomi Cortex, Paeoniae Radix, Angelicae Acutilobae Radix, Rehmanniae Radix, Cnidii Rhizoma, Ginseng Radix, Poria Sclerotium, Atractylodis Rhizoma, Glycyrrhizae Radix</i>
22. Shosaikoto	<i>Bupleuri Radix, Pinelliae Tuber, Scutellariae Radix, Ginseng Radix, Ziziphi Fructus, Glycyrrhizae Radix, Zingiberis Rhizoma</i>
23. Shoseiryuto	<i>Ephedrae Herba, Cinnamomi Cortex, Paeoniae Radix, Asiasari Radix, Zingiberis Processum Rhizoma,</i>

	<i>Schisandrae Fructus, Pinelliae Tuber, Glycyrrhizae Radix</i>
24. Shimbuto	<i>Poria Sclerotium, Paeoniae Radix, Atractylodis Rhizoma, Zingiberis Rhizoma, Aconiti Radix</i>
25. Daikenchuto	<i>Ginseng Radix, Zingiberis Processum Rhizoma, Zanthoxyli Piperiti Pericarpium, Koi</i>
26. Daisaikoto	<i>Bupleuri Radix, Pinelliae Tuber, Scutellariae Radix, Paeoniae Radix, Ziziphi Fructus, Aurantii Fructus Immaturus, Zingiberis Rhizoma, Rhei Rhizoma</i>
27. Chotosan	<i>Gypsum Fibrosum, Uncariae Uncis cum Ramulus, Citri Unshiu Pericarpium, Pinelliae Tuber, Ophiopogonis Radix, Ophiopogonis Radix, Ophiopogonis Radix, Chrysanthemi Flos, Saposhnikoviae Radix, Glycyrrhizae Radix, Zingiberis Rhizoma</i>
28. Tokakujokito	<i>Persicae Semen, Rhei Rhizoma, Cinnamomi Cortex, Glycyrrhizae Radix, Sal Mirabilis</i>
29. Tokishakuyakusan	<i>Paeoniae Radix, Atractylodis Rhizoma, Alismatis Tuber, Poria Sclerotium, Cnidii Rhizoma, Angelicae Acutilobae Radix</i>
30. Ninjinto	<i>Ginseng Radix, Glycyrrhizae Radix, Zingiberis Processum Rhizoma, Atractylodis Rhizoma</i>
31. Bakumondoto	<i>Ophiopogonis Radix, Pinelliae Tuber, Oryzae Fructus, Ziziphi Fructus, Ginseng Radix, Glycyrrhizae Radix</i>
32. Hachimijogon (decoction)	<i>Rehmanniae Radix, Corni Fructus, Dioscoreae Rhizoma, Alismatis Tuber, Poria Sclerotium, Moutan Cortex, Cinnamomi Cortex, Aconiti Radix</i>
33. Hangekobokuto	<i>Pinelliae Tuber, Poria Sclerotium, Magnoliae Cortex, Perilla Herba, Zingiberis Rhizoma</i>
34. Hangeshashito	<i>Pinelliae Tuber, Scutellariae Radix, Glycyrrhizae Radix, Zingiberis Processum Rhizoma, Ginseng Radix, Ziziphi Fructus, Coptidis Rhizoma</i>
35. Byakkokaninjinto	<i>Gypsum Fibrosum, Anemarrhenae Rhizoma, Oryzae Fructus, Glycyrrhizae Radix, Ginseng Radix</i>
36. Boiogito	<i>Sinomeni Caulis et Rhizoma, Astragali Radix, Atractylodis Rhizoma, Ziziphi Fructus, Zingiberis</i>

	<i>Rhizoma, Glycyrrhizae Radix</i>
37. Bofutsushosan	<i>Rhei Rhizoma, Sal Mirabilis, Ephedrae Herba, Saposhnikoviae Radix, Schizonepetae Spica, Menthae Herba, Kasseki, Gardeniae Fructus, Gypsum Fibrosum, Platycodi Radix, Forsythiae Fructus, Scutellariae Radix, Cnidii Rhizoma, Angelicae Acutilobae Radix, Paeoniae Radix, Atractylodis Rhizoma, Glycyrrhizae Radix, Zingiberis Rhizoma</i>
38. Hochuekkito	<i>Ginseng Radix, Atractylodis Rhizoma, Astragali Radix, Angelicae Acutilobae Radix, Bupleuri Radix, Citri Unshiu Pericarpium, Ziziphi Fructus, Zingiberis Rhizoma, Glycyrrhizae Radix, Cimicifugae Rhizoma</i>
39. Maoto	<i>Ephedrae Herba, Armeniacae Semen, Cinnamomi Cortex, Glycyrrhizae Radix</i>
40. Maobushisaishinto	<i>Aconiti Radix, Asiasari Radix, Ephedrae Herba</i>
41. Unkeito	<i>Pinelliae Tuber, Ophiopogonis Radix, Angelicae Acutilobae Radix, Paeoniae Radix, Cnidii Rhizoma, Asini Corii Collas, Moutan Cortex, Ginseng Radix, Cinnamomi Cortex, Glycyrrhizae Radix, Zingiberis Rhizoma, Euodiae Fructus</i>
42. Unseiin	<i>Angelicae Acutilobae Radix, Processi Rehmanniae Radix, Paeoniae Radix, Cnidii Rhizoma, Scutellariae Radix, Gardeniae Fructus, Coptidis Rhizoma, Phellodendri Cortex</i>
43. Ogikenchuto	<i>Cinnamomi Cortex, Zingiberis Rhizoma, Ziziphi Fructus, Astragali Radix, Paeoniae Radix, Glycyrrhizae Radix, Koi</i>
44. Kambakutaisoto	<i>Glycyrrhizae Radix, Ziziphi Fructus, Triticum Semen</i>
45. Kyukikyogaito	<i>Rehmanniae Radix, Angelicae Acutilobae Radix, Paeoniae Radix, Cnidii Rhizoma, Asini Corii Collas, Artemisiae Folium, Glycyrrhizae Radix</i>
46. Keigairengyoto	<i>Angelicae Acutilobae Radix, Paeoniae Radix, Cnidii Rhizoma, Rehmanniae Radix, Coptidis Rhizoma, Phellodendri Cortex, Scutellariae Radix, Gardeniae</i>

	<i>Fructus, Forsythiae Fructus, Saposhnikoviae Radix, Menthae Herba, Schizonepetae Spica, Glycyrrhizae Radix, Aurantii Pericarpium, Bupleuri Radix, Angelicae Dahuricae Radix, Platycodi Radix</i>
47. Keishikashakuyakuto	<i>Cinnamomi Cortex, Paeoniae Radix, Zingiberis Rhizoma, Ziziphi Fructus, Glycyrrhizae Radix</i>
48. Keishikajutsubuto	<i>Cinnamomi Cortex, Paeoniae Radix, Zingiberis Rhizoma, Ziziphi Fructus, Glycyrrhizae Radix, Atractylodis Rhizoma, Aconiti Radix</i>
49. Keishikaryukotsuboreito	<i>Cinnamomi Cortex, Paeoniae Radix, Zingiberis Rhizoma, Ziziphi Fructus, Glycyrrhizae Radix, Fossilia Osis Mastodi, Ostreae Testa</i>
50. Keishishakuyakuchimoto	<i>Ephedrae Herba, Saposhnikoviae Radix, Cinnamomi Cortex, Paeoniae Radix, Zingiberis Rhizoma, Anemarrhenae Rhizoma, Atractylodis Rhizoma, Glycyrrhizae Radix, Aconiti Radix</i>
51. Kososan	<i>Cyperii Rhizoma, Perilla Herba, Citri Unshiu Pericarpium, Glycyrrhizae Radix, Zingiberis Rhizoma</i>
52. Goshajinkigan	<i>Rehmanniae Radix, Achyranthis Radix, Cornus Fruit, Dioscoreae Rhizoma, Plantaginis Semen, Alismatis Tuber, Poria Sclerotium, Moutan Cortex, Aconiti Radix, Cinnamomi Cortex</i>
53. Goshakusan	<i>Atractylodis Rhizoma, Poria Sclerotium, Tachibana Pericarpium, Pinelliae Tuber, Magnoliae Cortex, Aurantii Fructus Immaturus, Platycodi Radix, Angelicae Dahuricae Radix, Glycyrrhizae Radix, Ephedrae Herba, Cinnamomi Cortex, Zingiberis Processum Rhizoma, Angelicae Acutilobae Radix, Paeoniae Radix, Cnidii Rhizoma</i>
54. Saikokeishikankyoto	<i>Bupleuri Radix, Cinnamomi Cortex, Scutellariae Radix, Ostreae Testa, Zingiberis Processum Rhizoma, Glycyrrhizae Radix, Trichosanthis Radix</i>
55. Saikoseikanto	<i>Bupleuri Radix, Angelicae Acutilobae Radix, Paeoniae Radix, Cnidii Rhizoma, Rehmanniae Radix, Coptidis Rhizoma, Scutellariae Radix, Phellodendri Cortex, Gardeniae Fructus, Forsythiae Fructus, Platycodi Radix,</i>

	<i>Arctii Fructus, Trichosanthis Radix, Menthae Herba, Glycyrrhizae Radix</i>
56. Saibokuto	<i>Bupleuri Radix, Pinelliae Tuber, Zingiberis Rhizoma, Scutellariae Radix, Ziziphi Fructus, Ginseng Radix, Glycyrrhizae Radix, Magnoliae Cortex, Poria Sclerotium, Perilla Herba</i>
57. Saireito	<i>Bupleuri Radix, Alismatis Tuber, Pinelliae Tuber, Scutellariae Radix, Atractylodis Rhizoma, Ziziphi Fructus, Polyporus, Ginseng Radix, Poria Sclerotium, Glycyrrhizae Radix, Cinnamomi Cortex, Zingiberis Rhizoma</i>
58. Jiinkokato	<i>Atractylodis Rhizoma, Rehmanniae Radix, Paeoniae Radix, Citri Unshiu Pericarpium, Angelicae Acutilobae Radix, Ophiopogonis Radix, Phellodendri Cortex, Glycyrrhizae Radix, Anemarrhenae Rhizoma, Asparagi Radix</i>
59. Shigyakusan (decoction)	<i>Bupleuri Radix, Paeoniae Radix, Aurantii Fructus Immaturus, Glycyrrhizae Radix</i>
60. Shakanzoto	<i>Glycyrrhizae Radix Praeparata, Zingiberis Rhizoma, Cinnamomi Cortex, Cannabidis Fructus, Ziziphi Fructus, Ginseng Radix, Rehmanniae Radix, Ophiopogonis Radix, Asini Corii Collas</i>
61. Jumihaidokuto	<i>Bupleuri Radix, Platycodi Radix, Pruni Cortex, Saposhnikoviae Radix, Poria Sclerotium, Cnidii Rhizoma, Araliae Cordatae Rhizoma, Schizonepetae Spica, Glycyrrhizae Radix, Zingiberis Rhizoma</i>
62. Shokenchuto	<i>Paeoniae Radix, Cinnamomi Cortex, Ziziphi Fructus, Glycyrrhizae Radix, Zingiberis Rhizoma, Koi</i>
63. Shofusan	<i>Angelicae Acutilobae Radix, Rehmanniae Radix, Gypsum Fibrosum, Saposhnikoviae Radix, Atractylodis Lanceae Rhizoma, Akebiae Caulis, Arctii Fructus, Anemarrhenae Rhizoma, Sesami Semen, Glycyrrhizae Radix, Cicadae Periostracum, Sophorae Radix, Schizonepetae Spica</i>
64. Seishinrenshiin	<i>Ophiopogonis Radix, Poria Sclerotium, Nelumbis Semen, Ginseng Radix, Plantaginis Semen, Scutellariae Radix,</i>

	<i>Astragali Radix, Lycii Cortex, Glycyrrhizae Radix</i>
65. Seihaito	<i>Angelicae Acutilobae Radix, Ophiopogonis Radix, Poria Sclerotium, Scutellariae Radix, Platycodi Radix, Armeniacae Semen, Gardeniae Fructus, Mori Cortex, Ziziphi Fructus, Citri Unshiu Pericarpium, Bambusae Caulis, Asparagi Radix, Fritillariae Bulbus, Glycyrrhizae Radix, Schisandrae Fructus, Zingiberis Rhizoma</i>
66. Sokeikakketsuto	<i>Paeoniae Radix, Rehmanniae Radix, Cnidii Rhizoma, Atractylodis Lanceae Rhizoma, Angelicae Acutilobae Radix, Persicae Semen, Poria Sclerotium, Achyranthis Radix, Citri Unshiu Pericarpium, Sinomeni Caulis et Rhizoma, Saposhnikoviae Radix, Gentianae Scabrae Radix, Clematidis Radix, Notopterygii Rhizoma, Glycyrrhizae Radix, Angelicae Dahuricae Radix, Zingiberis Rhizoma</i>
67. Daiokanzoto	<i>Rhei Rhizoma, Glycyrrhizae Radix</i>
68. Daiobotampito	<i>Benincasae Semen, Rhei Rhizoma, Persicae Semen, Moutan Cortex, Sal Mirabilis</i>
69. Daibofuto	<i>Angelicae Acutilobae Radix, Paeoniae Radix, Rehmanniae Radix, Astragali Radix, Saposhnikoviae Radix, Eucommiae Cortex, Atractylodis Rhizoma, Cnidii Rhizoma, Ginseng Radix, Notopterygii Rhizoma, Achyranthis Radix, Glycyrrhizae Radix, Ziziphi Fructus, Zingiberis Rhizoma, Aconiti Radix</i>
70. Chikujountanto	<i>Pinelliae Tuber, Citri Unshiu Pericarpium, Poria Sclerotium, Glycyrrhizae Radix, Aurantii Fructus Immaturus, Bambusae Caulis, Ziziphi Fructus, Bupleuri Radix, Coptidis Rhizoma, Cyperi Rhizoma, Platycodi Radix, Ophiopogonis Radix, Ginseng Radix</i>
71. Choijokito	<i>Rhei Rhizoma, Sal Mirabilis, Glycyrrhizae Radix</i>
72. Choreito	<i>Polyporus, Poria Sclerotium, Kasseki, Alismatis Tuber, Asini Corii Collas</i>

73. Tokishigyakukagoshuyusho kyoto	<i>Ziziphi Fructus, Angelicae Acutilobae Radix, Paeoniae Radix, Cinnamomi Cortex, Akebiae Caulis, Glycyrrhizae Radix, Asiasari Radix, Euodiae Fructus, Zingiberis Rhizoma</i>
74. Ninjin'Yoeito	<i>Ginseng Radix, Astragali Radix, Atractylodis Rhizoma, Poria Sclerotium, Angelicae Acutilobae Radix, Rehmanniae Radix, Cinnamomi Cortex, Paeoniae Radix, Citri Unshiu Pericarpium, Polygalae Radix, Schisandrae Fructus, Glycyrrhizae Radix</i>
75. Hangebyakujutsutemmato	<i>Pinelliae Tuber, Citri Unshiu Pericarpium, Fructus Hordei Germinatus, Poria Sclerotium, Astragali Radix, Ginseng Radix, Alismatis Tuber, Atractylodis Rhizoma, Atractylodis Lanceae Rhizoma, Gastrodiae Tuber, Massa Medicata Fermentata, Phellodendri Cortex, Zingiberis Rhizoma, Zingiberis Processum Rhizoma</i>
76. Bukuryoin	<i>Poria Sclerotium, Atractylodis Rhizoma, Ginseng Radix, Zingiberis Rhizoma, Tachibana Pericarpium, Aurantii Fructus Immaturus</i>
77. Heiisan	<i>Atractylodis Lanceae Rhizoma, Magnoliae Cortex, Citri Unshiu Pericarpium, Ziziphi Fructus, Zingiberis Processum Rhizoma, Glycyrrhizae Radix</i>
78. Makyokansekito	<i>Ephedrae Herba, Armeniacae Semen, Glycyrrhizae Radix, Gypsum Fibrosum</i>
79. Makyoyokukanto	<i>Ephedrae Herba, Armeniacae Semen, Coicis Semen, Glycyrrhizae Radix</i>
80. Yokuininto	<i>Ephedrae Herba, Angelicae Acutilobae Radix, Atractylodis Rhizoma, Coicis Semen, Cinnamomi Cortex, Paeoniae Radix, Glycyrrhizae Radix</i>
81. Yokukansan	<i>Atractylodis Rhizoma, Poria Sclerotium, Angelicae Acutilobae Radix, Cnidii Rhizoma, Uncariae Uncis cum Ramulus, Bupleuri Radix, Glycyrrhizae Radix</i>
82. Rikkunshito	<i>Ginseng Radix, Atractylodis Rhizoma, Poria Sclerotium, Glycyrrhizae Radix, Citri Unshiu Pericarpium, Pinelliae Tuber, Ziziphi Fructus, Zingiberis Rhizoma</i>

83. Ryutanshakanto	<i>Gentianae Scabrae Radix, Angelicae Acutilobae Radix, Rehmanniae Radix, Alismatis Tuber, Akebiae Caulis, Plantaginis Semen, Scutellariae Radix, Gardeniae Fructus, Glycyrrhizae Radix</i>
84. Ryokyojutsukanto	<i>Poria Sclerotium, Atractylodis Rhizoma, Zingiberis Processum Rhizoma, Glycyrrhizae Radix</i>
85. Ryokeijutsukanto	<i>Poria Sclerotium, Cinnamomi Cortex, Atractylodis Rhizoma, Glycyrrhizae Radix</i>
86. Rokumigan (decoction)	<i>Rehmanniae Radix, Corni Fructus, Dioscoreae Rhizoma, Alismatis Tuber, Poria Sclerotium, Moutan Cortex, Cinnamomi Cortex, Aconiti Radix, Alismatis Tuber, Poria Sclerotium, Moutan Cortex</i>

Chapter 2

Suppression of plasmacytoid dendritic cell migration to colonic isolated lymphoid follicles abrogates the development of colitis

1. Introduction

Dendritic cells (DCs) can initiate immune responses by migrating to tissues when they are needed (Audiger et al., 2017). DCs are mainly divided into 2 subtypes: conventional DCs (cDCs) and plasmacytoid DCs (pDCs). pDCs are known to perform massive type-I interferon (IFN) secretion in the context of viral infection to induce antiviral responses. In addition, pDC participate in the activation of adaptive immune cells (McKenna et al., 2005). Recent studies on the pathophysiological role of pDCs have revealed the importance of pDCs in the pathology of immune diseases. pDCs have been reported to be involved in the pathogenesis of autoimmune diseases, such as systemic sclerosis (Ye, Ricard et al., 2020) and systemic lupus erythematosus (SLE) (Ye, Gaugler et al., 2020). On the opposite, pDCs are capable of exerting regulatory functions to induce regulatory FoxP3⁺ CD4⁺ T cells in a tolerogenic microenvironment (Bonnetfooy et al., 2011). Thus, pDCs play pivotal roles in protecting immune responses to pathogenic foreign antigens and immune tolerance (Uto et al., 2018). During these immune processes, pDCs are required to migrate to organs and tissues to exert their functions. C-C chemokine receptor type 7 (CCR7) expressed on mature pDCs guides pDCs into the lymph nodes (LNs) or inflamed tissues via its ligand chemokine (C-C motif) ligand 21 (CCL21) (Lv et al., 2018).

Recently, it was found that pDCs are committed to the onset of inflammatory bowel disease (IBD). Numerous pDCs infiltrate the colonic mucosa of IBD patients (Smrekar et al., 2018, Baumgart et al., 2011). In addition, it has been reported that pDCs are highly enriched in the inflamed colon of ulcerative colitis (UC) and Crohn's disease patients, and this enrichment correlates with disease severity (Liu, Dasgupta et al., 2019). Furthermore, Mitsialis V et al. have reported that pDCs are increased in the peripheral blood mononuclear cells and colonic mucosa of IBD patients using single-cell analysis by mass cytometry methods (Mitsialis et al., 2020). However, there is also a report that pDCs are decreased in the peripheral blood of UC patients (Baird et al., 2016). In a murine dextran sulfate sodium (DSS)-induced colitis, the population of pDCs is increased in the mouse colon (Liu, Dasgupta et al., 2019, Arimura et al., 2017) and Arimura K et al. have demonstrated that the depletion of pDCs suppresses inflammation in the colon of DSS-induced colitis mice (Arimura et al., 2017). On the other hand, the depletion of pDCs impairs gut barrier function and caused heavy colitis in a *Citrobacter rodentium*-induced colitis model (Pöysti et al., 2021). Furthermore, ablating type-I IFN signaling in Wiskott-Aldrich syndrome protein (WASp) null mice rescues colitis in a WAS disease model (Prete et al., 2013), while Sawai et al. reported that pDCs do not have a major role in the pathology of colitis caused

by deficiency in WASp or interleukin (IL)-10 (Sawai et al., 2018). Therefore, these contradictory reports suggest that pDCs perform multiple functions in the intestine. Moreover, it is reported that the ability of pDCs in the peyer's patch of the small intestine is lower levels of type-I IFN production than that of pDCs in spleen (Contractor et al., 2007). Peyer's patch pDCs as a specific phenotype of pDCs has regulatory functions (Li et al., 2011). Taking together, pDC in the gastrointestinal tract is distinct from pDCs in other organ and tissue and play both pro-inflammatory responses and regulatory responses. Furthermore, the previous studies show that immature pDCs express chemokine receptor CCR9 and primarily migrate into the small intestine, but not colon during gut inflammation (Wendland et al., 2007, Mizuno et al., 2012), while CCR7 allow mature pDCs to migrate into T cell areas of the gut-associated lymphoid tissue (GALT) where they prime naive T cells and promote the differentiation of effector T cells (Seth et al., 2011). In addition, it has been reported that CCR9 or chemokine (C-C motif) ligand 25 (CCL25) knockout mice exacerbated DSS colitis and CCR9⁺ pDCs are potent inducers of regulatory T cell function and suppresses antigen-specific immune responses both *in vitro* and *in vivo* (Wurbel et al., 2014, Hadeiba et al., 2008). These previous studies raise the possibility that CCR7/CCL21 signaling is crucial for pDC migration during colonic inflammation. The pathophysiological role of pDCs in the pathology of IBD remains to be elucidated, but detailed investigation on mature pDC migration will provide new insight in designing better strategies to control IBD.

To the best of our knowledge, no drugs have been found to effectively and potently regulate pDC functions, especially pDC migration. Therefore, we utilized traditional Japanese herbal medicines as a resource for drug discovery. Traditional Japanese herbal medicines have been widely used for various immune diseases, such as rheumatoid arthritis, type 1 diabetes and IBD (Watanabe et al., 2017, Won et al., 2020). In addition, many researchers have a great interest in the effects of compounds extracted from herbal medicines on the pathological role of DCs in immune diseases (Liu et al., 2018, Aldahlawi, 2016). Recent studies have revealed that enhanced DC migration results in the aggravation of inflammatory injuries (Liu, Zhang et al., 2019).

In this study, we hypothesized that the migration of pDCs plays pivotal roles in the development and pathology of colitis. Therefore, the purpose of this study was to identify compounds that regulate the migration of pDCs and use these compounds to investigate whether the migration of pDCs is involved in the development and pathogenesis of colitis and whether inhibition of pDC migration can effectively suppress colitis.

2. Materials and methods

2.1 Mice

Male BALB/cCrSlc mice (7 weeks old) were purchased from Japan SLC (Shizuoka, Japan). Mice were allowed free access to food and water and housed in the animal facility at the University of Toyama. This study was performed in strict accordance with the recommendations in the Guide for the Care and Use of Laboratory Animals of the National Institutes of Health. The Animal Experiment Committee at the University of Toyama approved all the animal care procedures and experiments (authorization No. A2012 INM-4, A2015 INM-3 and A2018 INM-4).

2.2 Derivation and differentiation of DCs

DCs were generated from bone marrow (BM) cells isolated from the femurs and tibias of male BALB/c mice. For pDC differentiation, BMs were cultured in RPMI 1640 medium (Wako, Osaka, Japan) supplemented with 10% fetal bovine serum (FBS) (Equitech-Bio, Kerrville, TX, USA), 55 μ M 2-mercaptoethanol (Invitrogen, Carlsbad, CA, USA), 100 units/mL penicillin (Gibco, Grand Island, NY, USA), 140 μ M streptomycin (Gibco), 2 mM L-glutamine (Gibco), and 100 ng/mL Flt3 ligand (R&D Systems, Minneapolis, MN, USA) for 6 to 9 days. CpG oligodeoxynucleotides (ODN-2216, 2 μ M) (Hokkaido System Science, Hokkaido, Japan) were used to induce BM-derived pDC (BMpDC) maturation. As shown in Figure 1, $93.2 \pm 3.3\%$ of BM-derived cells using Flt3 ligand was CD11c^{int} mPDCA1⁺ (mean \pm SE, n = 4). For cDC differentiation, BM cells were cultured in RPMI 1640 medium supplemented with 10% FBS, 55 μ M 2-mercaptoethanol, 100 units/mL penicillin, 140 μ M streptomycin, 2 mM L-glutamine, and 10 ng/mL GM-CSF for 7 days. Lipopolysaccharide (LPS, 1 μ g/mL) (Sigma-Aldrich, St. Louis, MO, USA) was used to induce BM-derived cDC (BMcDC) maturation.

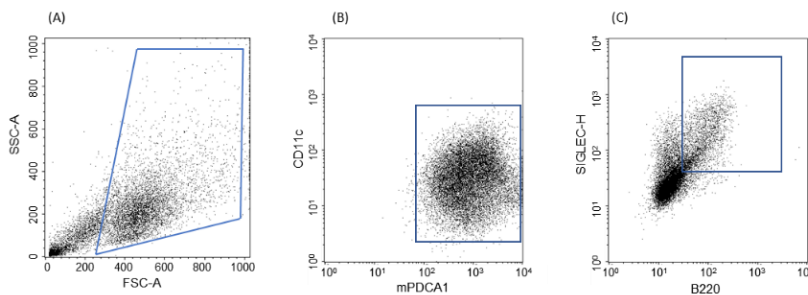


Figure 1. Frequency of CD11c^{int} mPDCA1⁺ B220⁺ SIGLEC-H⁺ BM-derived cells.

The frequency of CD11c^{int} mPDCA1⁺ B220⁺ SIGLEC-H⁺ BM-derived cells was detected by flow cytometry analysis (A-C). $93.2 \pm 3.3\%$ of BM-derived cells using Flt3 ligand was CD11c^{int} mPDCA1⁺ (B). CD11c^{int} mPDCA1⁺ BM-derived cells using Flt3 ligand contained $9.3 \pm 0.2\%$

B220⁺ SIGLEC-H⁺ CD11c^{int} mPDCA1⁺ BM-derived cells (C). Data are expressed as the mean ± SE (n = 4).

2.3 Compound preparation and treatment

Compounds were extracted from traditional Japanese herbal medicines provided by the Joint Usage/Research Center for Science-Based Natural Medicine, Institute of Natural Medicine, University of Toyama, and the Knowledge Cluster Initiative Program (Second Stage) of the Ministry of Education, Culture, Sports, Science and Technology of Japan (**Table 1**).

Matured BM-derived DCs (BMDCs) were incubated with 1 μM each compound at 37°C for 30 minutes. BMDCs were resuspended in modified RPMI 1640 medium (Sigma-Aldrich) supplemented with 1% FBS to prepare for chemotaxis studies.

2.4 Chemotaxis assay

The chemotaxis of BMDCs was measured with an EZ-TAXIScan system (GE Healthcare, Little Chalfont, UK), which allows observation of the horizontal migration of BMDCs according to the manufacturer's protocol. BMpDC chemotaxis was induced by CCL21 (R&D Systems), and BMcDC chemotaxis was induced by CXCL12 (R&D Systems). Matured BMDCs treated with each compound were suspended in modified RPMI 1640 medium containing 1% FBS. 1 μL of BMDC suspension (1×10⁶ cells/mL) was injected into one side of the chamber, and 1 μL of 250 μg/mL chemokine was injected into the contralateral chamber. A chemokine concentration gradient was formed, and BMDC migration toward the chemokine along the concentration gradient was observed. BMDC migration was automatically recorded every 30 seconds for 3600 seconds.

TAXIScan Analyzer 2 (GE Healthcare) was used to analyze the migration of BMDCs. The number of BMDCs migrating into the subject area was automatically counted every 30 seconds. The migration track of BMDCs was generated by a sequence of time-lapse imaging. The velocity and direction of BMDC migration were calculated and analyzed by a TAXIScan Analyzer 2 every 30 seconds.

2.5 Cell apoptosis

The toxicity of compounds used to treat BMDCs was detected by staining with an annexin V-FITC kit according to the manufacturer's protocol (Beckman Coulter, Brea, CA, USA). Briefly, after treatment with compounds at 37°C for 30 minutes, BMDCs were stained with 5 μL of annexin V-FITC and 2.5 μL of propidium iodide (PI) in binding buffer in the dark at room temperature for 10 minutes. Stained BMDCs were analyzed with a FACSCanto II. The

percentages of apoptotic cells (stained with annexin V only) and necrotic cells (stained with annexin V and PI) in the total cell population were used to evaluate the compound toxicity.

2.6 GTP-RAC1 detection and western blot analysis

Mature BMpDCs were treated with astragaloside IV (As-IV) or oxymatrine (Oxy) for 12 hours, followed by induction with CCL21 for 1 hour at 37°C. GTP-RAC1 in BMpDCs was extracted with the Active RAC1 Detection Kit (Cell Signaling Technology, Beverly, MA, USA) and detected by western blot analysis according to the manufacturer's protocol. The expression of GTP-RAC1 was detected with the primary anti-RAC1 mouse monoclonal antibody (mAb) (1:1000, Cell Signaling Technology) from the Active RAC1 Detection Kit and a secondary rabbit anti-mouse immunoglobulins/HRP antibody (1:1000, Dako, New Delhi, India). The bands in western blots were detected with an ImageQuant LAS4000 (GE Healthcare) and analyzed with ImageJ software.

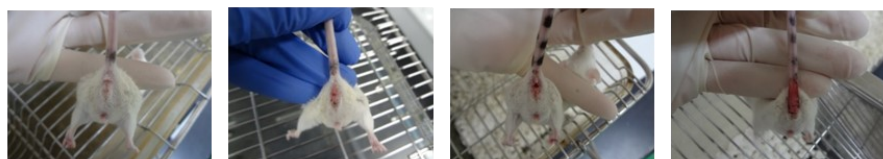
2.7 RNA extraction and microarray analysis

Mature BMpDCs sorted with a BD FACSAria SORP (BD Biosciences, San Jose, CA, USA) were used for RNA extraction. The frequency of CD11c^{int} mPDCA1⁺ BMpDCs in sorted cells is 98.5 ± 0.5 %. Mature BMpDCs were treated with As-IV or Oxy for 12 hours, followed by induction with CCL21 for 1 hour at 37°C. Then, RNA was extracted and purified with the RNeasy Mini Kit (Qiagen, Crawley, UK) according to standard procedures. Microarray analysis was performed by using the Clariom S Array Mouse (Affymetrix, Santa Clara, CA, USA). Measurement of RNA quality and analysis of the microarray were outsourced to Takara Bio Inc. (Osaka, Japan). Data were analyzed by GeneSpring (Silicon Genetics, Redwood City, CA, USA) and Ingenuity Pathway Analysis (IPA; Ingenuity Systems, Redwood City, CA, USA).

2.8 DSS-induced colitis model and compound treatments

Male BALB/c mice (8 weeks old) were given 3% DSS (MP Biomedicals, Santa Ana, CA, USA) in the drinking water for 7 days. Body weight was measured every day. The symptoms of DSS-induced colitis were monitored daily. The disease activity index (DAI) was defined as the combined scores for diarrhea and bloody stool, as previously described (Arimura et al., 2017). Diarrhea was scored as: 0 (normal), 1 (soft stool), 2 (loose stool) and 3 (diarrhea) as follows. Bloody stool was scored as: 0 (normal), 1 (fecal occult blood), 2 (visible blood) and 3 (rectal bleeding) as follows. As-IV (50 mg/kg) or Oxy (100 mg/kg) was administered by intraperitoneal (i.p.) injection each day during 3% DSS treatment. Mice were given saline injection as the control. According to all established animal welfare guidelines, the mice with the heavy body weight loss were euthanized.

Score of diarrhea and bleeding



Diarrhea	0	1	2	3
Bleeding	0	1	2	3

2.9 Isolation of cells and flow cytometry analysis

The colon was excised from model mice and washed with ice-cold saline. Lamina propria (LP) cells were isolated from the colon as previously described (Arimura et al., 2017). In brief, the colon was dissected into short segments and incubated in RPMI 1640 medium containing 2% FBS and 0.5 mM EDTA at 37°C for 20 minutes. The colon segments were flushed with ice-cold RPMI 1640 medium, and LP cells were dissociated according to an enzymatic procedure using collagenase (Wako). Discontinuous Percoll density-gradient centrifugation using 40% and 75% Percoll was performed to purify LP cells.

The mesenteric lymph nodes (MLNs) and spleen were excised from model mice. After tissue shredding, cells were dissociated according to an enzymatic procedure using collagenase (Wako).

To analyze isolated pDCs by flow cytometry, isolated pDCs were stained with an APC-conjugated anti-mPDCA1 antibody (Miltenyi Biotec), a PE-conjugated anti-CD11c antibody (BD Biosciences), a Pacific Blue-conjugated anti-CD45R/B220 antibody (BioLegend, San Diego, CA, USA), a FITC-conjugated anti-SIGLEC-H antibody (BioLegend) and a solution of 7-amino-actinomycin D (BD Via-Probe, Becton Dickinson, San Jose, CA, USA). Flow cytometry analysis was performed with a FACSCanto II (BD Biosciences).

2.10 Immunohistochemical staining

Colons were excised, fixed in 4% paraformaldehyde for 24 hours and then embedded in OCT compound. 30 µm sections cut by using a cryostat (Leica, Nussloch, Germany) were soaked in 0.3% Triton X (Sigma, Missouri, USA) for 2 hours and 2% Block Ace (DS Pharma Biomedical, Osaka, Japan) for 1 hour. Then, the colon sections were stained with the primary antibodies rat IgG anti-mouse B220 (1:200, BioLegend, San Diego, CA, USA), hamster IgG anti-mouse CD11c (1:100, BioLegend) and goat IgG anti-mouse CCL21 (1:200, R&D Systems). Alexa Fluor 488-conjugated donkey IgG anti-rat IgG (1:400, Jackson ImmunoResearch, West Grove, PA, USA), Cy3-conjugated goat IgG anti-hamster IgG (1:400, Jackson ImmunoResearch) and Alexa Fluor 647-conjugated goat anti-rat IgG (1:400, Invitrogen) were used as secondary antibodies. The

stained sections were detected with a fluorescence microscope (IX71 system; Olympus, Tokyo, Japan) and quantitated with ImageJ software.

2.11 pDC adoptive transfer model and compound treatments

Matured BMpDCs were labeled with 2.5 μ M carboxyfluorescein diacetate succinimidyl ester (CFSE) (Wako) for 10 minutes at 37°C and then transferred into male BALB/c mice via tail vein injection. The recipient mice were administered As-IV (50 mg/kg), Oxy (100 mg/kg) or saline by i.p. injection and monitored 24 hours after pDC adoptive transfer.

2.12 Statistical analysis

Data are expressed as the mean \pm standard error (SE). Statistical analyses were performed by using a paired or unpaired two-tailed Student's t-test, and multiple comparisons were analyzed with Bonferroni/Dunnett tests. A P value less than 0.05 for comparisons between the experimental conditions and the control was considered statistically significant.

3. Results

3.1 Levels of pDCs in a DSS-induced colitis model

Several clinical and basic studies have reported that pDCs are involved in the pathogenesis of human IBD and murine colitis models; however, the role of pDCs remains unclear. Therefore, to elucidate the pathophysiological role of pDCs in colitis, we first investigated whether the proportion of pDCs is altered in the mucosal immune system-related tissues of colitis mice. The subtypes and characteristics of the gut-specific pDCs that we are focusing on in this study are still not fully elucidated at present. Thus, we have defined CD11c^{int} mPDCA1⁺ DCs as pDCs (Figure 2). Administration of a 3% DSS solution significantly caused body weight losses (Figure 3A, $p < 0.05$) and increases in DAI scores (Figure 3B, $p < 0.05$). In addition, the colon length was markedly decreased in DSS-induced colitis mice (Figure 3C, $p < 0.05$). CD11c^{int} mPDCA1⁺ pDCs scarcely infiltrated the colonic LP of control mice, while the proportion of CD11c^{int} mPDCA1⁺ pDCs was markedly increased in the colonic LP cells of DSS-induced colitis mice compared with those of the control mice (Figure 3D, $p < 0.05$). Additionally, there were no significant changes in the proportion of CD11c^{int} mPDCA1⁺ pDCs in the MLN cells or splenocytes of colitis mice compared to the proportion of the corresponding population of control mice (Figure 3E and F). These results raise the possibility that pDCs in the colonic LP are involved in the development of DSS-induced colitis.

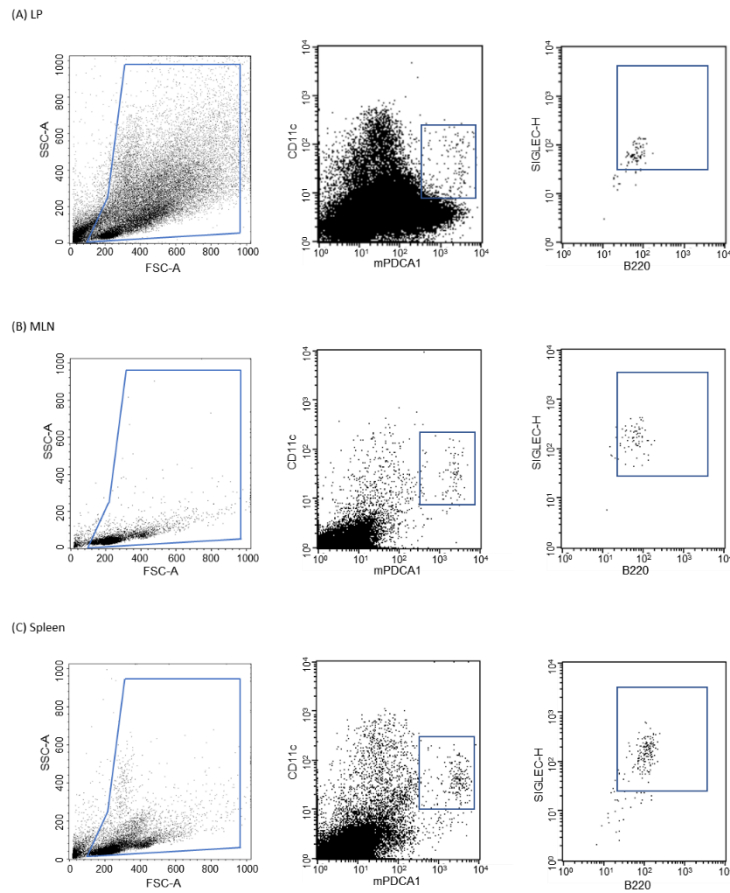


Figure 2. Frequency of CD11c^{int} mPDCA1⁺ B220⁺ SIGLEC-H⁺ pDCs.

The frequency of CD11c^{int} mPDCA1⁺ B220⁺ SIGLEC-H⁺ pDCs in CD11c^{int} mPDCA1⁺ pDCs of the colonic lamina propria (LP) (A), mesenteric lymph node (MLN) (B) and spleen (C) detected by flow cytometry analysis was $66.1 \pm 4.2\%$, $94.9 \pm 0.7\%$ and $66.0 \pm 1.8\%$, respectively. Data are expressed as the mean \pm SE ($n = 4$).

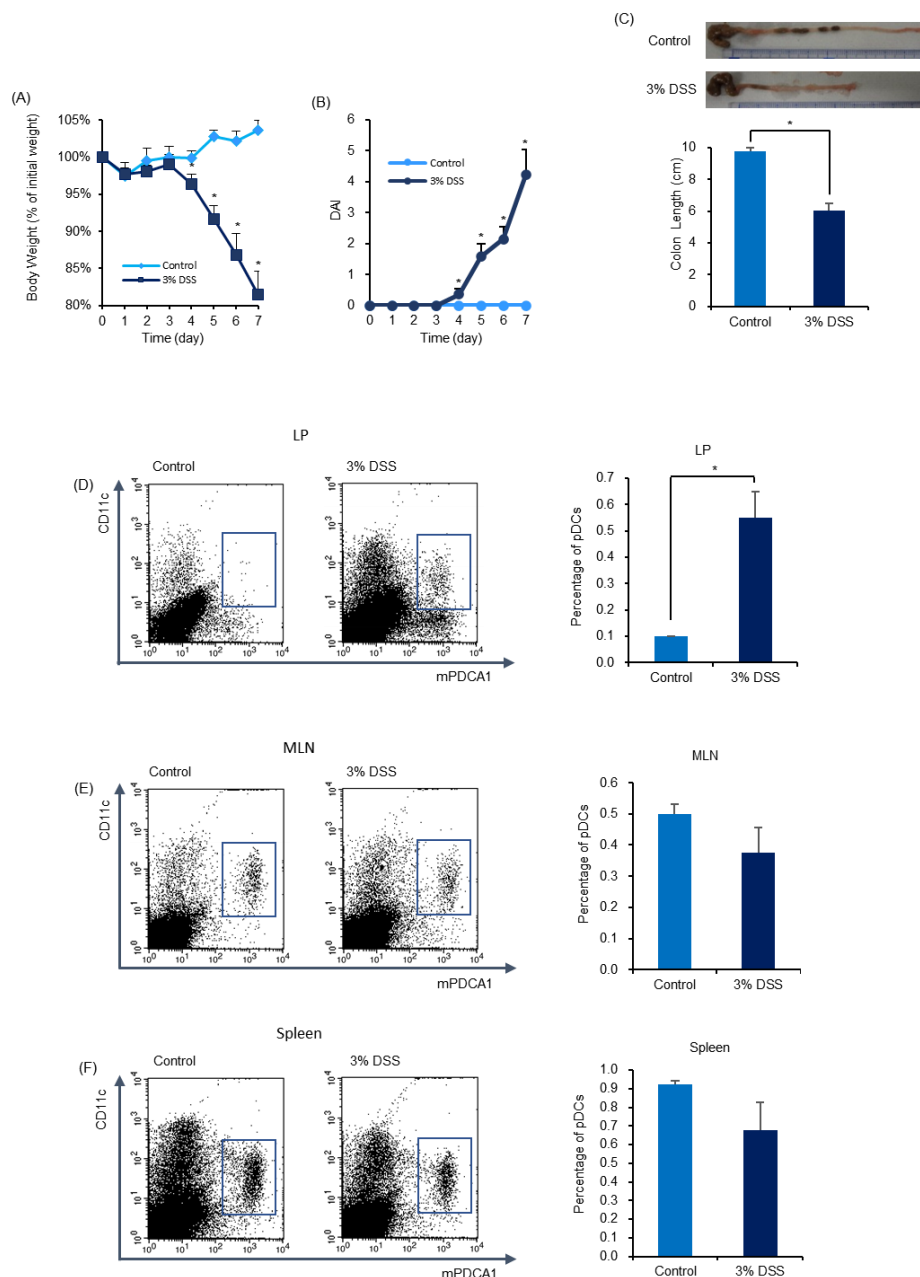


Figure 3. Levels of pDCs in a DSS-induced colitis model. The body weight changes (A), DAI scores (B) and colon length (C) were monitored for 7 days. Photos of typical changes in colon length are shown (C). Data are expressed as the mean \pm SE (* $p < 0.05$, $n = 6$). On day 7, the frequency of CD11c^{int} mPDCA1⁺ pDCs in the lamina propria (LP) (D), mesenteric lymph node (MLN) (E) and spleen (F) was detected by flow cytometry analysis. Typical data for CD11c^{int} mPDCA1⁺ pDCs and summarized data for the percentage of CD11c^{int} mPDCA1⁺ pDCs in the CD11c⁺ cell population are shown (D, E, F). Data are expressed as the mean \pm SE (* $p < 0.05$, $n = 4$).

3.2 BMDC migration along chemokine concentration gradients

Since pDCs were increased in sites of inflammation in the colon, we speculated that inhibition of pDC migration would lead to elucidation of the pathophysiological role of pDCs in the colitis model. Thus, we searched for specific inhibitors of pDC migration with a chemotaxis assay using an EZ-TAXIScan system. BMpDCs migrated toward the higher concentration side according to the concentration gradient of CCL21 (Figure 4A). The number of migrated BMpDCs was significantly increased at each time point from 810 seconds to 3600 seconds (Figure 4B and C, $p < 0.05$).

To investigate the inhibitors of pDC migration, we tested the benefit of 80 naturally occurring compounds. After treatment with each of the 80 compounds derived from natural medicines (1 μ M) at 37°C for 30 minutes, the chemotactic responses of BMpDCs were assessed by monitoring migration along a CCL21 concentration gradient over 3600 seconds (Figure 5). 10 compounds reduced the number of migrated BMpDCs by more than 50% but less than 70% compared to vehicle (partial inhibition of pDC migration), and 10 compounds reduced the number of migrated BMpDCs by more than 70% compared to vehicle (potent inhibition of pDC migration) (**Table 2**). Besides, there were 7 compounds increased the number of migrated BMpDCs by more than 50% (**Table 3**). Among these potent inhibitors of pDC migration, As-IV (Jiang, Lu et al., 2017, Jiang, Sun et al., 2017), berberine (Ber) (Yu et al., 2018, Cui et al. 2018), curcumin (Cur) (Zhang, Xue et al., 2019, Yue et al., 2019), isofraxidine (Iso) (Niu et al., 2015, Liu et al., 2015) and Oxy (Chen et al., 2017) have been well reported to influence immune responses, and Ber, Cur and Oxy have been particularly reported to have therapeutic effects on colitis models (Yu et al., 2018, Cui et al. 2018, Zhang, Xue et al., 2019, Yue et al., 2019, Chen et al., 2017). Thus, we further verified the effects of these 5 compounds on the migration of BMpDCs. As-IV, Ber, Cur, Iso and Oxy markedly reduced the number of migrated BMpDCs to $7.3 \pm 0.07\%$ (Figure 4D, $p < 0.05$), $10.0 \pm 0.04\%$ (Figure 4E, $p < 0.05$), $16.7 \pm 0.05\%$ (Figure 4F, $p < 0.05$), $6.7 \pm 0.10\%$ (Figure 4G, $p < 0.05$) and $32.4 \pm 0.06\%$ (Figure 4H, $p < 0.05$) of the control migrated BMpDC number, respectively, at 3600 seconds. In addition, the apoptosis and necrosis of pDCs following the treatment with each compound were detected using an annexin V-FITC kit to evaluate the compound toxicity. The percentages of annexin V-positive/PI-negative (apoptotic) cells or annexin V/PI-positive (necrotic) cells in the total BMpDC population were measured by flow cytometry. These 5 compounds did not induce either apoptosis or necrosis in BMpDCs compared to vehicle (**Table 4**, $p > 0.05$), indicating that these compounds inhibit pDC migration without inducing cell death.

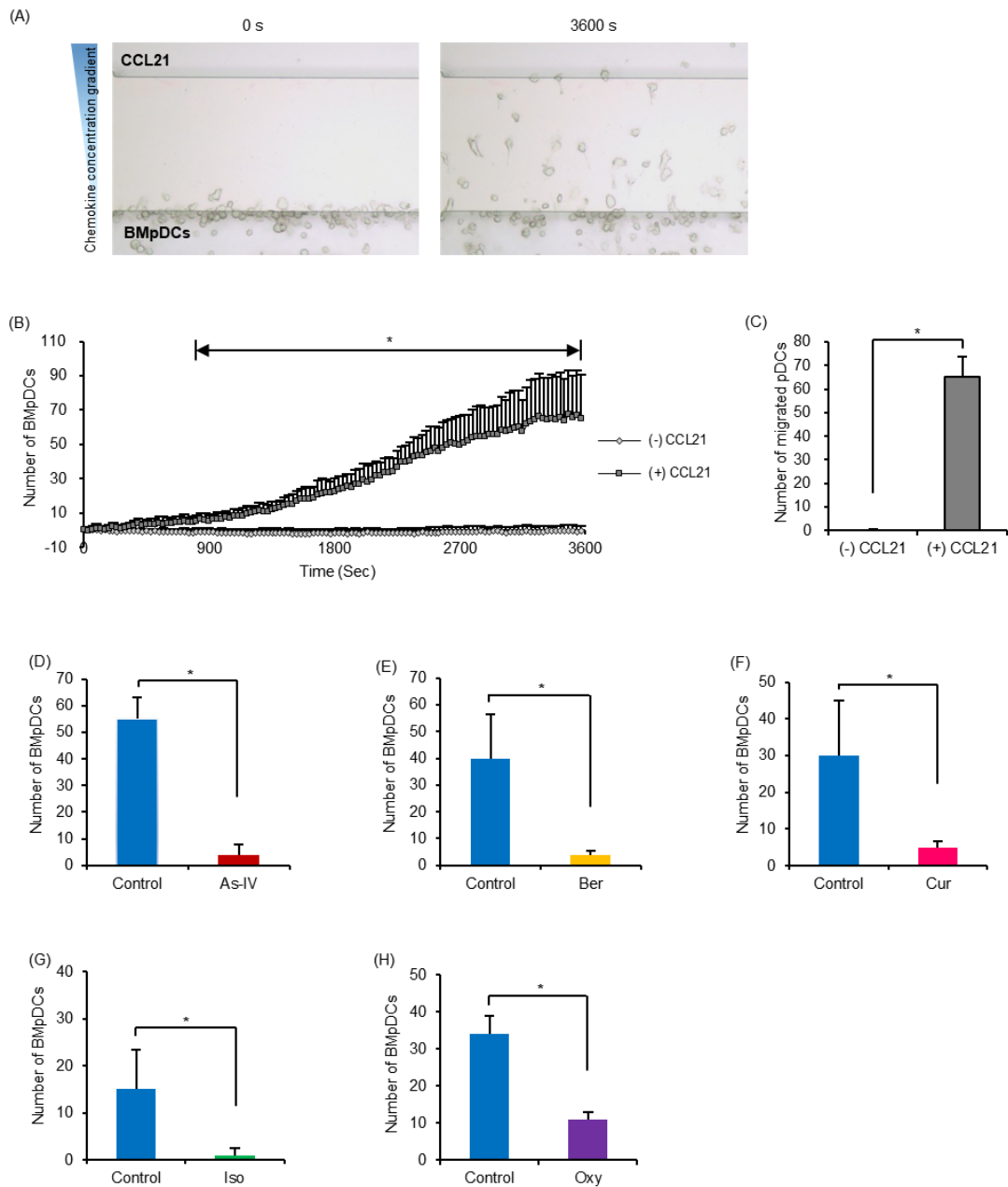


Figure 4. Inhibitors of BmpDC migration induced by CCL21. BmpDC chemotaxis experiments were performed with an EZ-TAXIScan system and analyzed with a TAXIScan Analyzer 2. Representative photos of BmpDCs migrated toward the more concentrated side of a CCL21 gradient at 0 and 3600 seconds are shown (A). The number of migrated BmpDCs during 3600 seconds is indicated by the line graph (B). The number of migrated BmpDCs at 3600 seconds is summarized in the bar graph (C). The numbers of migrated BmpDCs following treatment with 1 μ M As-IV (D), Ber (E), Cur (F), Iso (G) or Oxy (H) for 3600 seconds are shown. Data are expressed as the mean \pm SE (* $p < 0.05$, $n = 3$).

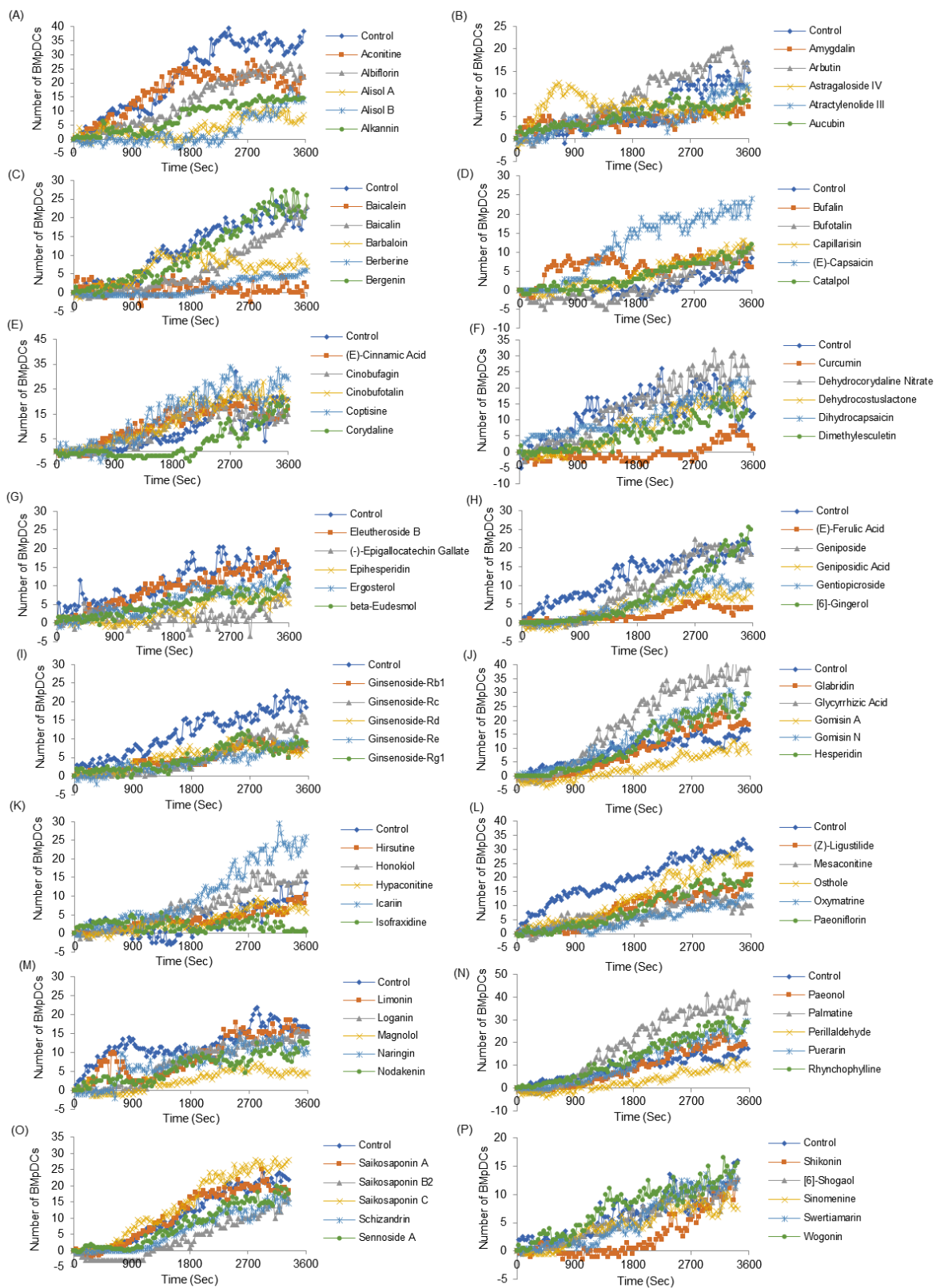


Figure 5. Typical data for the 80 compounds on the migration of BMpDCs. (A) Aconitine, albiflorin, alisol A, alisol B and alkannin. (B) Amygdalin, arbutin, astragaloside IV, atractylenolide III and aucubin. (C) Baicalein, baicalin, barbaloin, berberine and bergenin. (D) Bufalin, bufotalin, capillarisin, (E)-capsaicin and catalpol. (E) (E)-cinnamic acid, cinobufagin, cinobufotalin, coptisine and corydaline. (F) Curcumin, dehydrocorydaline nitrate, dehydrocostuslactone, dihydrocapsaicin and dimethylesculetin. (G) Eleutheroside B, (-)-epigallocatechin gallate, epihesperidin, ergosterol and beta-eudesmol. (H) (E)-ferulic acid, geniposide, geniposidic acid, gentiopicroside and [6]-gingerol. (I) Ginsenoside-Rb1, ginsenoside-Rc, ginsenoside-Rd, ginsenoside-Re and ginsenoside-Rg1. (J) Glabridin, glycyrrhizic acid, gomisin A, gomisin N and hesperidin. (K) Hirsutine, honokiol, hypaconitine, icariin and isofraxidine. (L) (Z)-ligustilide, mesaconitine, osthole, oxymatrine and paeoniflorin. (M) Limonin, loganin, magnolol, naringin and nodakenin. (N) Paeonol, palmatine, perillaldehyde, puerarin and rhynchophylline. (O) Saikosaponin A, saikosaponin B2, saikosaponin C, schizandrin and sennoside A. (P) Shikonin, [6]-shogaol, sinomenine, swertiamarin and wogonin.

We next investigated whether these 5 compounds influence cDC migration. cDCs expressing CXCR4 are guided by the CXCR4 ligand CXCL12 and migrate to inflamed sites and the LNs (Lopez et al., 2018, Tiberio et al., 2018). The number of BMcDCs that migrated along a CXCL12 concentration gradient was significantly increased at each time point from 390 seconds to 3600 seconds (Figure 6A and B, $p < 0.05$). As-IV had no significant effects on the number of migrated BMcDCs or the velocity or the direction of BMcDC migration (Figure 6C). Ber markedly decreased the number of migrated BMcDCs to $61.5 \pm 0.12\%$ of the control migrated BMcDC number and significantly decreased the velocity and direction of BMcDC migration (Figure 6D, $p < 0.05$). Cur slightly reduced the number of migrated BMcDCs and significantly decreased the velocity and direction of BMcDC migration (Figure 6E, $p < 0.05$). Iso markedly decreased the number of migrated BMcDCs to $48.2 \pm 0.12\%$ of the control migrated BMcDC number and decreased the velocity and direction of BMcDC migration (Figure 6F, $p < 0.05$). Oxy had no significant effects on the number of migrated BMcDCs or the velocity or the direction of BMcDC migration (Figure 6G).

Taken together, these results indicate that As-IV and Oxy have selective inhibitory effects on pDC migration, whereas Ber, Cur, and Iso have inhibitory effects on both cDC migration and pDC migration. In addition, the effects of As-IV and Oxy were concentration dependent (Figure 7).

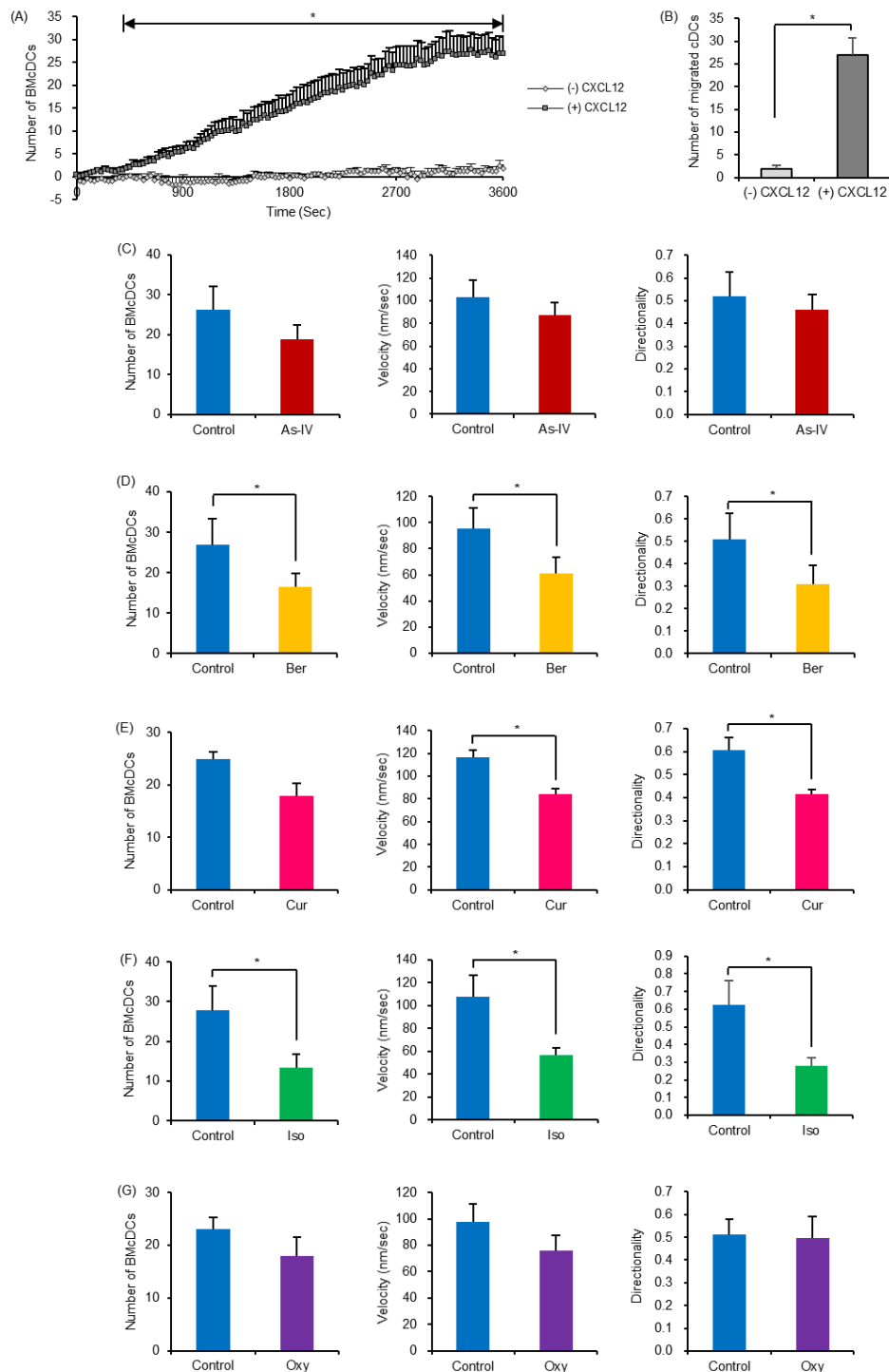
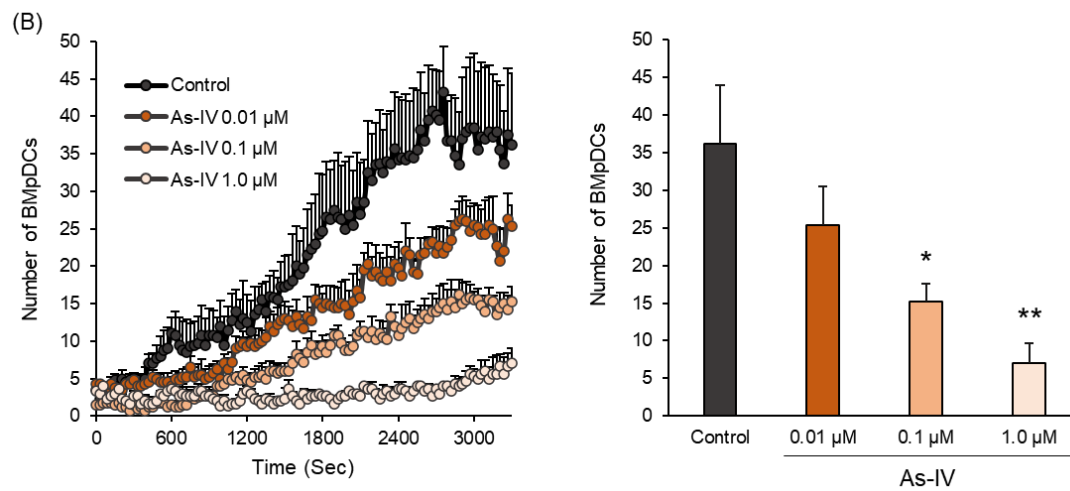
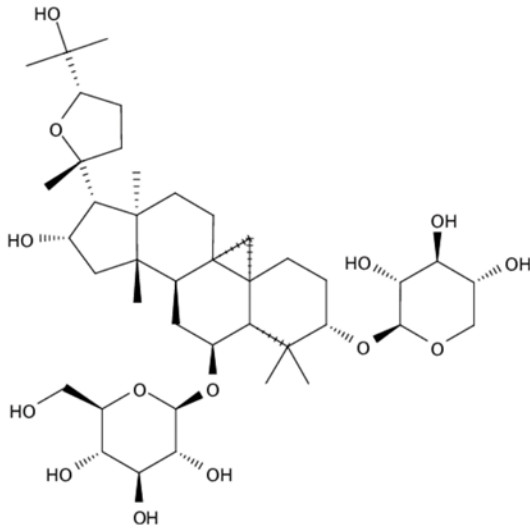


Figure 6. Effects of inhibitors of BMpDC migration on BMcDC migration induced by CXCL12. BMcDC chemotaxis experiments were performed with an EZ-TAXIScan system and analyzed with a TAXIScan Analyzer 2. The number of BMcDCs migrated toward the more concentrated side of a CXCL12 gradient from 0 to 3600 seconds is indicated by the line graph (A). The number of migrated BMcDCs at 3600 seconds is indicated by the bar graph (B). The

number, velocity and directionality of migrated BMpDCs following treatment with 1 μM As-IV (C), Ber (D), Cur (E), Iso (F) or Oxy (G) at 3600 seconds are shown. Data are expressed as the mean \pm SE (* $p < 0.05$, $n = 5$).

(A) The chemical structure of Astragaloside IV



(C) The chemical structure of oxymatrine

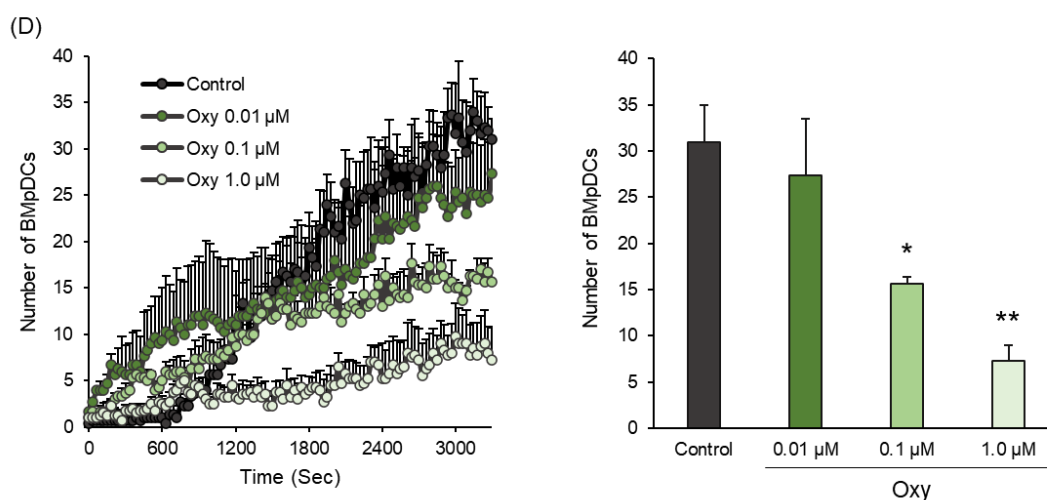
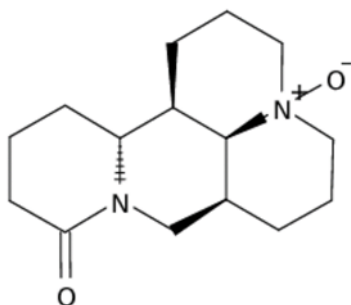


Figure 7. Concentration-dependent effects of As-IV and Oxy. The chemical structure of As-IV (A) and Oxy (C) are shown. Concentration-dependent effects of As-IV or Oxy on BMpDC migration at 0.01 μM , 0.1 μM and 1.0 μM were examined with an EZ-TAXIScan system and analyzed with a TAXIScan Analyzer 2. The number of migrated BMpDCs at 3600 seconds following treatment with As-IV (B) or Oxy (D) are shown. Data are expressed as the mean \pm SE (* $p < 0.05$, ** $p < 0.01$, $n = 3-4$).

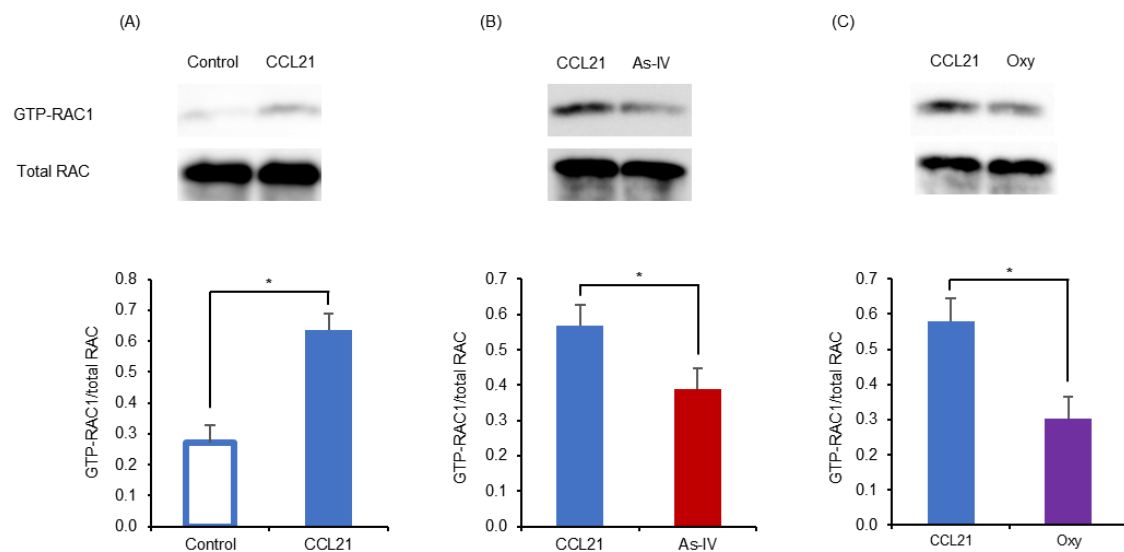
3.3 Effects of As-IV and Oxy on RAC1 activation

We next investigated the detailed mechanisms of the inhibition of BMpDC migration by As-IV or Oxy. It has been reported that activation of RAC1 is critically involved in CCL21-induced pDC migration (Gotoh et al., 2008). Therefore, to clarify the involvement of RAC1 activation in the inhibitory effects of As-IV and Oxy, we examined GTP-RAC1 expression by using an active RAC1 detection kit. GTP-RAC1 expression in BMpDCs was significantly induced by CCL21 stimulation (Figure 8A, $p < 0.05$). Treatment with As-IV (Figure 8B, $p < 0.05$) or Oxy (Figure 8C,

$p < 0.05$) significantly reduced the levels of GTP-RAC1 expression, which led to inhibition of the migration of BMpDCs.

To comprehensively analyze the inhibitory effects of As-IV and Oxy on BMpDC migration, microarray analysis of BMpDCs treated with CCL21 following treatment with As-IV or Oxy was performed using the Clariom S Array Mouse. In particular, the genes with large changes in expression are listed (**Table 5**). GO analysis by GeneSpring showed no significant evidence for DCs function of candidate genes. Next, we analyzed changes in expression levels for genes related to cell migration. A heatmap displaying results for each treatment analyzed by GeneSpring is shown in Figure 8D. The heatmap is composed of 117 candidate genes involved in cell migration. According to the heatmap for the regulation of cell migration, gene expression patterns were clearly different between the As-IV and Oxy treatments. Oxy treatment slightly increased the expression of *sema4a*, which activates NF κ B via phosphorylation of RAC1 and AKT (Zhang, Wei et al., 2019). Oxy treatment decreased the expression of *Ikkkap*, which is elevated by MAPK/ERK signaling pathway activation (Donyo et al., 2016), and *Fgf18*, which induces MAPK/ERK signaling pathway activation (Zhai et al., 2017). As-IV treatment decreased the expression of *Ajuba*, which blocks JAK1/STAT1 signaling pathway activation (Jia et al., 2017), *Hgf*, which induces JAK2/STAT3 signaling pathway activation (Li et al., 2018), and *Dpep1*, which activates the PI3K/AKT signaling pathway (Cui et al., 2019), while Oxy treatment increased the expression of these genes. Although the gene expression patterns were clearly different between the As-IV and Oxy treatments, these gene expression patterns were not consistent with the canonical cell migration pathways in IPA analysis or GeneSpring analysis.

Taken together, these results indicate that As-IV and Oxy significantly suppress RAC1 activation in CCL21-induced pDC migration, although the inhibitory effects of As-IV and Oxy on pDC migration are induced by different mechanisms.



(D)

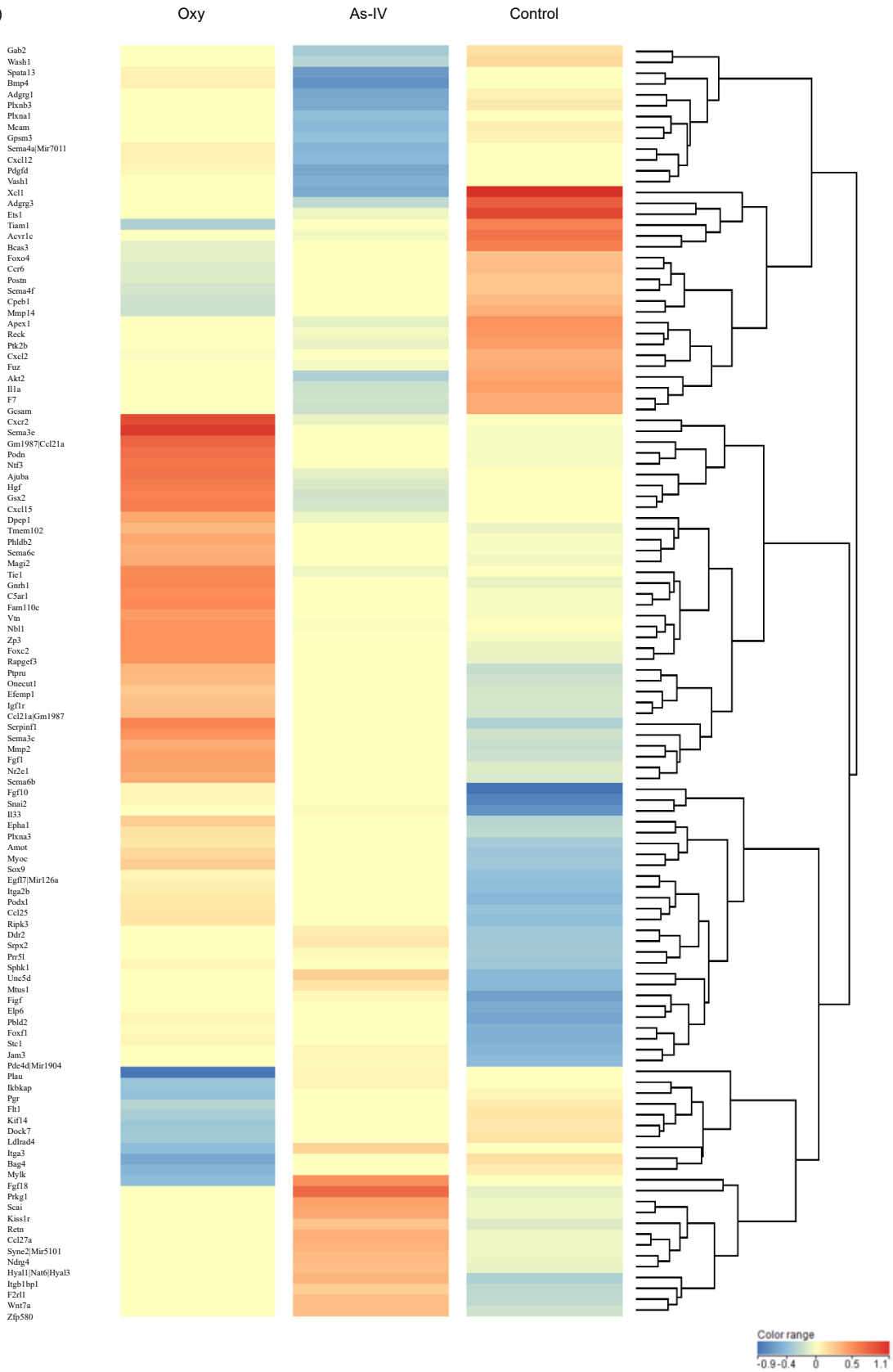


Figure 8. Effects of 1 μ M As-IV or Oxy on RAC1 activation. RAC1 activation was detected by evaluating the expression of the GTP-RAC1 protein by using a western blot analysis kit. A representative image and the quantification of the band intensity for GTP-RAC1 relative to that of total RAC1 are shown in A-C. (A) Representative western blot analysis of GTP-RAC1 in BMpDCs induced with CCL21 and quantification of the band intensity are shown (5 independent experiments). Data are expressed as the mean \pm SE (* $p < 0.05$, $n = 5$). Representative western blot analysis of GTP-RAC1 in CCL21-induced migrated BMpDCs following treatment with As-IV (B) or Oxy (C) and the quantification of band intensity are shown (7 independent experiments). Data are expressed as the mean \pm SE (* $p < 0.05$, $n = 7$). Microarray analysis of BMpDCs induced with a CCL21 gradient following treatment with As-IV or Oxy was performed by using the Clariom S Array Mouse. The differential expression of genes in BMpDCs induced with a CCL21 gradient following treatment with vehicle (control), As-IV or Oxy is displayed in the heatmap (D). The red and blue colors indicated the up-regulation normalized intensity values (\log_2) and down-regulation normalized intensity values (\log_2) of each RNA in each sample.

3.4 Effects of selective inhibitors of pDC migration on a DSS-induced colitis model

We next examined the effects of As-IV and Oxy on the development of DSS-induced colitis. Based on previous studies, we used 50 mg/kg of As-IV (Jiang, Lu et al., 2017, Bao et al., 2016, Chen et al., 2016) or 100 mg/kg of Oxy (Chen et al., 2017) as a dose with adequate efficacy and without adverse side effects. In the DSS-induced colitis model, As-IV (50 mg/kg) or Oxy (100 mg/kg) administration significantly reduced the body weight loss (Figure 9A, $p < 0.05$) and elevated DAI compared to DSS-induced colitis mice treated with vehicle (3% DSS) (Figure 9B, $p < 0.05$). In addition, As-IV obviously attenuated colon atrophy (Figure 9C, $p < 0.05$). However, as shown in Figure 9D and 9E, neither As-IV nor Oxy reduced the increased percentage of CD11c^{int}mPDCA1⁺pDCs in the colonic LP of DSS-induced colitis mice.

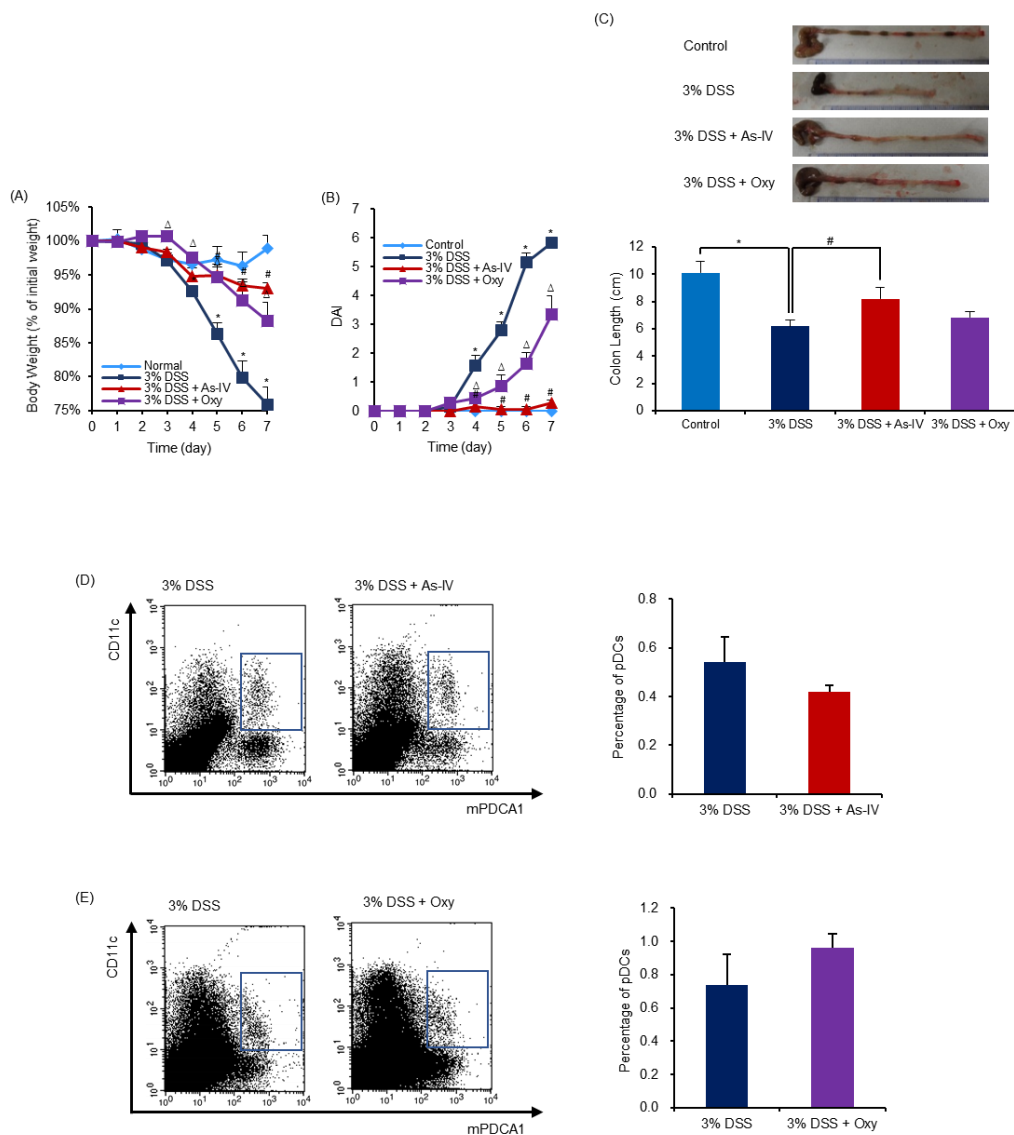


Figure 9. Effects of As-IV or Oxy on the DSS-induced colitis model and levels of pDCs. The body weight changes (A), DAI scores (B) and colon length (C) were monitored for 7 days. Photos of typical changes in colon length are shown (C). Data are expressed as the mean \pm SE (* $p < 0.05$ 3% DSS vs control, # $p < 0.05$ As-IV vs 3% DSS, $\Delta p < 0.05$ Oxy vs 3% DSS, $n = 6$). On day 7, the frequency of CD11c^{int} mPDCA1⁺ pDCs in the LP of DSS-induced colitis model mice treated with AS-IV (D) or Oxy (E) was detected by flow cytometry analysis. Representative data for CD11c^{int} mPDCA1⁺ pDCs and summarized data for the percentage of CD11c^{int} mPDCA1⁺ pDCs in the CD11c⁺ cell population are shown (D, E). Data are expressed as the mean \pm SE ($n = 4$).

3.5 Effects of selective inhibitors of pDC migration on the colonic LP and ILFs of mice

We investigated the effects of As-IV and Oxy treatment on the distribution of pDCs in the colonic LP of DSS-induced colitis mice. Hamada et al. reported that a cluster of B220⁺ B cells is

compartmentalized in the central region of isolated lymphoid follicles (ILFs), which is surrounded by a large number of CD11c⁺ DCs in the mouse intestine (Hamada et al., 2002). In the colon of DSS-induced colitis mice, a cluster of B220⁺ B cells was localized in the central region of ILFs (Figure 10A-C left), and most of the CCL21 immunoreactivity was obviously observed around the cluster of B220⁺ B cells in the ILFs (Figure 10A central and right). However, As-IV (Figure 10B central and right) and Oxy (Figure 10C central and right) both failed to affect the morphology.

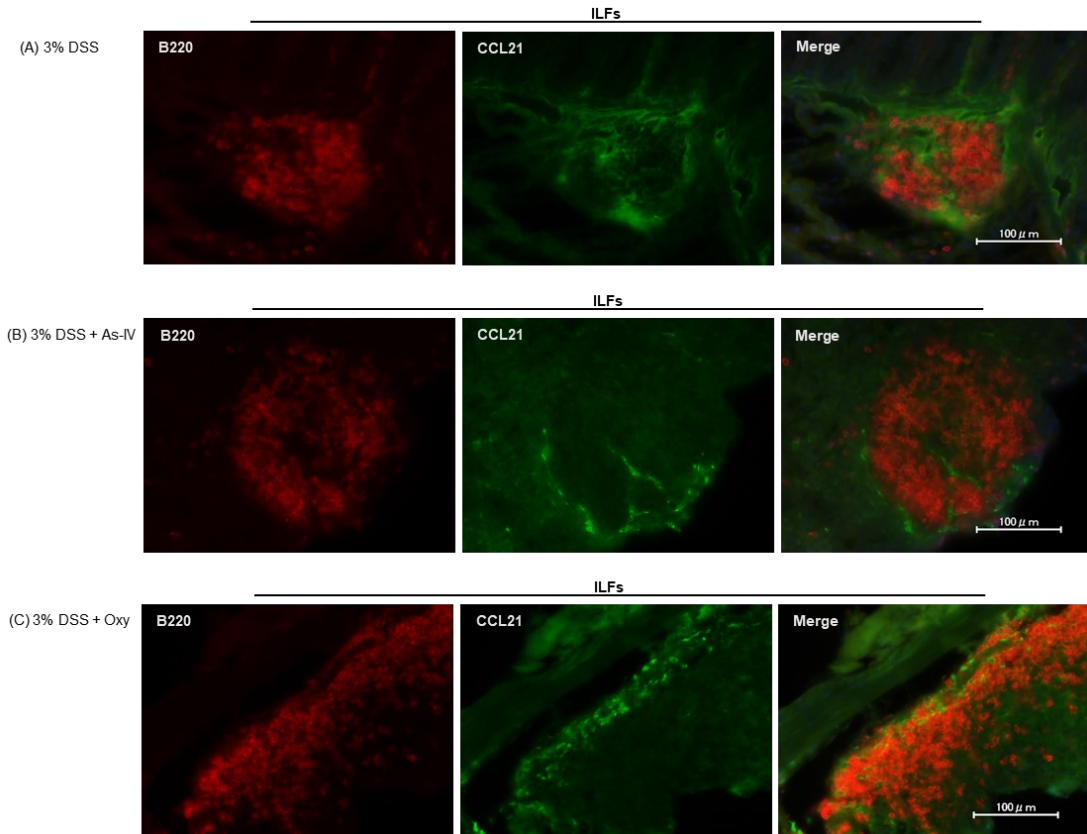


Figure 10. Effects of As-IV or Oxy on the distribution of CCL21 in the DSS-induced colitis model. The distribution of CCL21 in the colonic ILFs of DSS-induced colitis mice treated with saline (A), As-IV (B) or Oxy (C) was identified by immunohistochemical staining of the colon. Immunohistochemical staining was performed on samples from 3 mice/group, and representative images are presented.

Additionally, CD11c⁺ B220⁺ pDCs were mainly localized in the colonic ILFs (Figure 11A upper) rather than the colonic LP (Figure 11A lower) of DSS-induced colitis mice. In contrast, CD11c⁺ B220⁺ pDCs were largely found in the colonic LP rather than the colonic ILFs of DSS-induced colitis mice administered As-IV or Oxy (Figure 11B and C). Overall, the altered distribution of pDCs could be attributed to the inhibition of pDC migration to colonic ILFs in DSS-induced colitis mice by treatment with As-IV or Oxy.

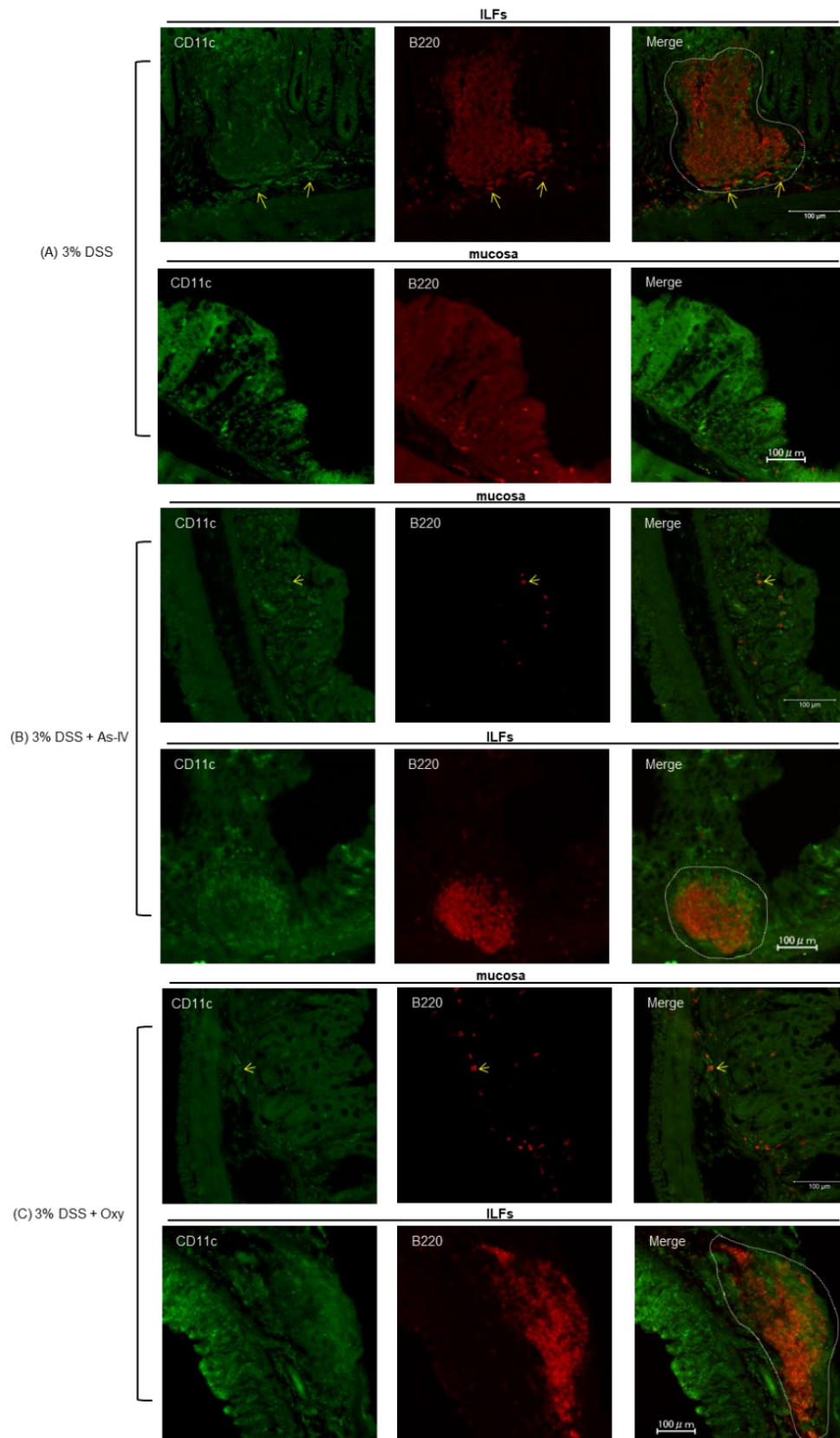


Figure 11. Effects of As-IV or Oxy on the distribution of pDCs in the DSS-induced colitis model. The distribution of CD11c⁺ B220⁺ pDCs in the colonic ILFs and the colonic LP of DSS-induced colitis mice treated with saline (A), As-IV (B) or Oxy (C) was identified by immunohistochemical staining of the colon. CD11c⁺ B220⁺ pDCs were observed in the colonic ILFs of DSS-induced colitis mice treated with saline (A) but mainly in the colonic LP after administration of As-IV (B) or Oxy (C). Immunohistochemical staining was performed on samples from 3 mice/group, and representative images are presented.

Furthermore, we investigated the distribution of pDCs in the colonic LP using a pDC adoptive transfer method. At 24 hours after adoptive transfer of CFSE⁺ BMpDCs into normal mice, the CFSE⁺ BMpDCs were distributed in both the lateral and inner sites of colonic ILFs (Figure 12A); in contrast, CFSE⁺ BMpDCs were mostly distributed in the lateral sites of colonic ILFs in As-IV- or Oxy-treated mice (Figure 12B and C). In addition, the number of CFSE⁺ BMpDCs that migrated to colonic ILFs was significantly decreased in As-IV- or Oxy-treated mice (Figure 12D, $p < 0.05$). Therefore, As-IV and Oxy suppressed pDC migration toward ILFs in the mouse colon and even altered the pDC distribution in colonic ILFs.

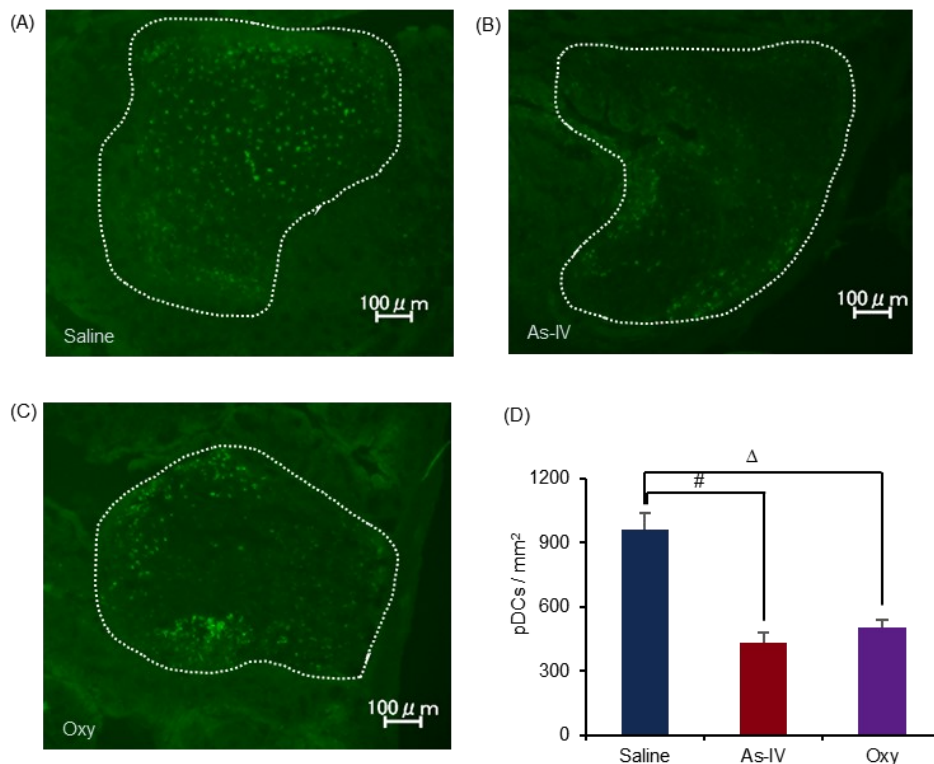


Figure 12. Effects of As-IV or Oxy on the migration of adoptively transferred pDCs. CFSE⁺ BMpDCs were adoptively transferred into BALB/c mice. The recipient mice were treated with As-IV (50 mg/kg) or Oxy (100 mg/kg). Male BALB/c mice were adoptively transferred with

CFSE⁺ BMpDCs and treated with saline (Saline). Representative images of colonic ILFs from pDC adoptively transferred mice treated with saline (A), As-IV (B) or Oxy (C) are presented. Data are from 3 independent experiments. The number of CFSE⁺ pDCs per unit area of ILFs is shown in the bar graph (D). Data are expressed as the mean \pm SE (# $p < 0.05$ As-IV vs saline, $\Delta p < 0.05$ Oxy vs saline, n = 4).

4. Discussion

DCs play important roles in the immune surveillance system as conductors of innate and acquired immune responses by migrating to the appropriate sites at the appropriate times. However, the pathophysiological role of DCs, especially that of pDCs, in intestinal inflammation is still not fully understood. In particular, the therapeutic implications of inhibiting pDC migration remain unknown, and one of the major reasons is the lack of available drugs that can inhibit the migration of pDCs.

In the present study, we identified As-IV and Oxy as selective inhibitors of pDC migration from 80 compounds contained in traditional Japanese herbal medicines. pDCs accumulated in the colonic LP and ILFs of the DSS-induced colitis model, and As-IV and Oxy, which attenuated DSS-induced colitis, simultaneously reduced pDC accumulation in the colonic ILFs but not the LP of DSS-induced colitis mice. Our results indicate that pDCs play an important role in the development of intestinal inflammation and that selective inhibitors of pDC migration toward GALTs have the potential to ameliorate intestinal inflammation.

We demonstrated that As-IV and Oxy are inhibitors of pDC migration but not cDC migration. pDCs serve as professional antigen-presenting cells and regulate immune responses in many immunological diseases (Ye, Gaugler et al., 2020). Previously, the pharmacological effects of As-IV and Oxy on immunological diseases were reported. As-IV alleviates allergic inflammation by downregulating inflammatory cytokine expression in a murine allergic contact dermatitis model (Bao et al., 2016) and suppresses 2,4,6-trinitrobenzene sulfonic acid-induced colitis in a rat model (Jiang, Sun et al., 2017). On the other hand, Oxy ameliorates skin lesions in allergic contact dermatitis mice (Xu et al., 2018) and alleviates DSS-induced colitis through the inhibition of PI3K/Akt signaling (Chen et al., 2017). However, there are no reports concerning the immunological effects of Oxy or As-IV on pDC functions, although there are some reports that pDCs are involved in the pathology of these diseases. Thus, it is speculated that the preventive effects of As-IV and Oxy on these immunological disease models may be partly attributed to the suppression of pDC migration.

In the present study, As-IV and Oxy inhibited the migration of pDCs along a concentration gradient of CCL21. CCL21 is indispensably required for pDC migration, and the recruitment of pDCs to the LNs is induced by a CCL21 concentration gradient (Tiberio et al., 2018). Furthermore, RAC1 activation plays a pivotal role in the migration of pDCs, and inhibition of RAC1 activation suppresses pDC migration (Gotoh et al., 2008). In addition, As-IV suppresses the expression of GTP-RAC1 in the breast cancer cell line MDA-MB-231 (Jiang, Lu et al., 2017). In the present study, our western blot results revealed that the rate of GTP-RAC1 under CCL21 stimulation was downregulated by As-IV or Oxy, indicating that the inhibitory effects of As-IV and Oxy on pDC migration are mediated by reducing the activation of RAC1.

Furthermore, in this study, microarray analysis revealed that As-IV and Oxy differed in the expression patterns of genes that regulate cell migration. As-IV slightly decreased the expression of *Ajuba* (Jia et al., 2017) and *Hgf* (Li et al., 2018), which are involved in JAK/STAT signaling pathway activation. Oxy decreased the expression of *Ikkkap* (Donyo et al., 2016) and *Fgf18* (Zhai et al., 2017), which are involved in MAPK/ERK signaling pathway activation. Although the mechanisms underlying pDC migration are not fully elucidated, our findings suggest that As-IV and Oxy affect different pathways to exert their inhibitory effects on pDC migration toward GALTs. In the additional analysis by IPA (Ingenuity® Pathway Analysis), refer to that As-IV suppressed the expression of iNOS on peritoneal macrophages (Liu et al., 2016), we infer that pathway of As-IV on RAC1 was As-IV-NOS2-RAC1 (Figure 13). Oxy decreased the expression of *Srebf1* in rat liver tissues (Shi et al., 2013). Interaction of SREBP-1 and HNF-4 α to suppress hepatic gluconeogenic activity (Yamamoto et al., 2004). So, we infer that pathway of Oxy on RAC1 was Oxy-Srebf1-HNF4 α -RAC1 (Figure 14).

Figure 13.

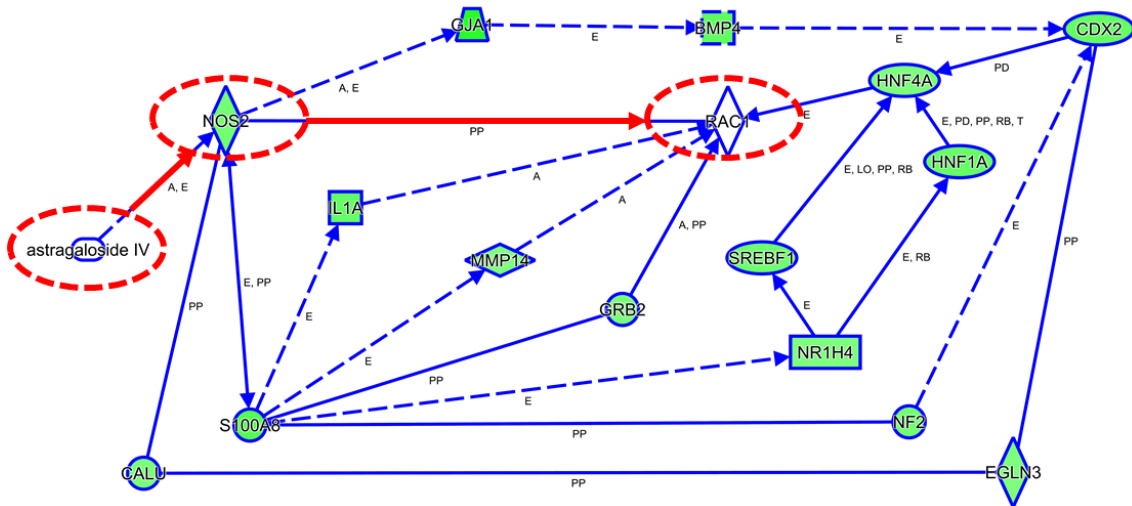
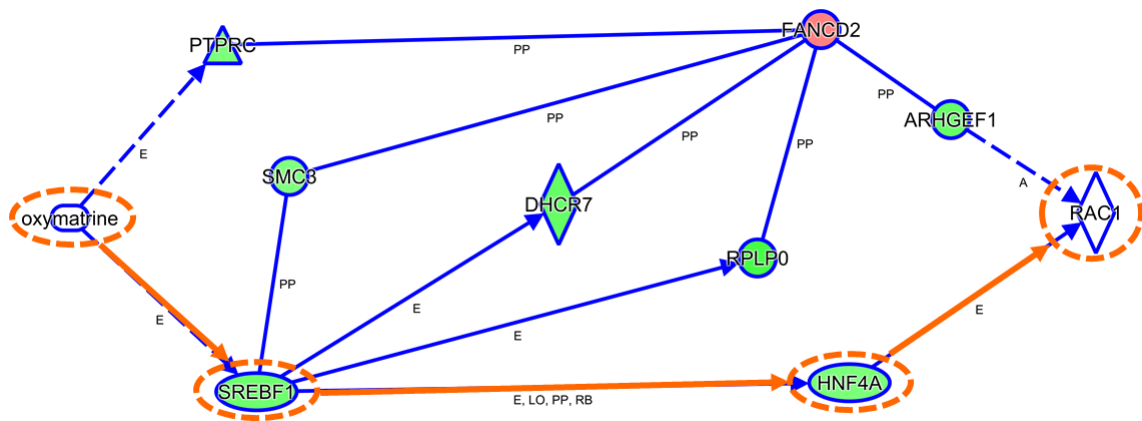


Figure 14.



It has been reported that pDCs are significantly increased in the colonic mucosa and MLNs of IBD patients and that the infiltration of pDCs into these tissues is closely involved in IBD (Baumgart et al., 2011). However, the pathophysiological role of pDCs in the pathology of IBD remains unclear. A recent study of a mouse colitis model also demonstrated that pDCs accumulate in the colonic mucosa of DSS-induced colitis mice (Arimura et al., 2017). In addition, pDC depletion relieves the symptoms of DSS-induced colitis, which are reversed by reconstitution of pDCs by using cell transplantation (Arimura et al., 2017). In our study, the population of pDCs was increased in the colonic LP but not changed in MLNs of DSS-induced colitis mice. Taken together, these findings suggest that pDCs migrate within the colonic mucosa and accumulate in the colonic mucosa rather than migrate from inflamed sites in the colon to the MLNs in DSS-induced colitis mice, which is considered to be deeply involved in the development of DSS-induced colitis. In contrast, a deficiency in pDCs cannot produce inhibitory effects on spontaneously developed chronic colitis induced by deletion of WASP or interleukin (IL)-10 (Sawai et al., 2018). Therefore, the pathophysiological role of pDCs in colitis needs further investigation based on symptoms and pathogenesis.

We demonstrated that As-IV and Oxy, which inhibited pDC migration, exerted preventive effects on DSS-induced colitis. However, treatment with As-IV or Oxy did not affect the population of pDCs in the colonic LP of DSS-induced colitis mice. We then investigated the distribution of pDCs and expression of CCL21 in the colon of DSS-induced colitis mice. CCL21 expression was obviously observed in colonic ILFs, and the distribution of pDCs in the colonic ILFs was decreased by As-IV or Oxy treatment, indicating that As-IV and Oxy inhibit the migration of pDCs to colonic ILFs. The inhibitory effects of As-IV and Oxy on the migration of pDCs to ILFs was also confirmed in a pDC adoptive transfer experiment. ILFs primarily contribute to the maintain of immune homeostasis in the colon via initiation of adaptive immune responses (Fenton et al., 2020). Yeung et al. have reported increased anomalous lymphoid follicular hyperplasia in

the colonic lamina propria of UC patients (Yeung et al., 2000). Likewise, a significant increase in ILF development is observed in the colon of DSS colitis mice (Sanderlin et al., 2017). Our results in this study demonstrate that inhibition of pDC migration to ILFs exerts preventive effects on DSS colitis, indicating that pDCs with antigen presenting function in the ILFs play a critical role in the induction of colitis. Therefore, we conclude that the migration of pDCs to ILF, a site of priming and differentiation of naive adaptive immune cells, contributes to the pathology of severe colonic inflammatory diseases.

Similar to our study, symptoms of DSS-induced colitis were found to be relieved in CCR7KO mice, although the proportion of pDCs in the colon was elevated (Kim et al., 2016). This study and our present study indicate that the CCL21/CCR7 interaction-related migration of pDCs within the colon of colitis mice contributes to the development of colitis.

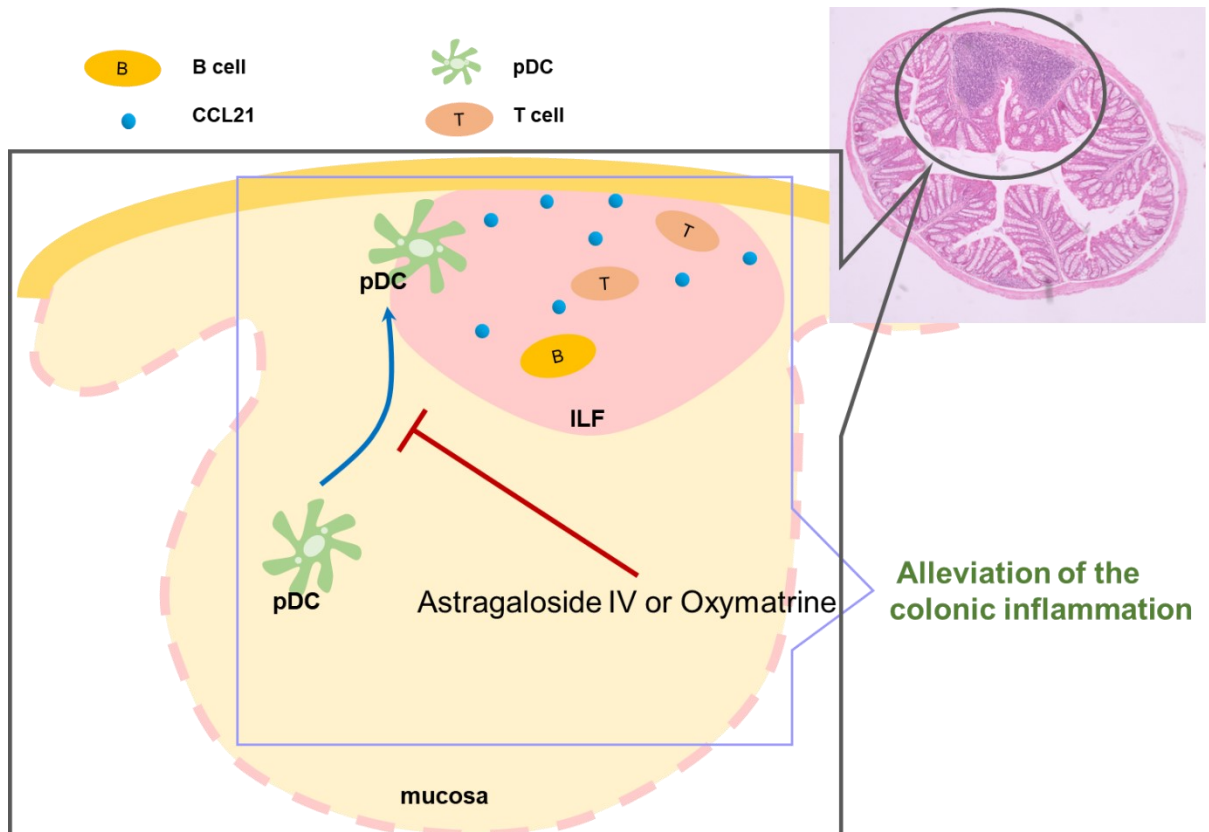
We discovered novel selective inhibitors of pDC migration and investigated their preventive effects on DSS-induced colitis. We demonstrated that the identified selective inhibitors of pDC migration suppressed the migration of pDCs into colonic ILFs and thereby significantly alleviated the symptoms of colitis.

The present study revealed the pathophysiological role of pDC migration within the inflamed colon and the therapeutic potential of suppressing pDC migration in colitis. Therefore, the identified selective inhibitors of pDC migration have great potential as innovative lead drug candidates with novel mechanisms of action for the treatment of colitis.

5. Conclusion

CCL21 expressed in ILFs induced pDC migration to the ILFs. Migration of pDCs to the ILFs is involved in the progression of colonic inflammation. Inhibitory effect of As-IV or Oxy on pDC migration to the ILFs alleviated the colonic inflammation. The selective inhibitors of pDC migration have great potential as innovative lead drug candidates with novel mechanisms of action for the treatment of colitis (Graphic conclusion 2).

Graphic conclusion 2



6. Tables

Table 1. List of Compounds

Aconitine	(E)-Cinnamic Acid	Ginsenoside-Rb1	Naringin
Albiflorin	Cinobufagin	Ginsenoside-Rc	Nodakenin
Alisol A	Cinobufotalin	Ginsenoside-Rd	Osthole
Alisol B	Coptisine	Ginsenoside-Re	Oxymatrine
Alkannin	Corydaline	Ginsenoside-Rg1	Paeoniflorin
Amygdalin	Curcumin	Glabridin	Paeonol
Arbutin	Dehydrocorydaline Nitrate	Glycyrrhizic Acid	Palmitine Chloride
Astragaloside-IV	Dehydrocostuslactone	Gomisin A	Perillaldehyde
Atractylenolide III	Dihydrocapsaicin	Gomisin N	Puerarin
Aucubin	Dimethylesculetin	Hesperidin	Rhynchophylline
Baicalein	Eleutheroside B	Hirsutine	Saikosaponin A
Baicalin	(-)-Epigallocatechin Gallate	Honokiol	Saikosaponin B2
Barbaloin	Epihesperidin	Hypaconitine	Saikosaponin C
Berberine	Ergosterol	Icariin	Schizandrin
Bergenin	beta-Eudesmol	Isofraxidine	Sennoside A
Bufalin	(E)-Ferulic Acid	(Z)-Ligustilide	Shikonin
Bufotalin	Geniposide	Limonin	(6)-Shogaol
Capillarisin	Geniposidic Acid	Loganin	Sinomenine
(E)-Capsaicin	Gentiopicroside	Magnolol	Swertiamarin
Catalpol	(6)-Gingerol	Mesaconitine	Wogonin

Table 2. Inhibitors of pDC migration

Potent inhibitor of pDC migration	Partial inhibitor of pDC migration
Alkannin	Alisol A
Amygdalin	Dehydrocostuslactone
Astragaloside-IV	Dimethylesculetin
Barbaloin	(-)-Epigallocatechin Gallate
Berberine	Epihesperidin
Curcumin	Ergosterol
Beta-Eudesmol	Gensenoside-Rd
(E)-Ferulic Acid	Hypoconitine
Isofraxidine	(6)-Shogaol
Oxymatrine	Sinomenine

Table 3. Accelerators of pDC migration

Accelerator of pDC migration
Bergenin
(E)-Capsaicin
Coptisine
Glycyrrhizic Acid
Gomisin N
Hesperidin
Palmatine Chloride

Table 4. The ratio of apoptotic and necrotic cells

	Apoptotic BMpDC (%)	Necrotic BMpDC (%)
Control	0.6 ± 0.6%	1.2 ± 0.4%
As-IV	0.4 ± 0.3%	2.0 ± 0.0%
Ber	0.4 ± 0.3%	1.9 ± 0.2%
Cur	0.5 ± 0.4%	1.8 ± 0.3%
Iso	0.8 ± 0.6%	2.1 ± 0.2%
Oxy	0.6 ± 0.5%	2.0 ± 0.2%

Table 5. List of genes selected by microarray analysis (1)

Gene Symbol	Description	Fold Change Log2 ratio (As-IV/control upregulation)
<i>Gm10944</i>	predicted gene 10944	4.05
<i>Mup12</i>	major urinary protein 12	3.19
<i>Cyp3a25</i>	cytochrome P450, family 3, subfamily a, polypeptide 25	3.03
<i>Olf1294</i>	olfactory receptor 1294	2.91
<i>Gm11115</i>	predicted gene 11115	2.90
<i>Vmn1r91</i>	vomeronasal 1 receptor 91	2.88
<i>Gm11084</i>	predicted gene 11084	2.83
<i>Gm5726;</i> <i>Gm8677</i>	predicted gene 5726; predicted gene 8677	2.66
<i>Nat3</i>	N-acetyltransferase 3	2.62
<i>Vmn1r101</i>	vomeronasal 1 receptor 101	2.60
Gene Symbol	Description	Fold Change Log2 ratio (As-IV/control downregulation)
<i>Gm11096</i>	predicted gene 11096	-10.96
<i>Xcl1</i>	chemokine (C motif) ligand 1	-3.10
<i>Wfdc9</i>	WAP four-disulfide core domain 9	-2.98
<i>Lmo7</i>	LIM domain only 7	-2.84
<i>Olf1459</i>	olfactory receptor 1459	-2.71
<i>Sh2b1</i>	SH2B adaptor protein 1	-2.59
<i>Gm17364</i>	predicted gene, 17364	-2.55
<i>Tecpr2</i>	tectonin beta-propeller repeat containing 2	-2.53
<i>Myo9a</i>	myosin IXa	-2.47
<i>Tceall</i>	transcription elongation factor A (SII)-like 1	-2.43

Table 5. List of genes selected by microarray analysis (2)

Gene Symbol	Description	Fold Change Log2 ratio (Oxy/control upregulation)
<i>Gm10944</i>	predicted gene 10944	6.90
<i>P4ha3</i>	procollagen-proline, 2-oxoglutarate 4-dioxygenase (proline 4-hydroxylase), alpha polypeptide III	3.58
<i>Esp1</i>	exocrine gland secreted peptide 1	3.53
<i>Astn1</i>	astrotactin 1	3.04
<i>Ccdc81</i>	coiled-coil domain containing 81	2.98
<i>Vmn2r98</i>	vomer nasal 2, receptor 98	2.94
<i>Defb46</i>	defensin beta 46	2.91
<i>Skint11</i>	selection and upkeep of intraepithelial T cells 11	2.79
<i>Dusp13</i>	dual specificity phosphatase 13	2.69
<i>Guca2a</i>	guanylate cyclase activator 2a (guanylin)	2.68
Gene Symbol	Description	Fold Change Log2 ratio (Oxy/control downregulation)
<i>Gm17482</i>	predicted gene, 17482	-9.83
<i>Gm11096</i>	predicted gene 11096	-7.96
<i>Olf193</i>	olfactory receptor 193	-3.30
<i>Lmo7</i>	LIM domain only 7	-3.01
<i>Gm17364</i>	predicted gene, 17364	-2.93
<i>Olf1392</i>	olfactory receptor 1392	-2.91
<i>Hist1h3a</i>	histone cluster 1, H3a	-2.63
<i>LOC102639117</i>	secretoglobin family 2A member 2-like	-2.53
<i>Olf1459</i>	olfactory receptor 1459	-2.52
<i>Vmn2r116</i>	vomer nasal 2, receptor 116	-2.40

Conclusion and Future Directions

These findings demonstrate that migration of pDCs is involved in the pathogenesis of immune diseases such as contact dermatitis and colonic inflammation. Inhibition of pDC migration contributes to alleviate the immune diseases which are related to pDC migration.

In the *Chapter 1* of our study, we prove that byakkokaninjinto which had an inhibitory effect on pDC migration may contribute to ameliorate the occurrence of allergic contact dermatitis. In the *Chapter 2* of our study, we prove that As-IV and Oxy as the specific inhibitor of pDC migration exerted preventive effects on colitis by suppressing pDC migration to colonic ILFs. Besides the inhibitors of pDC migration, we discovered the accelerators of pDC migration both in the *Chapter 1* and *Chapter 2*. Thus, it is expected that effects of accelerators of pDC migration on models of various infectious diseases will be elucidated in near future. In the *Chapter 2*, we have surmised the pathways of As-IV or Oxy towards the inactivation of RAC1 using IPA, while we couldn't make out the pathways. Therefore, the underlying mechanisms of the inhibitors should be elucidated in further studies.

Conventionally, the function of pDCs is characterized by the secretion of massive type-I IFN to prevent virus infection in an innate immune response. In addition, the hypersecretion of IFN from pDCs is known for its roles in autoinflammatory. In recent years, regulation of pDCs in the adaptive immune system was clearly identified. The findings of my present studies indicated that pDC had a pathophysiologic role in the immune diseases mediated by adaptive immune responses. Immune diseases were alleviated by inhibition of pDC migration. Hitherto, the therapeutic agents which target on the inhibition of pDC migration have not been reported. We provide a new therapeutic direction in immunological diseases which were related to pDC migration. In addition, a new therapeutic agent by inhibition of pDC migration is considered to be able to be used in combination with current therapeutic drugs due to the different pharmacological mechanisms. And then, inhibitors of pDC migration have the potential to improve treatment efficiency and reduce side effects by leading to reducing the amount of current treatments.

References

- Ah Kioon MD, Tripodo C, Fernandez D, Kirou KA, Spiera RF, Crow MK, Gordon JK, Barrat FJ. Plasmacytoid dendritic cells promote systemic sclerosis with a key role for TLR8. *Sci Transl Med* 2018; 10: eaam8458.
- Aldahlawi AM. Modulation of dendritic cell immune functions by plant components. *J Microsc Ultrastruct* 2016; 4: 55-62.
- Arimura K, Takagi H, Uto T, Fukaya T, Nakamura T, Chojookhuu N, Hishikawa Y, Yamashita Y, Sato K. Crucial role of plasmacytoid dendritic cells in the development of acute colitis through the regulation of intestinal inflammation. *Mucosal Immunol* 2017; 10: 957-970.
- Arumugam S, Watanabe K. Japanese Kampo medicines for the treatment of common diseases: focus on inflammation. New York: Elsevier Inc 2017.
- Audiger C, Rahman MJ, Yun TJ, Tarbell KV, Lesage S. The Importance of Dendritic Cells in Maintaining Immune Tolerance. *J Immunol* 2017; 198: 2223-2231.
- Baird AC, Mallon D, Radford-Smith G, Boyer J, Piche T, Prescott SL, Lawrance IC, Tulic MK. Dysregulation of innate immunity in ulcerative colitis patients who fail anti-tumor necrosis factor therapy. *World J Gastroenterol* 2016; 22: 9104-9116.
- Bao KF, Yu X, Wei X, Gui LL, Liu HL, Wang XY, Tao Y, Jiang GR, Hong M. Astragaloside IV ameliorates allergic inflammation by inhibiting key initiating factors in the initial stage of sensitization. *Sci Rep* 2016; 6: 38241.
- Baumgart DC, Metzke D, Guckelberger O, Pascher A, Grötzinger C, Przesdzing I, Dörffel Y, Schmitz J, Thomas S. Aberrant plasmacytoid dendritic cell distribution and function in patients with Crohn's disease and ulcerative colitis. *Clin Exp Immunol* 2011; 166: 46-54.
- Bonnefoy F, Perruche S, Couturier M, Sedrati A, Sun Y, Tiberghien P, Gaugler B, Saas P. Plasmacytoid dendritic cells play a major role in apoptotic leukocyte-induced immune modulation. *J Immunol* 2011; 186: 5696-5705.

Chen Q, Duan X, Fan H, Xu M, Tang Q, Zhang L, Shou Z, Liu X, Zuo D, Yang J, Deng S, Dong Y, Wu H, Liu Y, Nan Z. Oxymatrine protects against DSS-induced colitis via inhibiting the PI3K/AKT signaling pathway. *Int Immunopharmacol* 2017; 53: 149-157.

Chen T, Wang R, Jiang W, Wang H, Xu A, Lu G, Ren Y, Xu Y, Song Y, Yong S, Ji H, Ma Z. Protective Effect of Astragaloside IV Against Paraquat-Induced Lung Injury in Mice by Suppressing Rho Signaling. *Inflammation* 2016; 39: 483-492.

Contractor N, Louten J, Kim L, Biron CA, Kelsall BL. Cutting edge: Peyer's patch plasmacytoid dendritic cells (pDCs) produce low levels of type I interferons: possible role for IL-10, TGFbeta, and prostaglandin E2 in conditioning a unique mucosal pDC phenotype. *J Immunol* 2007; 179: 2690-2694.

Cui H, Cai Y, Wang L, Jia B, Li J, Zhao S, Chu X, Lin J, Zhang X, Bian Y, Zhuang P. Berberine Regulates Treg/Th17 Balance to Treat Ulcerative Colitis Through Modulating the Gut Microbiota in the Colon. *Front Pharmacol* 2018; 9: 571.

Cui X, Liu X, Han Q, Zhu J, Li J, Ren Z, Liu L, Luo Y, Wang Z, Zhang D, Fan Y, Zhang D, Dong G. DPEP1 is a direct target of miR-193a-5p and promotes hepatoblastoma progression by PI3K/Akt/mTOR pathway. *Cell Death Dis* 2019; 10: 701.

Donyo M, Hollander D, Abramovitch Z, Naftelberg S, Ast G. Phosphatidylserine enhances IKBKAP transcription by activating the MAPK/ERK signaling pathway. *Hum Mol Genet* 2016; 25: 1307-1317.

Dubois B, Joubert G, Gomez de Agüero M, Gouanvic M, Goubier A, Kaiserlian D. Sequential Role of Plasmacytoid Dendritic Cells and Regulatory T Cells in Oral Tolerance. *Gastroenterology* 2009; 137: 1019-1028.

Eichele DD, Kharbanda KK. Dextran sodium sulfate colitis murine model: An indispensable tool for advancing our understanding of inflammatory bowel diseases pathogenesis. *World J Gastroenterol* 2017; 23: 6016-6029.

Fenton TM, Jørgensen PB, Niss K, Rubin SJS, Mørbe UM, Riis LB, Da Silva C, Plumb A, Vandamme J, Jakobsen HL, Brunak S, Habtezion A, Nielsen OH, Johansson-Lindbom B, Agace

WW. Immune Profiling of Human Gut-Associated Lymphoid Tissue Identifies a Role for Isolated Lymphoid Follicles in Priming of Region-Specific Immunity. *Immunity* 2020; 52: 557-570.

Garzorz-Stark N, Lauffer F, Krause L, Thomas J, Atenhan A, Franz R, Roenneberg S, Boehner A, Jargosch M, Batra R, Mueller NS, Haak S, Groß C, Groß O, Traidl-Hoffmann C, Theis FJ, Schmidt-Weber CB, Biedermann T, Eyerich S, Eyerich K. Toll-like receptor 7/8 agonists stimulate plasmacytoid dendritic cells to initiate TH17-deviated acute contact dermatitis in human subjects. *J Allergy Clin Immunol* 2018; 141: 1320-1333.

Geremia A, Biancheri P, Allan P, Corazza GR, Di Sabatino A. Innate and adaptive immunity in inflammatory bowel disease. *Autoimmun Rev* 2014; 13: 3-10.

Gotoh K, Tanaka Y, Nishikimi A, Inayoshi A, Enjoji M, Takayanagi R, Sasazuki T, Fukui Y. Differential requirement for DOCK2 in migration of plasmacytoid dendritic cells versus myeloid dendritic cells. *Blood* 2008; 111: 2973-2976.

Goubier A, Dubois B, Gheit H, Joubert G, Villard-Truc F, Asselin-Paturel C, Trinchieri G, Kaiserlian D. Plasmacytoid Dendritic Cells Mediate Oral Tolerance. *Immunity* 2008; 29: 464-475.

Hadeiba H, Sato T, Habtezion A, Oderup C, Pan J, Butcher EC. CCR9 expression defines tolerogenic plasmacytoid dendritic cells able to suppress acute graft-versus-host disease. *Nat Immunol* 2008; 9: 1253-1260.

Hamada H, Hiroi T, Nishiyama Y, Takahashi H, Masunaga Y, Hachimura S, Kaminogawa S, Takahashi-Iwanaga H, Iwanaga T, Kiyono H, Yamamoto H, Ishikawa H. Identification of Multiple Isolated Lymphoid Follicles on the Antimesenteric Wall of the Mouse Small Intestine. *J Immunol* 2002; 168: 57-64.

Hashizume H, Horibe T, Yagi H, Seo N, Takigawa M. Compartmental imbalance and aberrant immune function of blood CD123+ (plasmacytoid) and CD11c+ (myeloid) dendritic cells in atopic dermatitis. *J Immunol* 2005; 174: 2396-2403.

Hauser MA, Legler DF. Common and biased signaling pathways of the chemokine receptor CCR7 elicited by its ligands CCL19 and CCL21 in leukocytes. *J Leukoc Biol* 2016; 99: 869-882.

Im K, Kim J, Min H. Ginseng, the natural effectual antiviral: Protective effects of Korean Red

Ginseng against viral infection. *J Ginseng Res* 2016; 40: 309-314.

Itoh K, Masuda M, Naruto S, Murata K, Matsuda H. Antiallergic activity of unripe Citrus hassaku fruits extract and its flavanone glycosides on chemical substance-induced dermatitis in mice. *J Nat Med* 2009; 63: 443-450.

Jia H, Song L, Cong Q, Wang J, Xu H, Chu Y, Li Q, Zhang Y, Zou X, Zhang C, Chin YE, Zhang X, Li Z, Zhu K, Wang B, Peng H, Hou Z. The LIM protein AJUBA promotes colorectal cancer cell survival through suppression of JAK1/STAT1/IFIT2 network. *Oncogene* 2017; 36: 2655-2666.

Jiang K, Lu Q, Li Q, Ji Y, Chen W, Xue X. Astragaloside IV inhibits breast cancer cell invasion by suppressing Vav3 mediated RAC1/MAPK signaling. *Int Immunopharmacol* 2017; 42: 195-202.

Jiang XG, Sun K, Liu YY, Yan L, Wang MX, Fan JY, Mu HN, Li C, Chen YY, Wang CS, Han JY. Astragaloside IV ameliorates 2,4,6-trinitrobenzene sulfonic acid (TNBS)-induced colitis implicating regulation of energy metabolism. *Sci Rep* 2017; 7: 41832.

Karuppagounder, V, Nomoto M, Watanabe, K. Antiinflammatory effects of Kampo medicines in atopic dermatitis. In: Arumugam S, Watanabe K, Japanese Kampo medicines for the treatment of common diseases: focus on inflammation. New York: Elsevier Inc 2017: 89-95.

Kim YI, Lee BR, Cheon JH, Kwon BE, Kweon MN, Ko HJ, Chang SY. Compensatory roles of CD8⁺ T cells and plasmacytoid dendritic cells in gut immune regulation for reduced function of CD4⁺ Tregs. *Oncotarget* 2016; 7: 10947-10961.

Lebre MC, van Capel TM, Bos JD, Knol EF, Kapsenberg ML, de Jong EC. Aberrant function of peripheral blood myeloid and plasmacytoid dendritic cells in atopic dermatitis patients. *J Allergy Clin Immunol* 2008; 122: 969-976.

Li HS, Gelbard A, Martinez GJ, Esashi E, Zhang H, Nguyen-Jackson H, Liu YJ, Overwijk WW, Watowich SS. Cell-intrinsic role for IFN- α -STAT1 signals in regulating murine Peyer patch plasmacytoid dendritic cells and conditioning an inflammatory response. *Blood* 2011; 118: 3879-3889.

Li N, Dou Z, Liu J, Chai B, Li Y, An X, Chu P, Zhang X. Therapeutic Effect of HGF on NASH Mice Through HGF/c-Met and JAK2-STAT3 Signalling Pathway. *Ann Hepatol* 2018; 17: 501-510.

Lin PY, Chu CH, Chang FY, Huang YW, Tsai HJ, Yao TC. Trends and prescription patterns of traditional Chinese medicine use among subjects with allergic diseases: A nationwide population-based study. *World Allergy Organ J* 2019; 12: 100001.

Liu H, Dasgupta S, Fu Y, Bailey B, Roy C, Lightcap E, Faustin B. Subsets of mononuclear phagocytes are enriched in the inflamed colons of patients with IBD. *BMC Immunol.* 2019; 20: 42.

Liu J, Zhang X, Chen K, Cheng Y, Liu S, Xia M, Chen Y, Zhu H, Li Z, Cao X. CCR7 Chemokine Receptor-Inducible Inc-Dpf3 Restrains Dendritic Cell Migration by Inhibiting HIF-1 α -Mediated Glycolysis. *Immunity* 2019; 50: 600-615.

Liu L, Mu Q, Li W, Xing W, Zhang H, Fan T, Yao H, He L. Isofraxidin protects mice from LPS challenge by inhibiting pro-inflammatory cytokines and alleviating histopathological changes. *Immunobiology* 2015; 220: 406-413.

Liu Q, Yin W, Han L, Lv J, Li B, Lin Y, Mi Q, He R, Lu C. Diarylheptanoid from rhizomes of *Curcuma kwangsiensis* (DCK) inhibited imiquimod-induced dendritic cells activation and Th1/Th17 differentiation. *Int Immunopharmacol* 2018; 56: 339-348.

Liu R, Jiang H, Tian Y, Zhao W, Wu X. Astragaloside IV protects against polymicrobial sepsis through inhibiting inflammatory response and apoptosis of lymphocytes. *J Surg Res* 2016; 200: 315-323.

Liu X, Mishra P, Yu S, Beckmann J, Wendland M, Kocks J, Seth S, Hoffmann K, Hoffmann M, Kremmer E, Förster R, Worbs T. Tolerance induction towards cardiac allografts under costimulation blockade is impaired in CCR7-deficient animals but can be restored by adoptive transfer of syngeneic plasmacytoid dendritic cells. *Eur J Immunol* 2011; 41: 611-623.

Lopez MJ, Seyed-Razavi Y, Jamali A, Harris DL, Hamrah P. The Chemokine Receptor CXCR4 Mediates Recruitment of CD11c⁺ Conventional Dendritic Cells Into the Inflamed Murine Cornea. *Invest Ophthalmol Vis Sci* 2018; 59: 5671-5681.

Lv J, Li L, Li W, Ji K, Hou Y, Yan C, Dai T. Role of the chemokine receptors CXCR3, CXCR4 and CCR7 in the intramuscular recruitment of plasmacytoid dendritic cells in dermatomyositis. *J Neuroimmunol* 2018; 319: 142-148.

McKenna K, Beignon AS, Bhardwaj N. Plasmacytoid dendritic cells: linking innate and adaptive immunity. *J Virol* 2005; 79: 17-27.

Mitsialis V, Wall S, Liu P, Ordovas-Montanes J, Parmet T, Vukovic M, Spencer D, Field M, McCourt C, Toothaker J, Bousvaros A; Boston Children's Hospital Inflammatory Bowel Disease Center; Brigham and Women's Hospital Crohn's and Colitis Center, Shalek AK, Kean L, Horwitz B, Goldsmith J, Tseng G, Snapper SB, Konnikova L. Single-Cell Analyses of Colon and Blood Reveal Distinct Immune Cell Signatures of Ulcerative Colitis and Crohn's Disease. *Gastroenterology* 2020; 159: 591-608.

Mizuno S, Kanai T, Mikami Y, Sujino T, Ono Y, Hayashi A, Handa T, Matsumoto A, Nakamoto N, Matsuoka K, Hisamatsu T, Takaishi H, Hibi T. CCR9+ plasmacytoid dendritic cells in the small intestine suppress development of intestinal inflammation in mice. *Immunol Lett* 2012; 146: 64-69.

Niu X, Wang Y, Li W, Mu Q, Li H, Yao H, Zhang H. Protective effects of Isofraxidin against lipopolysaccharide-induced acute lung injury in mice. *Int Immunopharmacol* 2015; 24: 432-439.

Owen JL, Vakharia PP, Silverberg JI. The Role and Diagnosis of Allergic Contact Dermatitis in Patients with Atopic Dermatitis. *Am J Clin Dermatol* 2018; 19: 293-302.

Pöysti S, Silojärvi S, Toivonen R, Hänninen A. Plasmacytoid dendritic cells regulate host immune response to *Citrobacter rodentium* induced colitis in colon-draining lymph nodes. *Eur J Immunol* 2021; 51: 620-625.

Prete F, Catucci M, Labrada M, Gobessi S, Castiello MC, Bonomi E, Aiuti A, Vermi W, Cancrini C, Metin A, Hambleton S, Bredius R, Notarangelo LD, van der Burg M, Kalinke U, Villa A, Benvenuti F. Wiskott-Aldrich syndrome protein-mediated actin dynamics control type-I interferon production in plasmacytoid dendritic cells. *J Exp Med* 2013; 210: 355-374.

Reizis B. Plasmacytoid Dendritic Cells: Development, Regulation, and Function. *Immunity* 2019;

50: 37-50.

Ridley AJ. Rho GTPase signalling in cell migration. *Curr Opin Cell Biol* 2015; 36: 103-112.

Saaddeh D, Kurban M, Abbas O. Update on the role of plasmacytoid dendritic cells in inflammatory/autoimmune skin diseases. *Exp Dermatol* 2016; 25: 415-421.

Sanderlin EJ, Leffler NR, Lertpiriyapong K, Cai Q, Hong H, Bakthavatchalu V, Fox JG, Oswald JZ, Justus CR, Krewson EA, O'Rourke D, Yang LV. GPR4 deficiency alleviates intestinal inflammation in a mouse model of acute experimental colitis. *Biochim Biophys Acta Mol Basis Dis* 2017; 1863: 569-584.

Sawai CM, Serpas L, Neto AG, Jang G, Rashidfarrokhi A, Kolbeck R, Sanjuan MA, Reizis B, Sisirak V. Plasmacytoid Dendritic Cells Are Largely Dispensable for the Pathogenesis of Experimental Inflammatory Bowel Disease. *Front Immunol* 2018; 9: 2475.

Seth S, Oberdörfer L, Hyde R, Hoff K, Thies V, Worbs T, Schmitz S, Förster R. CCR7 essentially contributes to the homing of plasmacytoid dendritic cells to lymph nodes under steady-state as well as inflammatory conditions. *J Immunol* 2011; 186: 3364-3372.

Shi LJ, Shi L, Song GY, Zhang HF, Hu ZJ, Wang C, Zhang DH. Oxymatrine attenuates hepatic steatosis in non-alcoholic fatty liver disease rats fed with high fructose diet through inhibition of sterol regulatory element binding transcription factor 1 (Srebf1) and activation of peroxisome proliferator activated receptor alpha (Ppar α). *Eur J Pharmacol* 2013; 714: 89-95.

Shimizu T. Efficacy of Kampo Medicine in Treating Atopic Dermatitis: An Overview. *Evid Based Complement Alternat Med* 2013; 2013: 260235.

Smrekar N, Drobne D, Smid LM, Ferkolj I, Stabuc B, Ihan A, Kopitar AN. Dendritic cell profiles in the inflamed colonic mucosa predict the responses to tumor necrosis factor alpha inhibitors in inflammatory bowel disease. *Radiol Oncol* 2018; 52: 443-452.

Sokol CL, Luster AD. The Chemokine System in Innate Immunity. *Cold Spring Harb Perspect Biol* 2015; 7: a016303.

Solitano V, D'Amico F, Fiorino G, Paridaens K, Peyrin-Biroulet L, Danese S. Key Strategies to

Optimize Outcomes in Mild-to-Moderate Ulcerative Colitis. *J Clin Med* 2020; 9: 2905.

Suzuki H, Jounai K, Ohshio K, Fujii T, Fujiwara D. Administration of plasmacytoid dendritic cell-stimulative lactic acid bacteria enhances antigen-specific immune responses. *Biochem Biophys Res Commun* 2018; 503: 1315-1321.

Swiecki M, Colonna M. The multifaceted biology of plasmacytoid dendritic cells. *Nat Rev Immunol* 2015; 15: 471-485.

Takagi H, Fukaya T, Eizumi K, Sato Y, Sato K, Shibazaki A, Otsuka H, Hijikata A, Watanabe T, Ohara O, Kaisho T, Malissen B, Sato K. Plasmacytoid Dendritic Cells Are Crucial for the Initiation of Inflammation and T Cell Immunity In Vivo. *Immunity* 2011; 35: 958-971.

Takayama S, Arita R, Kikuchi A, Ohsawa M, Kaneko S, Ishii T. Clinical Practice Guidelines and Evidence for the Efficacy of Traditional Japanese Herbal Medicine (Kampo) in Treating Geriatric Patients. *Front Nutr* 2018; 5: 66.

Tatsumi T, Yamada T, Nagai H, Terasawa K, Tani T, Nunome S, Saiki I. A Kampo formulation: Byakko-ka-ninjin-to (Bai-Hu-Jia-Ren-Sheng-Tang) inhibits IgE-mediated triphasic skin reaction in mice: the role of its constituents in expression of the efficacy. *Biol Pharm Bull* 2001; 24: 284-290.

Tiberio L, Del Prete A, Schioppa T, Sozio F, Bosisio D, Sozzani S. Chemokine and chemotactic signals in dendritic cell migration. *Cell Mol Immunol* 2018; 15: 346-352.

Tohda C, Sugahara H, Kuraishi Y, Komatsu K. Inhibitory effect of Byakko-ka-ninjin-to on itch in a mouse model of atopic dermatitis. *Phytother Res* 2000; 14: 192-194.

Uto T, Takagi H, Fukaya T, Nasu J, Fukui T, Miyanaga N, Arimura K, Nakamura T, Chojjookhuu N, Hishikawa Y, Sato K. Critical role of plasmacytoid dendritic cells in induction of oral tolerance. *J Allergy Clin Immunol* 2018; 141: 2156-2167.

Vatti RR, Ali F, Teuber S, Chang C, Gershwin ME. Hypersensitivity Reactions to Corticosteroids. *Clin Rev Allergy Immunol* 2014; 47: 26-37.

Villadangos JA, Young L. Antigen-presentation properties of plasmacytoid dendritic cells.

Immunity 2008; 29: 352-361.

Vittorakis S, Samitas K, Tousa S, Zervas E, Aggelakopoulou M, Semitekolou M, Panoutsakopoulou V, Xanthou G, Gaga M. Circulating conventional and plasmacytoid dendritic cell subsets display distinct kinetics during in vivo repeated allergen skin challenges in atopic subjects. *Biomed Res Int* 2014; 2014: 231036.

Wang G, Fyhrquist-Vanni N, Wolff H, Dieu-Nosjean MC, Kemeny L, Homey B, Lauerma AI, Alenius H. Immunostimulatory sequence CpG elicits Th1-type immune responses in inflammatory skin lesions in an atopic dermatitis murine model. *Int Arch Allergy Immunol* 2008; 147: 41-51.

Wang PL, Kaneko A. Introduction to Kampo medicine for dental treatment - Oral pharmacotherapy that utilizes the advantages of Western and Kampo medicines. *Jpn Dent Sci Rev* 2018; 54: 197-204.

Wang Y, Shou Z, Fan H, Xu M, Chen Q, Tang Q, Liu X, Wu H, Zhang M, Yu T, Deng S, Liu Y. Protective effects of oxymatrine against DSS-induced acute intestinal inflammation in mice via blocking the RhoA/ROCK signaling pathway. *Biosci Rep* 2019; 39: BSR20182297.

Wang Z, Cai J, Fu Q, Cheng L, Wu L, Zhang W, Zhang Y, Jin Y, Zhang C. Anti-Inflammatory Activities of Compounds Isolated from the Rhizome of *Anemarrhena asphodeloides*. *Molecules* 2018; 23: 2631.

Watanabe K, Karuppagounder V, Sreedhar R, Harima M, Arumugam S. Kampo medicines for autoimmune disorders: rheumatoid arthritis and autoimmune diabetes mellitus. In: Arumugam S, Watanabe K. *Japanese Kampo medicines for the treatment of common diseases: focus on inflammation*. New York: Elsevier Inc 2017: 103-110.

Wendland M, Czeloth N, Mach N, Malissen B, Kremmer E, Pabst O, Förster R. CCR9 is a homing receptor for plasmacytoid dendritic cells to the small intestine. *Proc Natl Acad Sci U S A* 2007; 104: 6347-6352.

Wollenberg A, Wagner M, Günther S, Towarowski A, Tuma E, Moderer M, Rothenfusser S, Wetzel S, Endres S, Hartmann G. Plasmacytoid dendritic cells: a new cutaneous dendritic cell subset with distinct role in inflammatory skin diseases. *J Invest Dermatol* 2002; 119: 1096-1102.

Won J, Lee BH, Jung WM, Chae Y, Lee H. Herbal medicine for inflammatory bowel diseases: development of pattern identification algorithms by retrospective analysis of case series data. *Eur J Integr Med* 2020; 36: 101114.

Wurbel MA, Le Bras S, Ibourk M, Pardo M, McIntire MG, Coco D, Geha RS, Fiebiger E, Snapper SB. CCL25/CCR9 Interactions Are Not Essential for Colitis Development but Are Required for Innate Immune Cell Protection from Chronic Experimental Murine Colitis. *Inflamm Bowel Dis* 2014; 20: 1165-1176.

Xu X, Xiao W, Zhang Z, Pan J, Yan Y, Zhu T, Tang D, Ye K, Paranjpe M, Qu L, Nie H. Anti-pruritic and anti-inflammatory effects of oxymatrine in a mouse model of allergic contact dermatitis. *J Dermatol Sci* 2018; 91: 134-141.

Yamamoto T, Shimano H, Nakagawa Y, Ide T, Yahagi N, Matsuzaka T, Nakakuki M, Takahashi A, Suzuki H, Sone H, Toyoshima H, Sato R, Yamada N. SREBP-1 interacts with hepatocyte nuclear factor-4 alpha and interferes with PGC-1 recruitment to suppress hepatic gluconeogenic genes. *J Biol Chem* 2004; 279: 12027-12035.

Ye Y, Gaugler B, Mohty M, Malard F. Plasmacytoid dendritic cell biology and its role in immune-mediated diseases. *Clin Transl Immunology* 2020; 9: e1139.

Ye Y, Ricard L, Siblany L, Stocker N, De Vassoigne F, Brissot E, Lamarthée B, Mekinian A, Mohty M, Gaugler B, Malard F. Arsenic trioxide induces regulatory functions of plasmacytoid dendritic cells through interferon- α inhibition. *Acta Pharm Sin B* 2020; 10: 1061-1072.

Yeung MM, Melgar S, Baranov V, Oberg A, Danielsson A, Hammarström S, Hammarström ML. Characterisation of mucosal lymphoid aggregates in ulcerative colitis: immune cell phenotype and TcR-gammadelta expression. *Gut* 2000; 47: 215-227.

Yu XT, Xu YF, Huang YF, Qu C, Xu LQ, Su ZR, Zeng HF, Zheng L, Yi TG, Li HL, Chen JP, Zhang XJ. Berberubine attenuates mucosal lesions and inflammation in dextran sodium sulfate-induced colitis in mice. *PLoS One* 2018; 13: e0194069.

Yue W, Liu Y, Li X, Lv L, Huang J, Liu J. Curcumin ameliorates dextran sulfate sodium-induced colitis in mice via regulation of autophagy and intestinal immunity. *Turk J Gastroenterol* 2019; 30: 290-298.

Zhai F, Song N, Ma J, Gong W, Tian H, Li X, Jiang C, Wang H. FGF18 inhibits MC3T3-E1 cell osteogenic differentiation via the ERK signaling pathway. *Mol Med Rep* 2017; 16: 4127-4132.

Zhang H, Wei Q, Xiang X, Zhou B, Chen J, Li J, Li Q, Xiong H, Liu F. Semaphorin 4A acts in a feed-forward loop with NF- κ B pathway to exacerbate catabolic effect of IL-1 β on chondrocytes. *Int Immunopharmacol* 2019; 69: 88-94.

Zhang L, Xue H, Zhao G, Qiao C, Sun X, Pang C, Zhang D. Curcumin and resveratrol suppress dextran sulfate sodium-induced colitis in mice. *Mol Med Rep* 2019; 19: 3053-3060.

Zhang YZ, Li YY. Inflammatory bowel disease: pathogenesis. *World J Gastroenterol* 2014; 20: 91-99.

Zhou X, Seto SW, Chang D, Kiat H, Razmovski-Naumovski V, Chan K, Bensoussan A. Synergistic Effects of Chinese Herbal Medicine: A Comprehensive Review of Methodology and Current Research. *Front Pharmacol* 2016; 7: 201.

Acknowledgements

Firstly, I would like to express my sincere gratitude to my advisor Prof. Makoto Kadowaki for giving me the opportunity to study here, for the clarifying comments and continuous supports, for the encouragement, motivation, enthusiasm and valuable advice in regard to my research. Thanks for his kindly advise and support so that I confirm my decision to continue my doctor course as a member of society. This is a really good decision I have made.

Besides my advisor, I would like to thank my thesis committee: Prof. Keiichi Koizumi, Prof. Takanori So, and Prof. Hiroaki Sakurai, for their insightful comments and encouragement, but also for the valuable questions which incited me to widen my research from various perspectives.

Besides, I would like to express deep thanks to my supervisor Dr. Takeshi Yamamoto who taught me how to perform and consider experiments as a researcher and for his great support and guidance in this work. My sincere thanks also go to Dr. Shusaku Hayashi for his valuable supports and comments.

I would like to appreciate all of my friends, my fellow lab mates at the Division of Gastrointestinal Pathophysiology, Dr. Kanwal, Ai Kigasawa, Emi Matsunami, for all their helps, nice party, great experiences and all of guidance during my living in Japan.

I am greatly honored to be accepted my research thesis for the degree of Doctor of University of Toyama. It is the most precious time in my life when I studied at Division of Gastrointestinal Pathophysiology, Institute of Natural Medicine, University of Toyama.

Last but not least I would like to thank my mother, my father and my sister for their deep love, my beloved Mr. W for all the accompanies and patience when I felt frustrated and confused.

Finally, I am grateful to myself for the perseverance when I decided to give up many times during these years.